ANTI-APOPTOTIC WILD-TYPE ALZHEIMER AMYLOID PRECURSOR PROTEIN SIGNALING INVOLVES THE p38 MITOGEN-ACTIVATED PROTEIN KINASE/MEF2 PATHWAY

BY

TERALEE BURTON

A Thesis

Submitted to the Faculty of Graduate Studies

in partial fulfillment of the requirements

for the degree of

MASTER OF SCIENCE

Department of Biochemistry and Medical Genetics

Faculty of Medicine

University of Manitoba

Winnipeg, Manitoba Canada

THE UNIVERSITY OF MANITOBA

FACULTY OF GRADUATE STUDIES

*****

MASTER'S THESIS/PRACTICUM FINAL REPORT

The undersigned certify that they have read the Master's Thesis/Practicum entitled:

Anti-Apoptotic Wild-Type Alzheimer Amyloid Precursor Protein Signaling Involves the p38 Mitogen-Activated Protein Kinase/MEF2 Pathway

submitted by

Teralee Burton

in partial fulfillment of the requirements for the degree of

M. Sc.

The Thesis/Practicum Examining Committee certifies that the thesis/practicum (and oral examination if required) is:

Approved

(Approved or Not Approved)

☒ **Thesis** **Advisor:** Thomas Hall

Spencer Gibson

Lorne Hyland

☐ **Practicum**

Date: 4th December 02

(forms\thereptm - 08/95)

THE UNIVERSITY OF MANITOBA

FACULTY OF GRADUATE STUDIES

*****

COPYRIGHT PERMISSION PAGE

Anti-Apoptotic Wild-Type Alzheimer Amyloid Precursor Protein Signaling Involves the p38 Mitogen-Activated Protein Kinase/MEF2 Pathway

BY

Teralee Burton

A Thesis/Practicum submitted to the Faculty of Graduate Studies of The University of Manitoba in partial fulfillment of the requirements of the degree

of

MASTER OF SCIENCE

ABSTRACT

Alzheimer amyloid precursor protein (APP) effectively protects against apoptosis in neuronal cells under stress, but the mechanisms of this anti-apoptotic effect remains largely unknown. Transcription factors act as critical molecular switches in promoting neuronal survival. The myocyte enhancer factor-2 (MEF2) is a transcription factor, and is known to be necessary for neurogenesis and activity dependent neuronal survival. This study examined the possible role of MEF2 in the anti-apoptotic signaling pathways activated by APP. We report that expression of wild-type human APP (hAPPwt) but not familial Alzheimer's disease mutant APP (FAD-hAPPmut) in APP-deficient rat B103 cells led to a significant increase in the level of phosphorylated MEF2. This differential phosphorylation was dependent on enhanced activation of p38 mitogen-activated protein kinase (p38 MAPK). Also, expression of hAPPwt mediated an increase in MEF2 DNA binding affinity that correlated with p38 MAPK dependent trans-activation of a MEF2-responsive reporter gene. Furthermore, over expression of dominant negative MEF2 in hAPPwt expressing cells enhanced staurosporine-induced apoptosis. In contrast, MEF2wt over expression in enhanced the capacity of hAPPwt to confer resistance to

apoptosis. Thus, MEF2 plays a critical role in APP mediated signaling pathways that inhibit neuronal apoptosis. A model of anti-apoptotic APP signaling is proposed where APP mediates p38 MAPK dependent phosphorylation and activation of MEF2. Once activated MEF2 regulates neuronal survival by stimulation of MEF2 dependent gene transcriptions. Alteration of this function by mutations in APP and aberrant APP processing, could contribute to neuronal degeneration seen in Alzheimer's disease (AD).

ACKNOWLEDGMENTS

First and foremost, I would like to thank Dr. Francis Amara, who is a great advisor and an even better friend. I am really grateful to have had the opportunity to study in his lab. I would like to thank my advisory committee Dr. Myal and Dr. Gibson for their advise and their time in guiding me through my Masters degree. I would like to thank my whole family who has supported me throughout all of my schooling. I would like to thank my dad for always being there to talk to and for doing anything to make sure I have what I need. I would like to thank my mom for helping me adapt to living in Winnipeg and for taking me out all the time to relax. I would like to thank my brother Tyler who has helped me a great deal. I would also like to thank Mark for being there to listen to me and for supporting me in the last year, I could not have chosen better person to share my time with.

TABLE OF CONTENTS

LIST OF FIGURES

LIST OF TABLES

LIST OF ABBREVIATIONS

aa	amino acid
AD	Alzheimer's disease
aPKC	atypical protein kinase C
APP	amyloid precursor proteins
APLP2	amyloid precursor like proteins
ATP	adenosine triphosphate
Aβ	amyloid-β
BCA	bicinchoninic acid
bHLH	basic helix-loop-helix
CaMK	calcium calmodulin-dependent protein kinase
CAT	chloramphenicol acetyltransferase
CIAP	calf intestinal alkaline phosphatase
cis-element	optimal MEF2 binding site sequence
CKII	casein kinase-II
CNS	central nervous system
cPKC	conventional protein kinase C
CRE	cAMP response element
dIdC	deoxyinosine-deoxycytidine

DIG	digoxigenin
DMSO	dimethyl sulfoxide
DN	dominant negative
DTT	dithiothreitol
dUTP	deoxyuridine triphosphate
ECL	enhanced chemiluminescence
EDTA	ethylene diaminetetraacetic acid
EGTA	ethyleneglycol bis (2-aminoethyl-ether) etraacetic acid
EMSA	electrophoretic mobility shift assay
FAD	familial Alzheimer's disease
GABA	γ-aminobutyric acid type A
GST	gluthathione S-transferase
G_0	guanine 5'-triphosphate GTP binding protein
hAPPwt	wild-type human APP
HAT	histone acetylase
HCl	hydrochloric acid
HDAC	histone deacetylase
IGF	insulin growth factor
KCl	potassium chloride
KN-93	CaMKII specific inhibitor

mAChR	muscarinic acetylcholine receptor
MADS	MCM1 agamous deficiens-serum response factor
MAPK	mitogen-activated protein kinase
MCK	muscle creatine kinase
MEF2	myocyte enhancer factor 2
$MgCl_2$	magnesium chloride
MTT	3-[4,5-dimentylthiazol-2-yl]-2-5-diphenyl tetrazolium bromide
NaCl	sodium chloride
NaF	sodium floride
Na_2PO_4	sodium phosphate
NFAT	nuclear factor of activated T cell
NMDA	N-Methyl-D-aspartate receptor
nPKC	novel protein kinase C
NR1	NMDA receptor subunit 1
p38 MAPK	p38 mitogen-activated protein kinase
PBS	phosphate buffered saline
PCV	packed cell volume
PDZ	PSD-95/Dlg/Z0-1 protein-protein domains
PID	phosphotyrosine-interaction domain

PI3-K	phosphoinositol-3-kinase
PKA	protein kinase A
PKB	protein kinase B
PKC	protein kinase C
PMSF	phenylmethylsulfonyl fluoride
PTB	phosphotyrosine-binding domain
SB	SB 202190 hydrochloride p38 MAPK inhibitor
SDS	sodium dodecylsulfate
SEM	standard error of the mean
SH2	Src homology
STS	staurosporine
TBE	Tris-borate-EDTA buffer
TBS	Tris-buffered saline
TBS-T	Tris-buffered saline/Tween 20
TGFβ	transforming growth factor β
Thr	threonine
TK	thymidine kinase
TLC	thin layer chromatography
TUNEL	terminal deoxynucleotidyl transferase mediated UTP-end labeling

Tyr	tyrosine
β-Gal	β-galactosidase

1.0 INTRODUCTION

1.1 ALZHEIMER AMYLOID PRECURSOR PROTEIN (APP)

There are three major isoforms of APP (APP_{770}, APP_{751} and APP_{695}). APP_{770} and APP_{751} are expressed in both neuronal and non-neuronal cells but APP_{695} is only expressed in high levels in the brain (1). The difference between the 770/751 and 695 isoforms is the presence of an exon that codes for a 56 amino acid (aa) motif that is homologous to the Kunitz type of serine protease inhibitor and an OX-2 antigen domain (2,3). Functions for APP that have been described *in vitro* and *in vivo* include: inhibition of certain proteases by APP_{751}/APP_{770}, and enhancement of cell substrate adhesion, neurotrophic and other growth promoting effects and neuroprotective properties, which are shown by all three isoforms (4).

1.1.1 The role of APP in the pathogenesis of Alzheimer's Disease (AD)

Amyloid precursor proteins have recently been implicated in the pathogenesis of AD (4,6,8). Alzheimer's disease is characterized by neurofibrillary tangles and amyloid plaque formation in the cerebral cortex,

which was first identified by Alois Alzheimer in 1907. The manifestation of AD is defined by three stages: the initial mild stage, where the patient shows short-term memory impairment often accompanied by symptoms of anxiety and depression; the moderate stage where symptoms appear to abate as neuropsychiatric manifestations such as visual hallucinations, false beliefs and reversal of sleep patterns; and the severe stage, where the patient becomes more sedentary and can no longer care for themselves (5).

One of the hallmarks of AD is the amyloid plaques found post-mortem in brain tissue. These characteristic plaques are composed of the amyloid-β (Aβ) protein, which is an insoluble product of endoproteolytic cleavage of APP (6). Aggregates of Aβ comprising of $A\beta_{40}$ and mostly $A\beta_{42}$ assemble into fibrils (7-10 nM) to form a dense plaques usually found in moderate or large numbers in the limbic structures and association neocortex (6). This plaque also usually contains degenerating axons and dendrites of neurons, activated microglia and astrocytes (6).

The principal cleavage sites on APP are important for proper cleavage of APP to soluble products that can be broken down further and recycled by the cell. APP has three specific sites that α, β and γ secretases recognize and cleave (Figure 1)(7). When α secretase cleaves APP, a large soluble segment is released and a small portion of the c-terminus fragment is

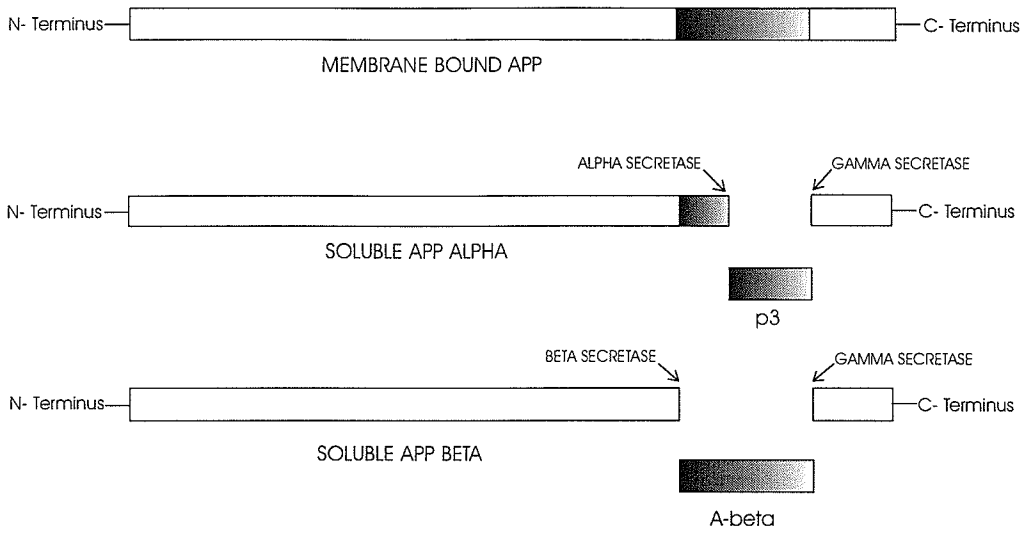

Figure 1. Secretase cleavage of APP by two alternative pathways. APP is either cleaved by alpha and gamma secretases to form the soluble APPalpha and p3 products, or beta and gamma secretases to form a soluble APPbeta peptide and an insoluble A-beta peptide.

retained in the membrane. The α secretase cleaves APP in the middle of the region that the Aβ peptide is located, therefore not allowing Aβ production. Cleavage of APP by β and γ secretases results in the formation the Aβ fragment, $A\beta_{42}$ (Figure 1) (6,7). The γ secretase can also cleave APP to form $A\beta_{40}$ and $A\beta_{41}$, but these fragments do not aggregate as readily to form a plaque as the $A\beta_{42}$ fragment.

The major theory that describes the cascade of AD progression is founded on the idea that missense mutations in genes that affect the endoproteolysis of APP results in an increase in production of Aβ42 and leads to a progressive accumulation and aggregation of Aβ42 in the brain and interstitial fluid (8). Deposition of aggregated Aβ42 then form diffuse plaques that also include Aβ40 and certain plaque associated proteins. This causes activation of the brain's resident macrophages, the microglia, that are in close proximity to Aβ deposits, which activate inflammatory cascades (123). *In vitro* exposure of microglia to Aβ leads to production of pro-inflammatory cytokines such as TNF-α (tumor necrosis factor alpha) and interleukin 1B that attenuate the inflammatory cascade. Also, Aβ plaque formation activates astrocytes (astrocytosis) resulting in upregulation of interleukin 1B production and inducible nitric oxide synthase (iNOS) that leads to inflammation (124). Neurons are then progressively injured within

the amyloid plaques and disruption of neural metabolic and ionic homeostasis contribute to oxidative injury, attenuating kinase/phosphatase activation and hyperphosphorylation of tau. Tau is a microtubule associating protein that is necessary for proper microtubule organization. When it is phosphorylated it loses its ability to associate with microtubules causing neurofibrillary tangles. The end result is widespread neuronal dysfunction and death in the hippocampus and cerebral cortex with progressive neurotransmitter deficiencies (8). On the other hand, there is evidence that the pathogenesis of AD is not caused by the Aβ plaques, but that they are a downstream effect of faulty APP metabolism. Recently, development of a theory that the fundamental basis of AD appears to relate directly to certain signaling mechanisms that are curtail for normal development that involves the metabolism of APP, therefore elucidating the normal function of APP may lead to understanding the causation of AD (19,20,21).

1.1.2 Functions of APP as a cell surface receptor

Amyloid precursor proteins (APPs) are type 1 integral membrane proteins that resemble glycosylated receptor proteins (9). They have a large N-terminus extracellular domain, a single transmembrane domain segment

and a short cytoplasmic tail. Although, the possible ligands of the extracellular domain of APP are still unknown, recent studies have shown that the carboxyl terminus of APP has a phosphotyrosine-binding domain (PTB). This domain consists of a highly conserved stretch of five amino acids (683-688) that resembles the consensus sequence surrounding a tyrosine that is auto phosphorylated in epidermal growth factor (10). Also centered on this PTB is a complex network of interacting proteins (Figure 2)(11-14). These results suggest that APP could be involved in signal transduction. Very little is known about the functions of membrane-bound APP; consequently our understanding of molecular mechanisms regulating APP signaling is largely unknown.

1.1.3 APP protein-protein interactions

1.1.3.1 Guanine 5'-triphosphate GTP binding protein (G_0)

G_0 has been found to bind the c-terminus (His 657-Lys676) of APP, which leads to its activation. The G_0 protein in neuronal cells is involved in propagating signals for adhesion (15), neurite outgrowth (16) and locomotion (17). When G_0 is treated with GTP-$\beta\gamma$, it loses the ability to associate with APP (18), thus APP is probably a receptor that regulates

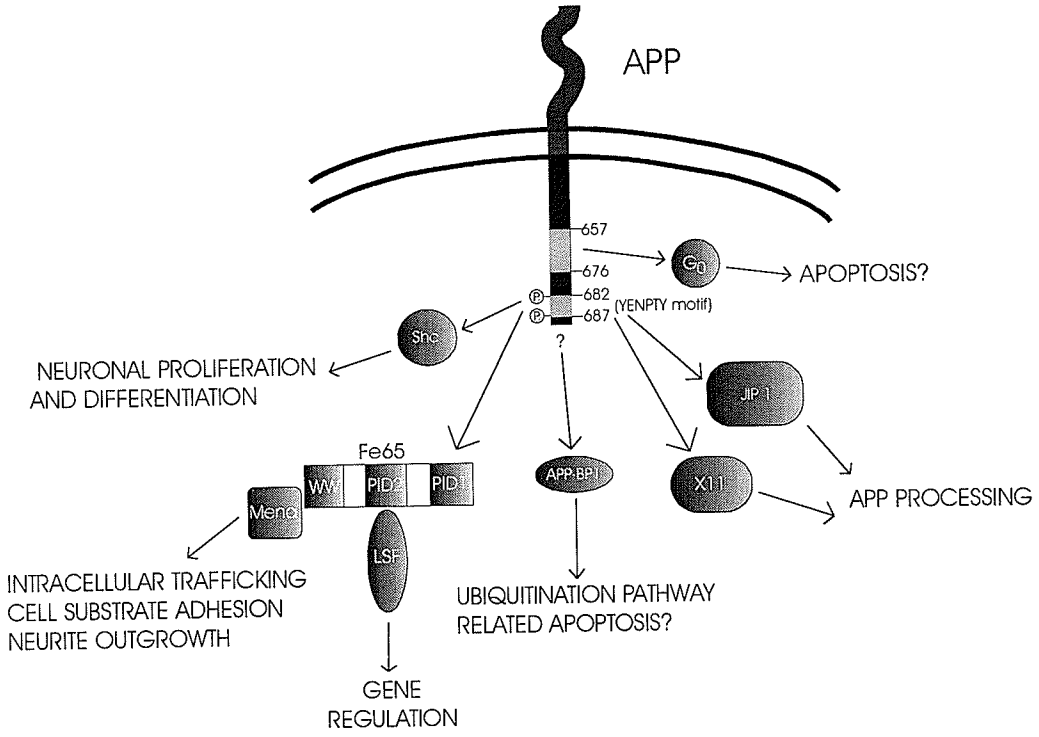

Figure 2. Schematic representation of the protein-protein interaction network centered around the cytoplasmic domain of APP.

intracellular signaling through G_0. This is supported by the fact that APP and G_0 have some of the same signaling characteristics in neuronal cells (19). In addition, the physiological role of APP signaling through G_0 has been studied in AD. Familial Alzheimer's disease (FAD) mutations in APP constitutively activate G_0 and induce apoptosis in NK1 cells and suppresses the cAMP response element (CRE) (19,20).

1.1.3.2 Fe65

The protein Fe65 has been found to interact with the last 33 c-terminal residues of APP (21). It has been suggested that Fe65 is an adapter protein that propagates signaling cascades through activation of specific proteins because it contains two distinct protein interaction domains: the phosphotyrosine-interaction domains (PIDs) and the WW domain (22). The PID domain is similar to the Shc family of proteins in that it recognizes phosphorylated NPXY motifs, and in addition is thought to be involved in signal transduction (21, 29).

1.1.3.3 LSF

A protein that complexes with the P1D domain of Fe65 is LSF which is a transcription factor that is involved in inducing expression of specific genes (22, 23). LSF is thought to control the internalization and processing of APP when it interacts with Fe65 (22). In AD, LSF is of interest because, apart from influencing global gene expression in cell growth and mitogenic stimulation (24), it interacts with gene products α-2 macroglobulin, GSKβ and viruses that have been suggested to have a role in the pathogenesis of AD (25,26,27).

1.1.3.4 Mena

Fe65 has also been found to interact with a protein called Mena through its WW domain (protein interaction domain). Mena is the mammalian homolog of the drosophila enabled protein (29), which is found in cellular sites where active actin remodeling occurs such as in lamellipodia (28). This suggests that Fe65 could function as an adaptor protein to alter cytoskeleton dynamics through Mena by APP stimulation. In addition Mena induces p19 neuronal cells to differentiate similar to the action of APP (28)

implicating that Mena may be involved in neurite outgrowth induced by APP signaling (29).

1.1.3.5 X11

Another protein that interacts with the c-terminus of APP is X11 (14). This protein interacts with APP through a PID/PTB domain similar to those found in Fe65. It has characteristics of being an adaptor protein because it possesses two PDZ (PSD-95/Dlg/Z0-1) protein-protein domains (29). X11 has been shown to modulate the metabolism of APP, and reduce secretion of Aβ. It achieves this through interaction with Munc18a at its n-terminus, where both X11 and Munc18a act in concert to suppress γ-secretase processing of APP (30).

1.1.3.6 JIP1

Proteins from the JNK (c-Jun NH_2-terminal kinase) signaling pathway selectively bind to scaffold proteins, such as the JIP family of proteins, which is important in specific stimulation of the JNK pathway (31,32). JIP1 interacts strongly with the cytoplasmic domain of APP. The interaction

between APP and JIP1 involves the phosphotyrosine interaction (PI) domain of JIP1 and GYENPTY motif in the APP cytoplasmic domain. The expression of JIP1 has been found to stabilize immature APP, suppress the production of the secreted large extracellular n-terminal domain of APP, the generation of a cleaved intracellular c-terminal fragment and the secretion of Aβ40 and Aβ42. This effect is independent of JIPs regulation of the JNK signaling cascade (31). This suggests that the interactions of JIP with APP plays an important role in the metabolism of APP (32,33).

1.1.3.7 APP-BP1

Another APP-binding protein called APP-BP1 has been isolated by yeast two hybrid system. It is similar to a protein encoded by the Arabidopsis AXR1 gene, which has a gene product that is a ubiquitin activating enzyme (34). This suggests that APP-BP1 may participate in a ubiquitinylation-related pathway that is stimulated by APP. Recent studies have shown that APP-BP1 also interacts with hUba3 (human Uba3), which activates the ubiquitin NEDD8 pathway, which has specifically been found to induce apoptosis in primary neurons through overexpression of APP-BP1 (35).

1.1.3.8 Shc

Recently, using the yeast-two hybrid system, the cytoplasmic domain of APP was found to interact with ShcA and ShcC (36). These proteins are cytoplasmic adaptor proteins that have phosphotyrosine binding (PTB) and Src homology (SH2) domains, which interact with receptor tyrosine kinases and activated growth factors (36). This is consistent with the findings that tyrosine phosphorylation of APP promotes the interaction between APP and Src. SrcC is highly expressed in the adult brain and has been found to modulate cellular and neuronal differentiation and proliferation therefore providing evidence for a link between APP signaling and the mediation of cell survival.

1.1.4 Anti-apoptotic action of APP in neuronal cells

APP has been implicated in the pathogenesis of AD. AD is characterized by memory impairment through neurodegeneration, which is mediated in part by activation of pro-apoptotic pathways and appears to contribute to AD and other important neurological diseases (37,38). During

apoptosis, degenerative cascades become activated and/or sustaining signaling pathways are too weak, causing degeneration of neuronal circuits, which manifest as disease (39). In the presence of apoptosis inducing stimuli overexpression of hAPPwt, but not FAD hAPPmut exhibits a protective effect against apoptosis in neuronal cells by post-translational modification of p53 and oxidative stress-induced apoptotic cell death (40,41,42). The protective capacity of APPwt in cells challenged with secondary insults is consistent with the observations that the synthesis of both APP and APLP2 (amyloid precursor like proteins) are upregulated during trophic factor withdrawl-induced neuronal apoptosis (43), secreted APPwt counteracts the pro-apoptotic action of mutant presinilin-1 (44), and that secreted APP protects neurons against excitotoxicity (45). In addition, the abnormal cleavage of APP seen in AD induces neuronal apoptosis by activating caspases (46,47). APPmut has also been found to have properties that induce apoptosis. For example, APPmut in contrast to APPwt constitutively activates G_0 (18) and provokes various effects including DNA fragmentation (20). Few studies have examined how mutations in APP or alteration in its signaling pathway counteract or impair specific APP functions. Knowledge about the molecular mechanisms involved in anti-

apoptotic APP signaling may provide insights into the pathogenesis and treatment of AD.

1.2 MEF2 FAMILY OF TRANSCRIPTION FACTORS

1.2.1 MEF2 structure and binding specificity

The myocyte enhancer factor 2 (MEF2) proteins belong to the MADS (MCM1 agamous deficiens serum response factor) family of transcription factors. There are four MEF2 isoforms reported in vertebrates (MEF2A-D) that share a high level of homology (Figure 3). Every isoform contains a MADS domain and a 29 amino acid (aa) MEF2 domain that constitutes approximately the first 100 aa from the N-terminus. These domains are involved binding to the A/T-rich DNA sequence (C/T)TA(A/T)$_4$TA(G/A) (48), and dimerization with other MEF2 family members or b-HLH transcription factors (49). MEF2 family members also contain a transactivation domain at the C-terminus that determines their ability to induce gene transcription. The induction of genes involved in myogenesis (50), myoblast differentiation (51), vascular development (52), and neuronal differentiation (53) have been found to be MEF2 dependent (54).

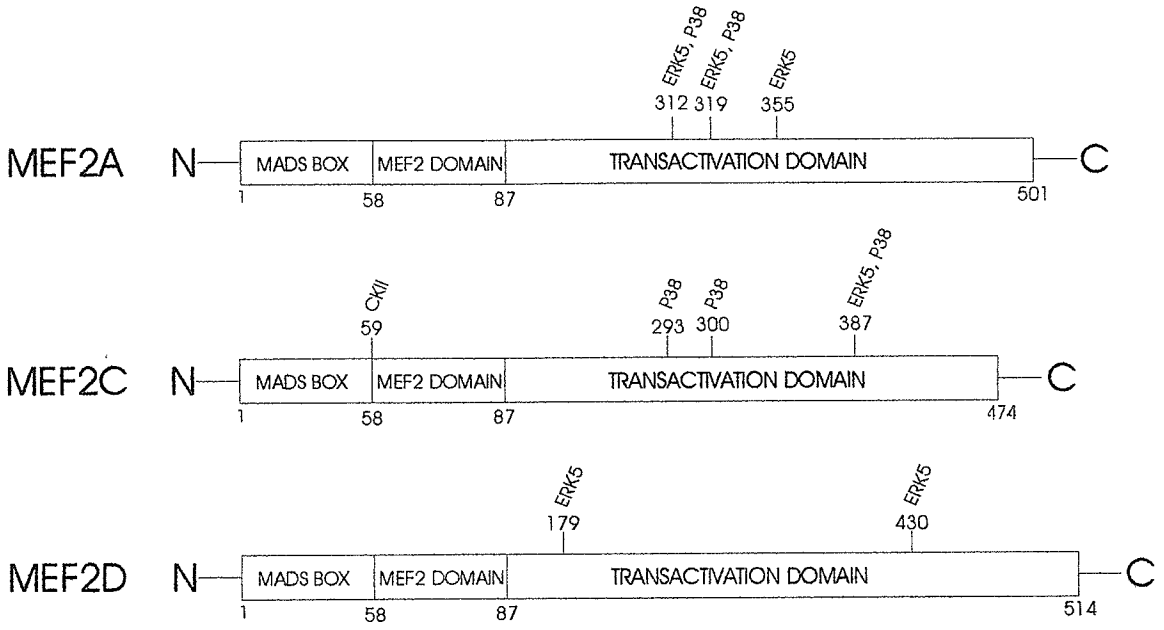

Figure 3. Members of the MEF2 family of transcription factors that are important in muscle differentiation, vascular development, differentation and survival. Known phosphorylation sites on MEF2 family members are identified (numbser indicates the amino acid position). These phosphorylation sites confer an increase in the transactivation potential of MEF2.

1.2.2 Function of MEF2 in muscle cells

The MEF2 family of proteins has been studied most extensively in muscle cells in view of their importance in muscle development (55). MEF2A, -C and -D proteins are detectable in cells from the developing mouse heart at embryonic day 8.5, and their expression then proceeds in a rostro-caudal direction concurrent with somite maturation (55). The essential role of MEF2 in muscle development is demonstrated by creating MEF2C-null mice, which are embryonic lethal due to heart malformation (50). Also, dominant negative forms of MEF2 expressed in myoblasts block myotube formation and differentiation (56, 57), and distamycin A (can out compete MEF2 for its binding to DNA) has been found to inhibit muscle-specific gene expression and myogenesis (58).

There is a proposed mechanism for the role of MEF2 proteins in myogenesis. This is, MEF2 proteins physically interact with myogenic transcription factors from the MyoD family and myogenin to initiate the muscle differentiation program by binding directly to the promoters or enhancers of muscle-specific genes furthermore increasing transcriptional activity (56, 57). The genes that have been identified to be involved in muscle differentiation that are regulated by a MEF2 *cis*-element in the

promoter are: myosin heavy chain in smooth muscle cells (57), troponin I and T genes in cardiac cells (59, 60), muscle creatine kinase (61), myosin light chain 2 in skeletal muscle (62) myogenin (63) (Table 1). MEF2 can also interact with TEF-1 which increases the activity of muscle specific genes and is also expressed in neurons in the development of the nervous system (64).

1.2.3 Function of MEF2 in neuronal cells

MEF2A, -C and -D are highly expressed in neurons located in the central nervous system (CNS), especially MEF2C (65). In cells from developing rat cerebral cortex, MEF2C expression is first detected at embryonic day 17 and peaks around day 21 (66). Increased MEF2C expression is found in the differentiating cells of the cortical plate but is not detectable in the actively dividing neuronal precursor cells that populate the ventricular zone, indicating that MEF2C may play a role in neurogenesis. Further evidence for this is shown by studies that have found that MEF2 has an anti-apoptotic effect on differentiating neuronal cells (67) and mediates neuronal activity dependent cell survival (68). Conversely, apoptosis levels

CELL TYPE		GENES CONTAING MEF2 BINDING SITES	FUNCTION
Muscle-specific	Smooth Muscle	Myosin heavy chain	Components of myosin, which is involved in the mechanics of muscle contraction
	Cardiac Muscle	Myosin light chain 2	
		Muscle creatine kinase	Involved in muscle energy metabolism
	Skeletal Muscle	Troponin T	Involved in calcium-dependent regulation of skeletal muscle contraction
		Troponin I	
		Myogenin	Activates expression of muscle-specific genes such as actin and myosin
Brain-specific	Neuronal	NMDA R1	Component of NMDA receptor, which is important in brain development and memory
		GABA receptor sigma subunits	Component of GABA receptor anion channel important in control of synaptic signaling
		Type II sodium channels	Important in generating charge for initiation of action potential propagation in neuronal signaling
		Neurogranin	Involved in dendritic spine development, learning and memory
		Neurofilament-light chain	Component of neuronal intermediate filaments, which form the primary cytoskeletal component of axons in mature neuronal cells
		Brain-specific creatine-kinase	Involved in brain energy metabolism
		Synapsin II	Modulates synaptic transmission for proper neuronal signaling

Table 1. Genes involved in differentiation and development that are regulated by a MEF2 *cis*-element in the promoter

are increased in cerebral cortical cells and cerebellar granule cells by expressing a dominant negative MEF2.

The mechanism by which MEF2 mediates neurogenesis is thought to be analogous to the model in myogenesis because MEF2 has been found to interact with NeuroD, KW8, neurogenin1, and MASH1 (69), (bHLH transcription factors to activate neural specific promoters (Table 1), leading to neurogenesis (68).

1.2.4 MEF2 dimer composition

Tissue-specific regulation of transcriptional regulatory proteins such as MEF2 is a critical component of cell fate specification and can be accomplished by post-translational control over MEF2 activity. There is evidence that MEF2 protein expression and DNA binding activity is not correlated with the capacity of transcriptional activity, rather there are differences in the composition of the MEF2 DNA binding complex in different cell types that may modulate its *trans*-activational potency. This is observed in the comparison of MEF2 dimer composition between muscle (C2C12) and non-muscle cells (Hela) (70). In differentiating muscle cells MEF2 is primarily found in a MEF2A:MEF2A homodimer, which *trans*-

activates a myosin heavy chain promoter reporter gene with MEF2 sites (PE102CAT), whereas in Hela cells the primary dimer composition is MEF2A:MEF2D which binds to the MEF2 *cis*-element but is inactive (70).

1.2.5 MEF2 responsive genes

1.2.5.1 c-*jun* transcription

The proto-oncogene c-*jun* is an immediate early gene expressed in quiescent cells in response to mitogens such as serum or other growth promoting stimuli. The regulation of c-*jun* transcription is partially due to a MEF2 binding site in the promoter region. Other transcription factors that bind to the promoter of c-*jun* , such as AP-1 and ATF1, are also required for the optimal activation of c-*jun* transcription.

The induction of c-*jun* expression, through AP-1, ATF1 and MEF2 activation is mediated by mitogens or signals from G protein-coupled receptors (71, 72). Evidence for this is shown in studies where serum induced G protein-coupled muscarinic acetylcholine receptor (mAChR) signaling initiated transcription of the c-*jun* promoter via activation of MEF2 (71, 72).

Recently, the regulation of c-jun through mAChRs has been described as the integration of numerous signals transduced by a highly complex network of MAPKs, rather than resulting from the stimulation of a linear protein kinase cascade. The pathways that are activated by mAChR signaling and in turn activate MEF2-dependent c-*jun* transcription are: the ERK5 pathway, and the p38 MAPK pathway (71, 72). Specifically, activation of ERK5, p38α and p38γ kinases induced a significant increase in the expression of c-*jun*. Conversely, mutation of the MEF2 sites in the promoter diminished the stimulatory effects of these kinases, suggesting that the MEF2 responsive element is essential for activation of c-*jun* expression by these kinases. Studies have shown that m1 muscarinic receptor activation leads to MEF2A and -C phosphorylation by ERK5, p38α and -γ, but only p38α and -γ phosphorylated MEF2D, and none of these kinases phosphorylated MEF2B. This increase in phosphorylation in MEF2A and -C increased their ability to stimulate c-*jun* transcription (71,72).

1.2.5.2 N-Methyl-D-aspartate Receptor (NMDA) signaling

The NMDA glutamate receptor is growth factor regulated and plays an important role in normal brain development as well as long term

potentiation (73). The NMDA receptor subunit 1 (NR1) appears to be essential for the receptor function, and its gene contains MEF2 consensus sites in its promoter that bind MEF2C (74). MEF2 binding to the promoter region of NR1 is important in activating transcription because inducing MEF2 binding site mutations abolished 44% of the NR1 promoter activity. This indicates that MEF2 is important in acting with another factor, specifically Sp1 to activate NR1 expression (73). Furthermore, many other neuronal genes that are important in the developing brain have been identified to contain MEF2 and Sp1 sites that regulate their transcription. Some of these include, γ-aminobutyric acid type A (GABA) receptor δ subunits, type II sodium channels, neurogranin, synapsin II, neurofilament-light chain and brain-specific creatine-kinase (73) (Table 1).

1.2.6 Signaling pathways that affect MEF2 transcriptional activity

Recent studies have suggested that expression of the MEF2 proteins and MEF2 DNA binding activity are not always correlated with the activation of MEF2 site-dependent target genes (70, 75). This observation supports the idea that the post-translational modification of these proteins by signaling pathways is an important regulatory step in controlling their

capacity to activate transcription. Further evidence for this is shown by amino acid sequence analysis of the MEF2 proteins, which indicates that they contain numerous putative phosphorylation sites for PKC, caesin kinase II, and MAPK classes of signaling molecules (Figure 4).

1.2.6.1 Mitogen-activated protein kinase pathways

Mitogen-activated protein kinase (MAPK) signal transduction pathways are widespread mechanisms of eukaryotic cell regulation. Each MAPK pathway is preferentially activated by distinct sets of stimuli, acting through different receptor families (tyrosine kinase receptors, and G-protein coupled receptors), thereby allowing the cell to respond coordinately to multiple divergent inputs. In turn, activation of MAPK pathways result in activation of gene transcription, protein synthesis, cell cycle machinery, cell death and differentiation (35).

All MAPK pathways involve a three component module conserved from yeast to humans. These modules include three kinases that establish the sequential activation pathway comprising of a MAPK kinase kinase (MKKK), a MAPK kinase (MKK), and a MAPK. MKKKs are activated by phosphorylation or interaction with small GTP binding proteins such as Ras,

Rac, Cdc42 and Rho. Furthermore, active MKKKs phosphoryate and activate MKKs which then phosphorylate and activate MAPKs. MAPK are proline directed kinases that are activated by concomitant tyrosine and threonine phosphorylation with in a conserved Thr-X-Tyr motif in the activation loop of the kinase domain. Other common principals that MAPK pathways share are, their signaling components are under multiple forms of regulation with more than one biological function. Also pathway organization is mediated by scaffolding proteins, which bind and sequester select MAPK pathway components to permit efficient action in response to specific stimuli.

The mammalian MAPKs are subdivided into five families that are defined as ERK1/2 (insulin/mitogen-regulated extracellular signal-related kinase), JNK (c-Jun NH_2-terminal kinase), p38, and ERK5/BMK1 (big mitogen-activated kinase). Two of these pathways are important in the regulation of MEF2, which are the p38 and ERK5/BMK1 pathways.

1.2.6.2 P38 MAPK signaling

The p38 mitogen-activated protein kinase (MAPK) family has four closely related isoforms (α, β, γ and δ) (76), which are activated via tyrosine

kinase receptors following exposure of cells to environmental stress or by treatment of cells with pro-inflammatory cytokines. The direct intracellular activators of p38 are MKK3 and MKK6. Recent studies have determined that MEF2A and MEF2C are phosphorylated directly by p38α (slightly by p38β) within their trans-activation domain. Specifically, MEF2C is phosphorylated at serine 387, and threonines 293 and 300; and MEF2A is phosphorylated at threonine 312 and 319 (Figure 3)(76, 77, 78). Furthermore, phosphorylation of these sites by p38α and p38β enhances the transcriptional activity of both MEF2A and MEF2C in response to inflammation (76, 79). This provides evidence support to the view that MEF2 is a key downstream effector of mitogenic signaling (Figure 4).

The specificity of p38 MAPK sites is determined by a highly conserved docking domain within MEF2A and MEF2C that confers phosphorylation of a consensus motif (ser/thr-pro) by p38α and p38β. This docking domain is sufficient to confer p38 responsiveness on heterologous substrates and can be functionally replaced by alternative kinase docking motifs from other transcription factors (77).

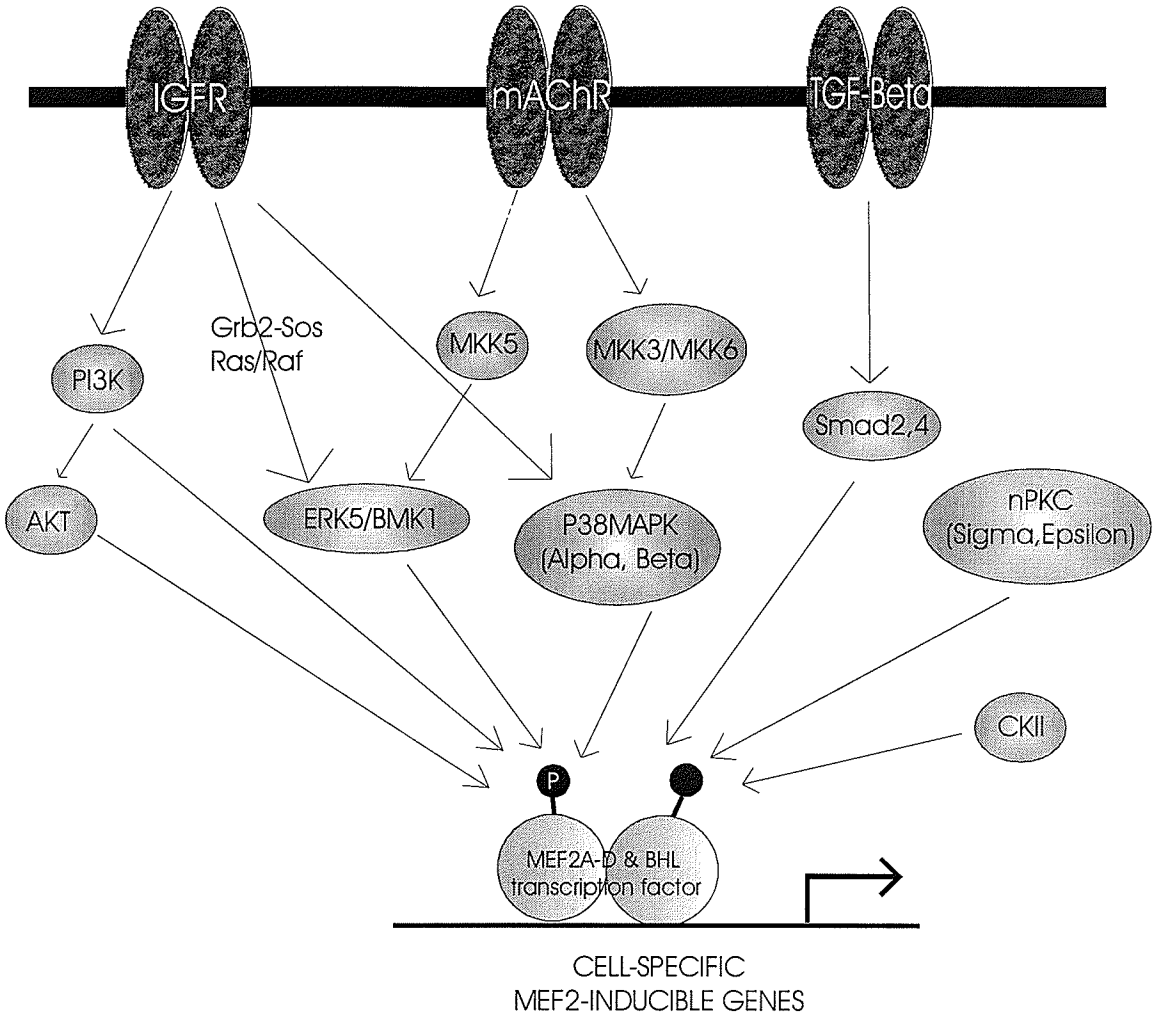

Figure 4. Signaling pathways that affect the phosphorylation state of MEF2 family members. Phosphoryation of MEF2 by these pathways up-regulates MEF2-dependent transactivation of target genes.

Phosphorylation of MEF2 family members by p38 has been linked to the activation of myoblast differentiation and myogenesis through insulin growth factor (IGF) and G protein coupled receptor signaling (51). Myogenesis and myoblast differentiation are initiated by induction of muscle-specific genes, such as muscle creatine kinase (MCK) and myogenin (51). Therefore the p38/MEF2 signaling pathway is postulated to fulfill a dual role during muscle differentiation, being mitogenic at the initial stage of myogenesis and promoting differentiation at a later stage in the differentiation program.

MEF2 phosphorylation by p38 in neuronal cells has been linked to neurogenesis and induces neuroprotective effects. This is shown in differentiating p19 embryonal carcinoma cells, where inhibition of p38α MAPK increased apoptosis levels. This effect could be reversed when cells are transfected with constitutively active MEF2C (67). Furthermore, transfecting p19 cells with MEF2C induced a mixed neurogenic/myogenic phenotype in addition to decreasing the amount of apoptotic cells.

Also, calcium influx into neurons has been shown to induce p38-dependent phosphorylation of MEF2 and increase its trans-activation of target genes, linking the p38/MEF2 pathway to regulation of calcium-dependent survival

in neurons that have made the appropriate synaptic connections during development (66).

1.2.6.3 ERK5/BMK1 signaling pathway

The ERK5/BMK1 pathway is activated by growth factors, oxidative stress, and hyperosmolarity and is required for growth factor-induced cells cycle progression through S phase (80). A yeast two-hybrid screen revealed that ERK5 interacts with amino acids 19-167 of MEF2D (81), and in addition MEF2C and MEF2A immunopercipitated with ERK5. A functional role for MEF2-ERK5 interaction was confirmed by a study that found that ERK5 phosphorylated MEF2A, C and D, (MEF2A phosphorylated on serine 355 and threonines 312 and 319; MEF2D on serine 430) when activated by EGF (Figure 3,4). Furthermore phosphorylation of MEF2A, MEF2C and MEF2D by ERK5 initiated transcription of a MEF2-responsive CAT-reporter gene (81) indicating that ERK5 induces MEF2-dependent gene transcription. Several groups have reported that, in a variety of cell types, MEF2 proteins play a role in growth factor and stress stimulus-induced early gene responses such as c-*jun*, through stimulation from the ERK5 pathway.

This has been the only target gene identified for MEF2 through the ERK5 pathway to date.

1.2.6.4 Protein kinase C (PKC) pathway

The PKC family of serine-threonine kinases participate in vital cellular processes such as growth and differentiation acting as components of several signal transduction cascades initiated by ligand stimulation of transmembrane receptor tyrosine kinases by growth factors (78). Receptors activate phospholipase C, which cleaves phosphoinositides to generate inositol-3-phosphate (IP_3) and diacylglyerol (DAG), then DAG activates PKC in conjuction with intracellular calcium. There are three groups of PKCs: the conventional cPKCs (α, β and γ); novel nPKCs (δ, ε, θ and η); and atypical PKCs (λ, ξ and μ) (78). Novel PKCs (δ and ε) have been found to phosphorylate MEF2A and MEF2C on serine residues in the trans-activation domain in differentiating COS muscle cells. Overexpressing PKCδ and PKCε with MEF2A in COS cells was found to significantly increase the activity of a MEF2 CAT reporter over MEF2A expressing cells, indicating a functional role for the phosphorylation of MEF2 by PKC (Figure 4)(78).

1.2.6.5 Phosphoinositol-3-kinase (PI3-K) Signaling

Insulin-like growth factors (IGFs) have been implicated in the control of skeletal muscle growth and differentiation (82, 83, 84). After myoblasts are withdrawn from the cell cycle, IGFs promote muscle differentiation by inducing the expression or activity of myogenic regulatory factors such as myogenin (involved in executing the differentiation program in myoblasts) through the PI3-K pathway (75, 82).

PI3-K has been found to activate downstream molecules such as protein kinase B (PKB) also known as Akt by converting phosphatidylinositol 4,5-bisphosphate to phosphatidylinositol 3,4,5-triphosphate, which in turn leads to phosphorylation of Akt. Akt has been found to induce muscle-specific transcription and functions as a positive mediator of muscle cell survival (85, 86). In contrast, the ability of myoblasts to differentiate was significantly repressed in cells grown in the presence of the PI3-K inhibitor compared to control conditions (82). Inhibition of PI3-K or Akt also repressed the activity of MEF2C to *trans*-activate a reporter gene, thereby implicating that the PI3-K/Akt pathway induces myoblast differentiation through activation of MEF2-dependent gene transcription. The PI3-K/Akt pathway attenuates this effect by

inducing a change in the phosphorylation state of MEF2 that is independent of MAPK pathways (Figure 4)(75, 82). Akt does not directly phosphorylate MEF2 but there is a possibility that Akt may directly phosphorylate an intermediate co-activator, p300/CBP, which in turn can complex with MEF2 to facilitate transcriptional activation (75).

1.2.6.6 Transforming growth factor β (TGFβ) signaling pathway

Growth factors such as TGFβ exert their effects by inducing an altered program of gene expression through trans-activation of a discrete set of genes important for the regulation of a variety of characteristics, including cell proliferation, extracellular matrix production, inflammatory responses and growth inhibition (87, 88). The properties of TGFβ in mediating such a diversity of cellular responses result from their ability to regulate the expression of a multitude of target genes. TGFβ receptor activation propagates a signal by phosphorylating R-Smads (Smads 1,2,3,5 and 8), which then complex with Co-Smads (Smads-4) and translocate to the nucleus where they control gene expression in a cell-type specific manner (87, 88). It has been recently discovered in C2C12 cells that Smad2 and Smad4 can associate *in vitro* with MEF2A and MEF2C. This interaction

enhances the activity of MEF2A and MEF2C, which is regulated by the TGFβ receptor, determined by a GAL4 activator/reporter assay (88). In addition, the activation of MEF2A and MEF2C by TGFβ stimulation is dependent on their phosphorylation by p38 MAPK, which suggests that there is cross-talk between TGF-β and the p38 MAPK signaling pathways. Furthermore, these results provide evidence that expression of MEF2 proteins may be a key switch in conveying Smad-dependent TGF-β signaling from an inhibitory to a stimulatory differentiation signal in muscle cells (88).

1.2.6.7 Casein kinase-II

Casein kinase-II (CKII) is a protein kinase with many substrates, the majority of which are proteins implicated in signal transduction, gene expression and other nuclear functions. Through these substrates CKII mediates a number of key biological functions, such as RNA synthesis, Wnt signaling, ubiquitination, and cell survival (89).

Studies have found that MEF2C is phosphorylated by casein kinase-II at serine 59, which falls between the MEF2 and MADS domain (Figure 3)(49). The phosphorylation of MEF2C by CKII induces an increase in

MEF2 DNA binding to sites in the MCK promoter (high affinity site) as well as α-MHC promoter (low affinity sites). An increase in MEF2 DNA binding enhances its transcriptional activity possibly through a mechanism whereby phosphorylation of serine 59 induces a conformational change in the MEF2 DNA-binding domain that favors interaction with DNA (49). This increase in binding activity has been shown to be due to phosphorylation because it can be reversed by expressing a mutant MEF2 (with serine 59 mutated to cystine) in cells or by treatment of cells with calf intestinal alkaline phosphatase, which would reduce overall phosphorylation (49).

1.2.7 Activation of MEF2 by calcium signaling

Calcium signaling is important for development and proliferation in neuronal, muscle and T cells. Calcium can activate CaM calmodulin-dependent kinase, calcineurin, PI3-K and p38 MAPK signaling pathways to initiate mechanisms by which cells can react to environmental stimuli. Recent studies have implicated MEF2 as a transcriptional effector of calcium signaling pathways that promote neuronal survival (68), control muscle differentiation and induce apoptosis in T cells.

Calcineurin is a calcium and calmodulin-dependent serine/threonine phosphatase that is activated by the binding of calcium and calmodulin, and is involved in many cellular processes including neuronal excitability (90). The main substrate of calcineurin is nuclear factor of activated T cell (NFAT), a transcription factor, which translocates to the nucleus in response to dephosphorylation by calcineurin to activate gene expression (90, 92). However, recent studies have demonstrated that MEF2 factors are also downstream targets of calcineurin in differentiating myoblasts, neurons and T cells (93).

i) Differentiating muscle cells

The influx of extracellular calcium signals are required for myogenin expression. Drugs that specifically inhibit calcineurin partially inhibit myogenin expression in C2C12 cells (94). Conversely, if calcineurin is activated in C2C12 cells by expression of calcineurin AΔ (constitutively active) MEF2-dependent myogenin expression is increased. Calcineurin also up-regulates slow or oxidative fiber-selective gene promoters in skeletal myocytes through activation of MEF2 with no change in DNA binding (95).

ii) Neurons

Calcium signals in cultured rat cerebellar granule neurons regulate the function of Mef2A through calcineurin. Inhibition of calcineurin and KCl withdrawl led to the hyper-phosphorylation of the MEFA protein, which was associated with an inhibition if MEF2A DNA binding activity and reduced MEF2-dependent reporter gene activity (68). The decrease in MEF2-dependent gene expression was associated with an increase in neuronal apoptosis. In contrast, calcineurin stimulation increased MEF2A DNA binding and transcriptional activity of a CAT reporter gene by dephosphoryation of MEF2A. This may potentiate expression of anti-apoptotic MEF2 target genes, but none have been identified to date.

iii) T-cells

Orphan steroid receptors including Nur77 and have been identified as crucial mediators of T-cell receptor-induced apoptosis through calcium signaling. The calcium-regulated elements in the Nur77 promoter are consensus sites for MEF2, implicating that MEF2 plays a role in the induction of apoptosis of T-cells (Figure 5). In these cells MEF2 is bound to

Cabin1, which affects the transcriptional activity of MEF2 (not DNA binding) because it is a repressor that recruits histone deacetylases (96). When T-cells are stimulated by calcium, calmodulin (CaM) dissociates Cabin1 from MEF2. Calcium also activates calcineurin, which dephosphorylates NFAT allowing its translocation to the nucleus where it increases its ability to bind and activate MEF2, inducing transcription of the Nur77 receptor (97). This effect is opposite to MEF2 signaling in neuronal cells, where it is mainly anti-apoptotic in nature, demonstrating that MEF2 signaling is cell-type specific.

1.2.8 Co-modulators that regulate MEF2 transcriptional activity

Histone acetylation and deacetylation are known to play critical roles in chromatin remodeling and gene expression. The enzymes that carry out these functions are called histone acetylases (HATs) and histone deacetylases (HDACs) respectively. Co-activators of transcription are associated with transcriptionally active regions of the genome, such as p300/CBP, which possesses intrinsic HAT activity. HATs acetylate histone tails, relaxing chromatin by weakening the electrostatic interactions between the positively charged histone tails and negatively charged DNA (93, 98).

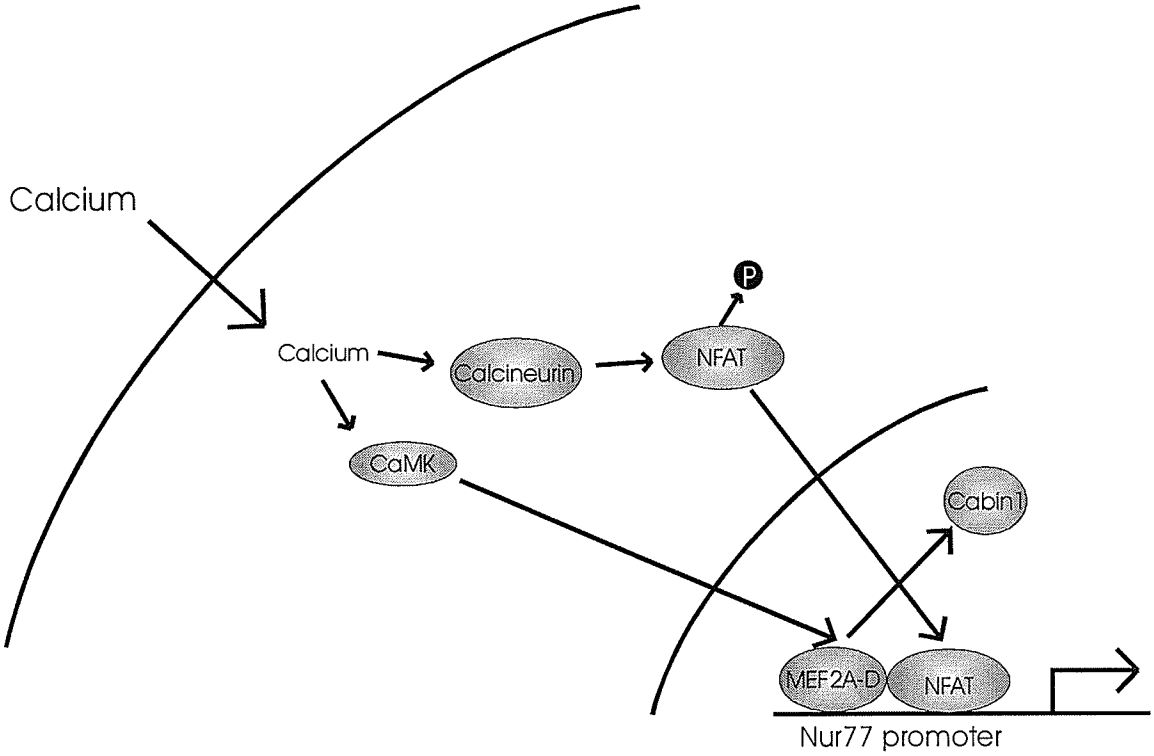

Figure 5. Calcium signaling in T-cells mediates apoptosis through MEF2 transactivation. Two pathways are activated by calcium in T-cells to increase the transcription of the Nur77 receptor, which induces apoptosis when expressed. Calcineurin is activated, which dephosphorylates NFAT to allow its translocation to the nucleus where it can bind to MEF2 to increase transcription of Nur77. Also CaMKIV/II are activated, which dissociates the repressor Cabin 1 from MEF2, activating Nur77 transcription.

Co-repressors recruit histone deacetylases, which repress transcription by deacetylating the N-terminal tails of core histones resulting in chromatin condensation.

1.2.8.1 Co-repressors involved in repression of MEF2 activity

i) Histone deacetylases (HDACs) mediated by Ca^{2+}/calmodulin (CaM)

The mammalian deacetylases belongs to a super-family of evolutionary conserved enzymes, which include HDAC1-7 (98). An 18 aa segment near the amino termini of HDAC4 and –5 (class II histone deacetylases that can deacetylate all four core histones) were found to complex with MEF2 A, -C and –D in 293T cells and this interaction conferred repression of MEF2 transcriptional activity of a reporter gene (99). Furthermore, this interaction occurs spanning the junction between the n-terminal MADS/MEF2 domain of MEF2 (amino acids 39-72) and residues 155-220 of HDAC4 and –5 (98, 100, 101).

HDAC4 expression has been reported to be the highest in skeletal muscle and brain (102), therefore suggesting that HDAC4 may play a role in MEF2-dependent regulation of differentiation (98). MEF2 translocation to

the nucleus depends on a c-terminus 13 aa nuclear localization signal, which is also required for efficient nuclear localization of HDAC4 in muscle cells. Transfected HDAC4 is largely cytoplasmic but when co-transfected with MEF2A or –C causes it to accumulate in the nucleus (103).

In cardiomyocytes, hypertrophic growth in response to serum can stimulate MEF2 trancriptional activity through CaMK and MAPK pathways (99). CaMKIV has been found to activate MEF2 in cardiac hypertrophic heart *in vivo* (2. through overcoming HDAC-mediated repression by dissociating HDACs from MEF2 (Figure 6). The MEF2 binding domain of HDAC overlaps a calcium-dependent CaMK binding domain that has a stronger affinity for HDAC (99). CaMK also stimulates nuclear export of HDAC5 by phosphorylating Ser-259 and Ser-498 and the 14-3-3 binds to these phosphorylated residues and causes nuclear export and therefore another mechanism by which CaMK reduces the amount of HDAC available to bind to MEF2 (104, 105). CaMK and MKK6 signaling were found to synergistically activate MEF2-dependent transcription (99), demonstrating that both pathways are necessary for optimal MEF2 trans-activation. In muscle cells inhibiting CaMKs can partially inhibit myogenin expression (94). It has been found that CaMKI and IV signaling can overcome HDAC-mediated repression of muscle gene expression stimulated by IGF signaling.

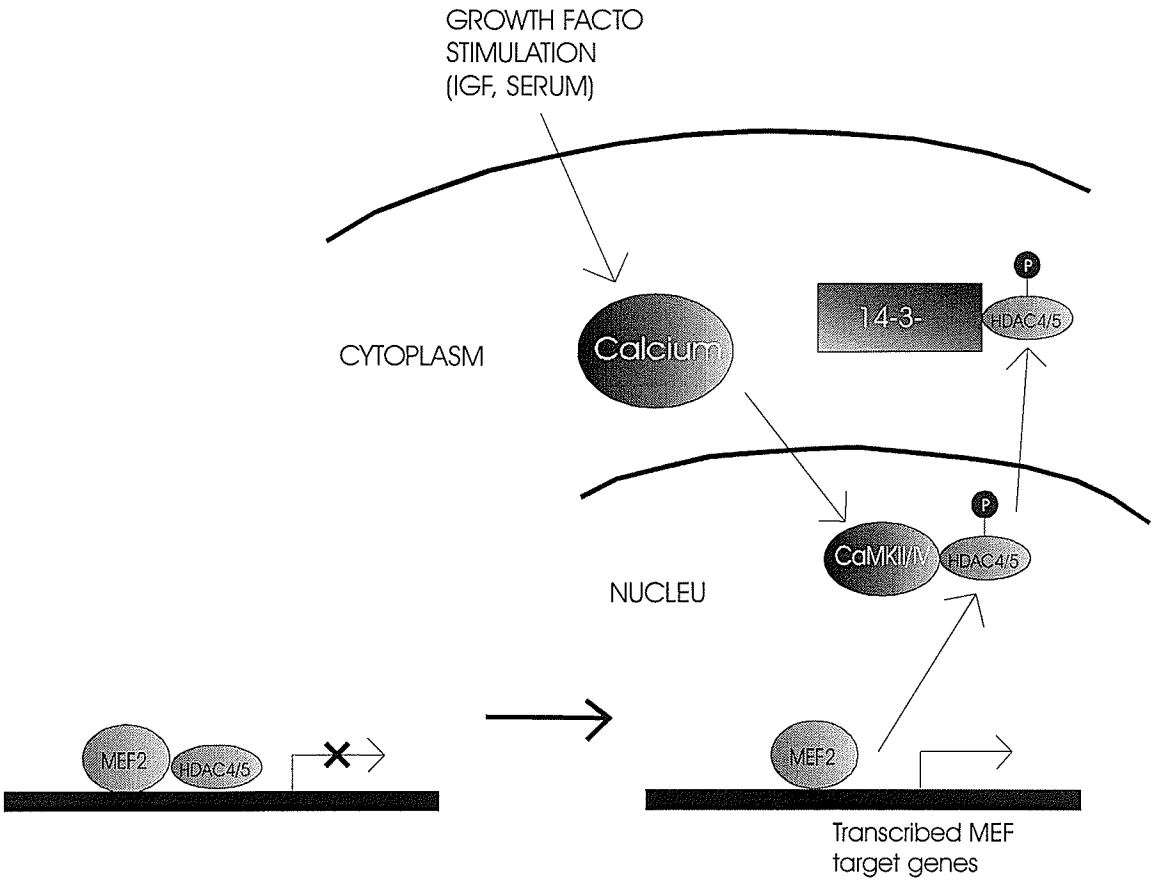

Figure 6. CaMK activates MEF2-dependent gene transcription by dissociating class II histone deacetylases (HDACs) from MEF2. CaMK also phosphoryalates HDAC creating a docking site for 14-3-3 proteins that stimulate nuclear export of HDACs.

Concurrently, the acetylation states of the myogenin promoter was significantly higher in differentiated myotubes compared to myoblasts and therefore establishing that CaMK reduces the activity of HDACs to induce myogenesis (106). Furthermore, HDAC4 and –5 also inhibit myogenesis in 10T1/2 fibroblasts through binding to MEF2, which is abolished when the MEF2 binding region is mutated (106). HDAC4 and –5 were also found to associate with 14-3-3 chaperone proteins. In unstimulated mammalian cells, 14-3-3 efficiently associates with HDAC4, but not HDAC5 (104). CaMK signaling promotes binding of 14-3-3 to HDAC5, and this binding appears to be required for CaMK-dependent disruption of MEF2-HDAC complexes, and can also affect myogenesis in differentiating myoblasts (Figure 6)(104, 107).

ii) Other co-repressors

Other repressors for MEF2 transcriptional activity have been identified, such as Dermo-1, which is a bHLH protein that inhibits transactivational activity of MEF2 by histone deacetylation (108). MITR (MEF2-interacting transcriptional repressor)is another repressor that binds MEF2 and recruits class II histone deacetylases (109). Finally, Cabin 1 is a

calcium dependant repressor of MEF2 in T-cells that recruits mSin3 and histone deacetylases and it competes with p300 for binding to MEF2 (110).

1.2.8.2 Co-activators involved in the repression of MEF2 activity

P300 and CBP are co-activators that are expressed in muscle cells and enhance MEF2C-dependent transactivation as well as MyoD-dependent transactivation of muscle specific genes including myogenin (111). They directly associate with the amino-terminal activation domain of MyoD (111) and the MADS domain of MEF2 and has been found to compete with HDAC4 for the binding to MEF2 (100). These studies implicate that p300, may promote myogenic differentiation by initiating transcription of Mef2 and MyoD responsive genes.

1.2.9 Caspase-mediated degredation of MEF2

MEF2 has been found to regulate neuronal survival and development (53, 65, 66). MEF2C is expressed in the post-mitotic differentiating cerebral cortical neurons and is required for the survival of these neurons (112). MEF2A and MEF2D have also been found to be pro-survival factors with

high DNA binding and transcriptional activity in post-mitotic cerebellar granule neurons (112). These neurons survive by a depolarization-dependent mechanism; therefore lowering extracellular potassium induces phosphorylation of MEF2A and MEF2D, which leads to apoptosis. The stress-induced phosphorylation of MEF2 induces cleavage of MEF2 by a caspase-sensitive pathway to N-terminal MEF2 fragments that lack the transactivation domain. These fragments were purified and it was found that MEF2A was cleaved by caspase-3, -6, -7 and –8; MEF2C by caspase-3 and –7; and MEF2D by caspase-7 at specific residues (Figure 7)(113). These fragments act as dominant-inactive transcription factors and are sufficient to block the pro-survival effects of MEF2A and MEF2D and induce apoptosis in mature cerebellar granule neurons (112).

NMDA stimulation activates neuronal caspase-3 and caspase-7 in cerebrocortical neurons, which cleaves MEF2 and induced apoptosis (113). The cleavage of MEF2 was also observed *in vivo* within 3 hours of the onset of insult in a mouse model of focal middle cerebral artery ischemia/reperfusion (113). This cleavage disrupts the normal pro-survival effects of the p38/MEF2 pathway and contributes to neuronal cells death.

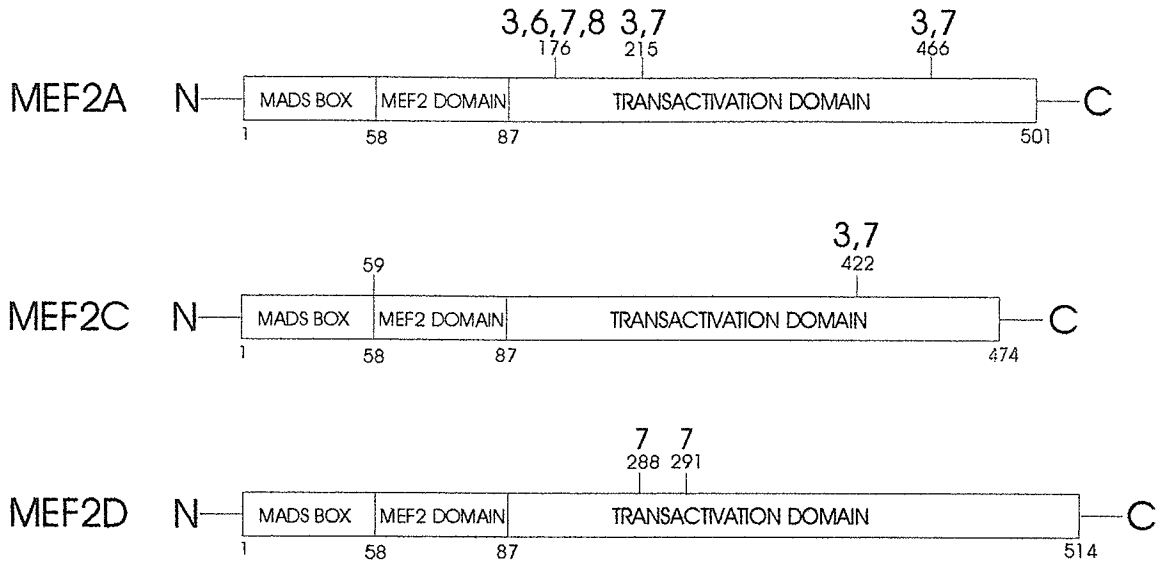

Figure 7. Stress-induced phosphorylation of MEF2 family members in neuronal cells leads to cleavage of MEF2 by a caspase-sensitive pathway. MEF2A, -C and –D are cleaved differentially by caspases 3,6,7 and 8 within their transactivation domains creating N-terminal MEF2 fragments that can act as dominant negative transcription factors. The position of the cleavage sites and specific caspases are indicated by the bottom and top numbers respectively.

2.0 RESEARCH AIMS AND HYPOTHESIS

Alzheimer amyloid precursor proteins (APPs) are conserved and diversely expressed across mammalian species, and mutations in these proteins are linked to familial Alzheimer's disease (FAD). This suggests APP has an important role in the central nervous system. Wild-type APP (hAPP695wt) has been demonstrated to effectively protect against apoptosis in neuronal cells through activating signaling pathways, but the mechanisms of this anti-apoptotic effect remains largely unknown.

Stress activated transcription factors function as critical molecular switches between life and death, and as such play important roles in the aberrant induction of apoptosis in largely irreplaceable cells such as neurons. In this study, we focused on the myocyte enhancer factor 2 (MEF2), a transcription factor that has an anti-apoptotic effect on differentiating neuronal cells and has recently been shown to be necessary for neurogenesis and activity dependent neuronal survival. There are several pathways known to mediate anti-apoptotic MEF2-dependent transcriptional activity in neuronal cells. These include the p38 MAPK and calcium calmodulin-dependent protein kinase (CaMK) pathway. This study investigated the possibility that the anti-apoptotic signaling of APP is mediated in part

through activation of p38 or CaMK signaling pathways to induce the transcriptional activity of MEF2 and lead to inhibition of apoptosis in neuronal cells.

3.0 MATERIALS

3.1 Reagents and chemicals

All chemicals and solvents were of reagent or analytical grade, and were obtained from one of the following sources: Amersham Pharmacia Biotech (Baie d'Urfe, PQ), Bio-Rad Laboratories (Mississauga, ON), Boehringer-Manheim (Laval, PQ), Fisher Scientific (Edmonton AB), Gibco-BRL (Burlington, ON), Sigma-Aldrich (Oakville, ON), VWR Canlab (Mississauga, ON).

Neurobasal-A medium, calf serum, G418, N-2 supplement and other cell culture products were obtained from Gibco-BRL (Burlington, ON). The pharmacological inhibitor SB 202190 hydrochloride (SB) specific for p38 MAPK was from Calbiochem (San Diego, CA). The calcium/calmodulin kinase II (CaMKII) specific inhibitor, KN-93, calf intestinal alkaline phosphatase (CIAP), staurosporine (STS), Hoechst 33258, monoclonal anti-CaMKII antibody and calcium phosphate DNA transfection reagents were purchased from Sigma-Aldrich (Oakville, ON). Digoxigenin (DIG) DNA gel shift kit and *in situ* DNA apoptosis detection kits were from Boehringer Mannheim (Laval, PQ). The chloramphenicol acetyltransferase (CAT)

reporter assay kit and β-galactosidase (β-Gal) enzyme assay system was from Promega (Madison WI). The MEF2 consensus wild type and mutant DNA binding site double stranded oligonucleotides was purchased from Santa Cruz Biotechnology (Santa Cruz, CA). [γ-^{32}P] was purchased from NEN Life Sciences (Guelph, ON).

3.2 Antibodies

The rabbit polyclonal anti-phospho-p38 MAPK, p38 MAPK antibody sampler kit and rabbit polyclonal anti-histone deacetylase antibodies were purchased from Cell Signaling Technology (NEB) (Mississauga, ON), rabbit polyclonal anti-MEF2 antibody (C-21), anti-IgG secondary antibody and goat polyclonal anti-APP antibody (C-20) was from Santa Cruz Biotechnology (Santa Cruz, CA). The anti-mouse and anti-rabbit fluorescence conjugate secondary antibody were purchaced from Amersham Pharmacia (Bai d'Urfe, PQ).

3.3 Expression vectors and reporter constructs

A plasmid encoding the β-gal gene under control of the SV40 early promoter and enhancer, pSVβ Gal was purchased from Promega (Madison WI). Plasmids encoding wild-type human APP_{695} (hAPPwt) and familial Alzheimer disease (FAD) associated V642F substitution (hAPPmut) [25], was kindly provided by Dr. Lennart Mucke. The plasmid pSV2neo was from Clontech (Scarborough, ON). The MEF2A wild type plasmid, (pMT2 hMEF2A), MEF2A dominant negative (DN) plasmid, (pcDNA 1-131) encoding the first 1-131 N-terminal amino acids, DNA binding domain, but lacking the carboxyl-terminal trans-activation domain of MEF2A (amino acids 132-507 deleted), were kindly provided by Dr. John C. Mcdermott. The MEF2A DN plasmid was tagged with GST fusion protein to ascertain its expression in transfected cell lines. The MEF2A DN plasmid is capable of binding specifically to the MEF2 *cis*-element and can abrogate trans-activation by MEF2wt [26]. The plasmid pcDNA3.1 (Invitrogen, Hornby ON) was used in co-transfections with plasmids lacking marker genes. The MEF2 CAT reporter expression plasmid (pMRE2wt-CAT) consisted of the CAT reporter gene driven by two copies of MEF2 consensus wild-type

binding sites upstream of the minimal thymidine kinase (TK) promoter, was kindly provided by Dr. Micheal E. Greenberg.

3.4 Equipment

The following equipment was used for the experimental methods carried out in this study: Biochrom Novaspec II spectrophotometer, Fisher Scientific Accumet Basic pH meter, Mettler Toledo AG104 balance, Eppendorf 5317C centrifuge, IEC Centra CL3R centrifuge, Beckman J2-HS centrifuge, Beckman TL-100 ultracentrifuge, Beckman LS6500 scintillation counter, E-C apparatus Corporation EC250-90 power supply, VWR Scientific 2300 incubator, Bio-Rad Mini-PROTEAN3 gel electrophoresis equipment, Bio-Rad PROTEAN II xi electrophoresis equipment, Bio-Rad Trans Blot electrophoretic transfer apparatus, Coulter 2169 flow cytometer, Zeiss LSM5 Pascal fluorescence microscope and Pentax TX100 35mm Camera.

4.0 EXPERIMENTAL METHODS

4.1 Cell culture and treatment

B103 cells lacking expression of endogenous APP and APP-like proteins (40) were kindly provided by Dr. Lennart Mucke, and were maintained in Dulbeco's modified Eagles Medium containing 10% fetal bovine serum and 5% horse serum at 37°C in a 5% CO_2 humidified atmosphere. After transfections in the undifferentiated state, cells were washed with serum free medium and cultured in Neurobasal A- medium containing N-2 supplement for differentiation as described previously (40). The N-2 supplement is an optimized serum substitute currently used routinely for the long-term growth and survival of primary neurons and differentiated neuroblastomas, without the need for exogenous growth factors. After 72 h, cytosine arabinoside (10 μM) was also added to differentiating cultures to limit the growth of undifferentiated cells. Differentiated B103 cells were exposed to 5 μM STS for 5 h (STS was diluted in differentiation medium), or 5 μM KN-93 or 2.5 μM SB for specified periods. Both KN-93 (specific CaMK inhibitor) and SB (specific p38 MAPK inhibitor) were diluted in dimethyl sulfoxide (DMSO) as the

carrier solvent (vehicle). In this study, all experiments were performed on differentiated B103 cells under the above conditions, unless otherwise specified.

4.2 Measurement of *in vitro* cytotoxicity

The *in vitro* toxicology assay kit, based on the reduction of 3-[4,5-dimentylthiazol-2-yl]-2-5-diphenyl tetrazolium bromide (MTT) to purple formazan by mitochondrial dehydrogenase activity, was used to determine cell survival in a colorimetric assay according to the manufacturer's instruction, Sigma-Aldrich (Oakville, ON). Cells were seeded in individual wells, 2×10^4 cells in 100µl of medium in each well, and cultured for 2 days at 37°C. The medium was then replaced with test medium under specified conditions. Microtitre plates containing 96 wells were cultured at appropriate time intervals after which the viability of the cells were determined by the MTT assay. Briefly, a stock solution of MTT (5 mg/ml) was added to the wells containing cells at 0.5 mg/ml, after first removing additives and medium. The plates were then incubated for 3 h at 37°C in 5% CO_2. Fifty microlitres of liquid was aspirated, leaving a total volume of 50µl in each well. The MTT formazan formed was solubilized by propanol.

The absorbency at 560 nm was measured and background values subtracted before conversion to percentage values relative to controls.

4.3 Western Blotting

Differentiated B103 cells under appropriate conditions were harvested, washed in chilled phosphate buffered saline (PBS) pH 7.4, resuspended in lysis buffer containing 20 mM Hepes, pH 7.4, 100 mM NaCl, 100 mM NaF, 1 mM sodium orthovanadate, 5 mM EDTA, 0.1% Triton X-100, and protease inhibitor cocktail (1 mM PMSF, 10 μg/ml aprotinin, 10 μg/ml leupeptin, 10 μg/ml pepstatin). Lysates were centrifuged at 10,000 *g* for 5 min at 4^0C. The resulting supernatant was collected and the total protein concentration was determined by using the micro bicinchoninic acid (BCA) assay (Pierce, Rockford Il). Samples were boiled for 3 min in SDS sample buffer (62.5 mM Tris HCl, pH 6.8, 2% SDS, 10% glycerol, 50 mM DTT and 0.1% v/v bromophenol blue). The protein samples were fractionated by SDS-PAGE with the use of 15% acrylamide gel, and the separated proteins were transferred to nitrocellulose membranes. Membranes were incubated in 20 mM Tris-buffered saline, pH 7.6, 0.2% v/v Tween 20 (TBS-T) with 5% w/v non-fat dried milk for 1 h, washed in TBS-

T (3 x 5 min), and incubated for 1 h with primary antibody in TBS-T containing 1% milk at room temperature for non -phosphospecific antibodies and overnight at 4°C for phosphospecific antibodies. The following dilutions were used for individual antibodies against different proteins: APP (1:1000); HDAC5 (1:1000); MEF2 (1:200); CaMKII (1:1000); p38 MAPK (1:1000); and phospho-p38 MAPK (1:1000). After further washes in TBS-T, membranes were incubated for 1 h with horseradish peroxidase-linked anti-IgG secondary antibody. The immunoreactive protein bands were detected by enhanced chemiluminescence (ECL) (Amersham Pharmacia, Baie d'Urfe PQ) as described by the supplier. Quantitative analysis of protein levels was performed by densitometric scanning of the autoradiograms with the Bio-Rad quantity one software, and each protein blot is representative of at least three independent experiments. The identity of the phosphorylated form of MEF2 was determined by incubating protein extracts that are diluted in alkaline phosphatase buffer (1 M Diethylenetriaminepenta acetic acid, 0.5 mM $MgCl_2$, pH 9.8) (10X), with 3 units of calf intestinal alkaline phosphatase (AP) for 15 min at 30°C, followed by Western blot analysis.

4.4 Immunostaining

Cells plated on cover glass slides were allowed to differentiate in serum free N-2 supplemented Neurobasal A- medium for at least 72 h. The cell culture medium was aspirated and cells washed with cold PBS with Ca^{2+} and Mg^{2+} (3 times). Cells were fixed for 15 min in 4% paraformaldehyde at 4°C and then blocked with 5% goat serum in PBS, washed with cold PBS once, permeabilized in PBS containing 0.1% Triton X-100 for 15 min at 4°C. Following three washes in PBS, cells were incubated with primary antibodies (anti-APP, and anti-MEF2) diluted in PBS containing 1% BSA for 2 h at room temperature. After three washes in PBS, cells were incubated with goat anti-mouse or anti-rabbit fluorescence conjugate secondary antibody (1:200) (Amersham Pharmacia, Baie d'Urfe PQ) for indirect immunofluorescence analysis and washed in cold PBS. For nuclear staining, cells were incubated with 20 μg/ml of Hoechst 33258 dye in PBS for 5 min, washed and mounted with ProLong anti-fade (Molecular Probes, Eugene OR). Images were collected with a Zeiss epifluorescence microscope.

4.5 Image analysis

Images were collected with Zeiss epifluorescence microscope equipped with a charge couple camera device, and Adobe Photoshop was used for presentation of the images. Image processing and quantification of nuclear fluorescence was carried out using the Image Pro Plus software (Media Cybernetics, USA). MEF2-positive and negative nuclei (after subtraction of the background) were then counted in several randomly selected fields from at least three different coverslips (>300 cells). Investigators were blinded to the types of cell cultures, STS treatments and transfections that were performed. To analyze the images, nuclear area of randomly selected control cells (untreated) was calculated from the segmented Hoechst image. This area with Hoechst image was defined as representing a cell. A segmentation area from the cell with minimal FITC intensity will then be reduced until a pixel with zero intensity was achieved. This was considered to be the background signal for MEF2 staining and was subtracted from all FITC images defined within the average nuclear area. FITC value of 0.0 thus denotes negative MEF2 fluorescence and value more than 1 represents a positive MEF2 immunoreactivity. These values were only integrated, if the MEF2 image was within the defined nuclear area of

Hoechst image. This was necessary to remove bias of different intensity of partial or predominantly MEF2 immuno stained nuclei. Negative FITC indicate loci that appear to be located outside of the visible limits of the Hoechst image due to improperly defined cells. In practice, because of variation in actual nuclear sizes, values of FITC were normalized using spatial coordinates. To assess the reproducibility of this method of analysis, the same set of 50 images, were analyzed independently by two different observers. This image analysis took into consideration both the number of nuclei, MEF2 positive nuclei and FITC intensity (MEF2 immunoreactivity) per nuclei above background levels. The results that were tested by one-way analysis of variation, showed that the component of variance between the inter territory position of FITC values in nuclei of different transfected cell populations was not significantly greater than the variance between intra territory positions within each transfected cell type.

4.6 p38 MAPK activity assay

p38 MAP kinase activity was measured using the non-radioactive immunoprecipitation p38 MAPK assay reagents, according to the supplier's instruction. Briefly, the cell pellets were resuspended in lysis buffer (20 mM

Tris, pH 7.5, 150 mM NaCl, 1 mM EDTA, 1 mM EGTA, 1% Triton, 2.5 mM sodium pyrophosphate, 1 mM 3-glycerolphosphate, 1 mM Na_2PO_4, 1 μg/ml Leupeptin), and then 200 μg of total protein was immunoprecipitated with 20 μl of resuspended anti-p38 MAPK antibody conjugated to protein A. The immunoprecipitates were washed thoroughly with lysis buffer and then with kinase reaction buffer (25 mM Tris, pH 7.5, 5 mM 3-glycerolphosphate, 2 mM DTT, 0.1 mM Na_2PO_4, 10 mM $MgCl_2$). The kinase reaction was assayed by incubating the immunoprecipitate in kinase reaction buffer supplemented with 200 μM ATP and 2 μg GST-ATF2 (codons 19-96) fusion protein for 30 min at 30°C. The reaction was terminated with 25 μl of 3 x SDS sample buffer, boiled for 5 min, vortexed, and then centrifuged for 2 min. The reaction products were separated by SDS-PAGE on a 12% gel and blotted onto nitrocellulose membrane. The extent of phosphorylation of ATF-2 at Thr 71 was measured by Western blotting using a phospho-ATF-2 (Thr 71) specific antibody, while control for loading of total protein was measured by reprobing the filter with anti-p38 MAPK antibody.

4.7 CaMKinase II activity assay

CaMKII activity was determined by using the CaMKII assay kit (Upstate Biotechnology, Lake Placid NY) according to the supplier's instructions. The assay kit is designed to measure the phosphotransferase activity of CaMKII in crude cell lysate and is based on the phosphorylation of the specific substrate peptide (KKALRRQETVDAL) by the transfer of γ-phosphate of ATP by CaMKII. Briefly, cell lysates (200 µg of total protein) were added to 10 µl inhibitor cocktail (This cocktail blocks the activity of other serine/threonine kinases such as PKA and PKC), [γ-^{32}P]ATP (3000 Ci/mmol) diluted to 1 µCi/µl with Mg^{2+}/ATP mixture and incubated for 10 min at 30°C. 25 µl of reaction aliquots were spotted onto P81 phosphocellulose paper to separate the phosphorylated substrate from the residual [γ -^{32}P]ATP. The assay square papers were washed three times with phosphoric acid (0.75%), and once with acetone. The cellulose papers were then transferred to a scintillation vial with scintillation cocktail and read in a scintillation counter. The specific activity of CaMKII was calculated as pmol of phosphate incorporated into CaMKII substrate peptide/min/1 µg of enzyme.

4.8 Preparation of nuclear extract

Cellular protein extracts under the appropriate conditions were prepared using the Nu-clear Extraction Reagents (Sigma-Aldrich, Oakville ON) based on methods described previously (114). All the steps in this procedure were carried out at 2-4°C. Using pre-cooled buffers after the indicated times, cells were harvested with 0.3% trypsin phosphate buffered saline, centrifuged at 450 *g* for 5 min. The packed cell volume (PCV) was estimated. 500 µl (5 x PCV) of lysis butter (100 mM Hepes, pH 7.9, 1.5 mM $MgCl_2$, 100 mM KCl) and DTT (0.1 mM) was added to 100 µl of packed cells. The cell pellet was gently resuspended in this lysis buffer, taking care to avoid foaming and incubated on ice for 15 min. Thirty-six µl of 10% IgePal CA-360 was added to the swollen cells in Lysis buffer, to a final concentration of 0.6% and vortexed vigorously for 10 sec. This was followed by centrifugation for 30 sec at 11,000 *g*, and the resulting supernatant transferred to a fresh tube. This fraction is the cytoplasmic lysate. Meanwhile, 1 µl of 0.1 M DTT and 1 µl of protease inhibitor cocktail were added to 98 µl of high salt nuclear extraction buffer (20 mM HEPES, ph 7.9, 10 mM $MgCl_2$, 0.42 M NaCl, 0.2 mM EDTA, 25% v/v glycerol). The resultant crude nuclei pellet was resuspended in 70 µl (2/3 x PCV) of

the above extraction buffer. The tubes were placed on a vortex mixer and agitated at medium speed for 30 min, centrifuged for 4 min at 21,000 *g*. The resulting supernatants (nuclear extracts) were snap-frozen as aliquots in liquid N_2 and stored at -70°C until ready. The extracts were quantified for protein concentration by the BCA method.

4.9 MEF2 DNA binding activity assay

Electrophoretic mobility shift assay (EMSA) was performed using digoxigenin (DIG) Gel Shift Kit (Boehringer-Mannheim, Laval PQ) according to the manufacturer's instruction. The nuclear extracts from the B103 hAPP wt/mut or mock transfectants were washed and tested to avoid contamination with cytoplasmic proteins. As the optimal MEF2 binding site sequence (*cis*-element), a double-stranded consensus oligonucleotide binding site for MEF2 transcription factors: 5'- GAT CGC TCT AAA AAT AAC CCT GTC –3' (MEF2 binding site underlined); for the control binding site the corresponding MEF2 mutant binding site oligomer 5`-GAT CGC TGT AAA CAT AAC CCT GTC -3`(C ⇒ G and A ⇒ C substitutions underlined) was used. Both MEF2 wt and mutant oligomers were purchased from Santa Cruz biotech (Santa Cruz, CA). The oligomers were DIG 3`-end

labeled with terminal transferase in a final volume of 20 µl containing 4 µl labeling buffer (5 x concentration), 4 µl $CoCl_2$ solution, 1 µl annealed oligonucleotide (100 ng/l), 1 µl DIG-11-ddUTP and 1 µl terminal transferase and incubated for 15 min at 37°C. A typical binding reaction contains 10 µg of nuclear protein, 0.3 ng of DIG labeled probe, 1 µl of deoxyinosine-deoxycytidine (dIdC) in 25 µl total volume. Samples were incubated for 15 min at room temperature. The protein-DNA complexes were analyzed on a 7% native (non-denaturing) polyacrylamide gels containing 3% glycerol and 0.25 x TBE (1.0 M Tris borate, 1 mM EDTA) in cold-room. After electrophoresis, the gels were transferred on to positively charged nylon membranes by contact blotting, followed by UV cross-linking of protein-DNA complexes onto the nylon membranes. The blotted membranes were processed for chemiluminescent detection and exposed to X-ray film.

4.10 Stable tranfections

B103 rat neuroblastoma cells were plated in a 10 cm dish at a density of 2 x 10^5, 24 h before transfection. Then 25 µg of the hAPPwt/mut expression vector (pCMV hAPP695wt/mut) and 1 µg of the neomycin resistant gene expression vector (pSVneo/pcDNA3.1) were co-transfected

by calcium phosphate precipitation, according to the supplier's instructions (Sigma-Aldrich, Oakville ON). In mock transfections, only the neomycin resistant gene expression vectors (without cDNA inserts for APP/MEF2A) were used. After 72 h, the cells were trypsinized and seeded onto tissue culture dishes (at 1:10 dilution). The transfected cells were selected by exposure to 400 µg/ml G418-containing medium. The selection medium was changed every 3 days. Expression levels of hAPP in stably transfected B103 cell lines were ascertained by Western blot analysis. For the establishment of B103 hAPPwt/mut cells stably expressing MEF2A wt/DN, hAPPwt/mut cells were transfected with 24 µg of an expression vector encoding MEF2Awt (pcDNA MEF2A) or MEF2A DN construct (pcDNA-131). The transfected cells were selected by exposure to 400 µg/ml G418. Stable clones expressing the MEF2A wt/ DN were ascertained by western blot analyses.

4.11 Transient transfections and reporter gene expression assays

B103 hAPPwt/mut and mock (vector only) stable cell lines were transiently transfected by the calcium phosphate precipitation method. For transfection experiments, the stable cell lines were seeded at a density of 2.5

x 10^5 cells in six well plates a day in advance. Transfections were performed in triplicate with 5 μg of MEF2 x 2 DNA binding sites (2 copies) CAT reporter gene and 1μg of pSVβ-Gal as an internal control for transfection efficiency. Cells were kept in normal culture media for at least 24 hours before being transferred into differentiation medium for another 48 hours. Finally, cells were washed with PBS, pH 7.4 and resuspended in reporter lysis buffer. The activities of β-galactosidase were measured using the β-Gal enzyme assay system (Promega, Madison WI) with o-nitrophenyl-β-D-galactopyranoside as the substrate. The cell extracts were incubated at 60°C for 10 min to inactivate endogenous deacetylase activity. CAT assays were performed using the CAT assay kit containing n-butyryl as substrate, according to the manufacturer's instructions (Promega, Madison WI) based on the method described previously (115). The butyrylated and non-butyrlyated chloramphenicol were separated by thin layer chromatography (TLC) and the their optical densities measured and were also quantified by liquid scintillation counting. The CAT activities were normalized to the corresponding β-gal activity.

4.12 Apoptotic assays

Apoptosis induced by 5 μM staurosporine for 5 hours in B103 stable transfectants were assessed by nuclear fragmentation using the cell death detection kit, according to the supplier's instruction. (Boehringer Mannheim, Laval PQ). Nuclear fragmentation was detected by *in situ* labeling with the terminal deoxynucleotidyl transferase mediated UTP-end labeling (TUNEL) assay. Briefly, cells in 6 well plates were fixed with 4% freshly prepared paraformaldehyde solution in PBS for 30 min at room temperature. Fixative was removed and cells were washed once with PBS and incubated with fluorescein labeled dUTP and terminal deoxynucleotidyl transferase for 60 min at 37°C in a humidified atmosphere in the dark. After three rinses with PBS, cells were resuspended in PBS to a final volume of 800 μl and analyzed by flow cytometry to determine the percentage of apoptotic cells.

4.13 Statistical analyses

Data were analyzed using the Stat View J5.0 software. Non-parametric Friedman analysis of variance for related samples was used to evaluate differences between sample repetitions within each transfected cell

line. Differences in nuclear MEF2 level before and after STS treatment for different transfected cells were assessed by χ^2 tests for independent samples using the average scores for control (mock transfected) and for each individual transfected cell culture. The control cells were not different from each other and, to minimize the number of comparisons, data from the control cells were pooled for comparison with data from the transfected cells. To correct for multiple comparisons, the experiment wise error was set $\alpha = 0.05$ and the comparison wise error at $\alpha' = 0.06$. Densitometry data of Western blots were analyzed by ANOVA, followed by Fisher's post-hoc tests for comparisons. Results are expressed as means ± standard error of the mean (SEM), and values of n indicate the number of independent experiments. $P < 0.05$ was considered significant.

5.0 RESULTS

5.1 Expression and distribution of wild type and mutant human APP in stable transfected B103 cells.

To assess the role of the myocyte enhancer factor 2 (MEF2), a 59 kDa protein, in the anti-apoptotic APP signaling, we transfected mock, wild type and FAD-mutant human APP into rat neuroblastoma (B103) cells. These cells are useful for comparing specific functions of wild type and mutant hAPP without interference by rodent APP, because they lack expression of endogenous APP and APP-like proteins. Wild type (MEF2A wt) and dominant negative MEF2A (MEF2A DN) were also expressed in these cells to enhance and block endogenous MEF2-DNA transcriptional activity respectively, and how this affected anti-apoptotic APP signaling. B103 cells share many typical neuronal properties with other commonly used APP-expressing neuronal cell lines, including outgrowth of neurites upon differentiation, synthesis of neurotransmitters, possession of neurotransmitter receptors and electrical excitability of surface receptors (116).

B103 cells were stably transfected with hAPPwt, hAPPmut or plasmid containing the CMV promoter, but no cDNA insert (mock). Western blot analysis was used to determine the expression levels of APP, and the results showed that APP expression levels in hAPPwt and hAPPmut expressing cells were similar (Figure 8a). Mock-transfected cells did not show any APP expression, serving as a negative control for the APP-deficient B103 cells. The endogenous expression of APP in human brain homogenate was used as a positive control for the APP_{695} isoform. The exogenously expressed hAPPwt and hAPPmut in these cells migrated with a similar molecular weight (98-110 kDa) as the endogenously expressed APP_{695} in human brain extract (Figure 8a). Indirect immunofluorescence analysis also showed that hAPPwt and hAPPmut had a similar intracellular distribution pattern in transfected B103 cells; APP immunoreactivity was detectable in the soma and neurites but not in the nucleus (Figure 8b). This expression pattern closely resembles the distribution of endogenous APP observed in untransfected primary neurons (40). Furthermore no cytotoxicity was associated with either wild type or mutant hAPP expression (Figure 8c).

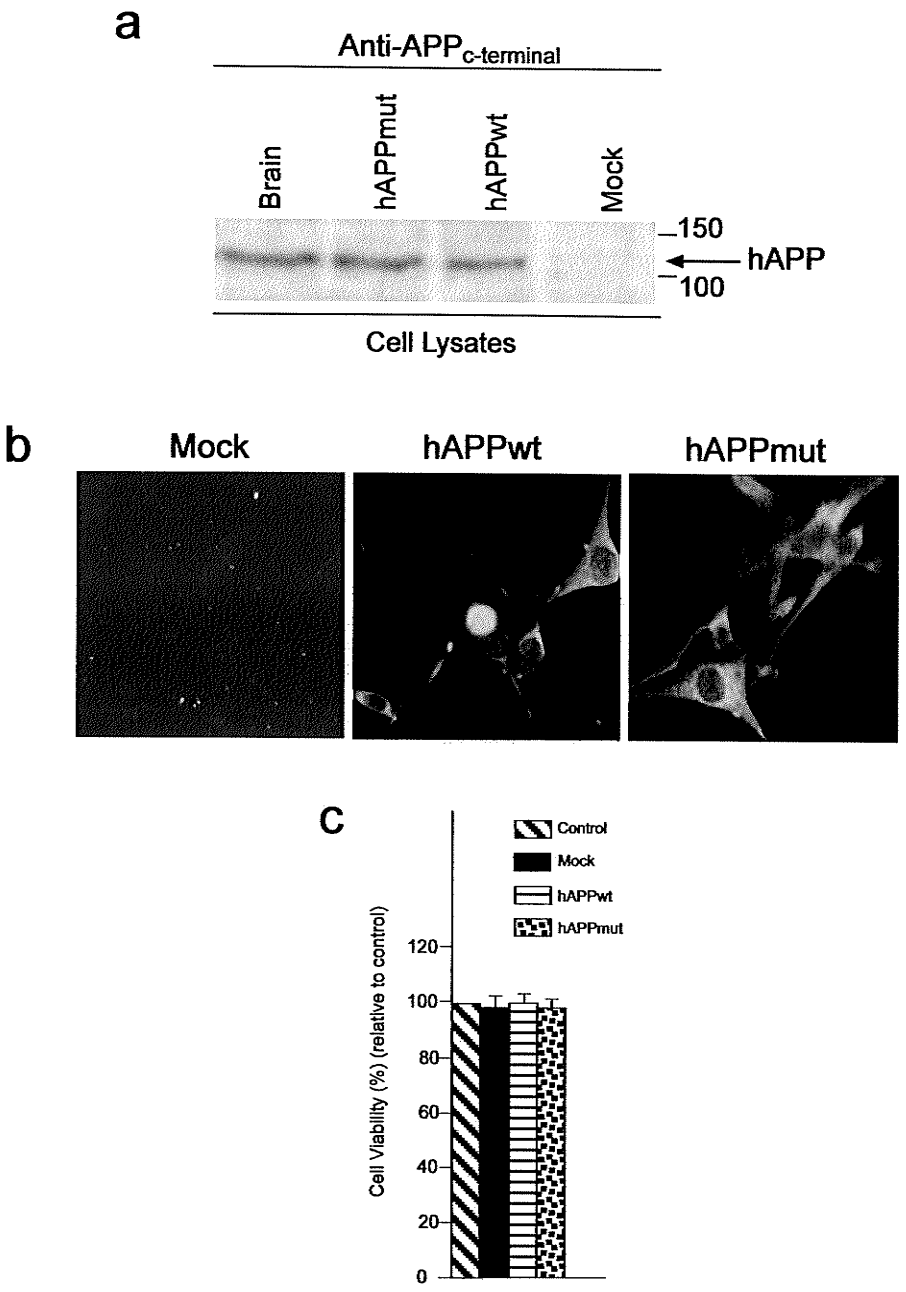

Figure 8. Stable expression of hAPPwt and hAPPmut in B103 cells. (a) Western blot analysis of APP expression in B103 cells transfected with hAPP695wt (hAPPwt), FAD-hAPP695mut (hAPPmut), or plasmid containing the CMV promoter but no cDNA insert (Mock). Positive control: human brain homogenate. APP was detected with anti-APP c-terminus antibody that, cross reacts with human and rodent APP (b) Similar intracellular distribution of hAPPwt and hAPPmut after transfection of B103 cells (epiflourescent images of anti-APP c-terminus immunostaining; x 40). (c) Determination of cell viability. Control (untransfected) and transfected cells were plated at 2.5×10^3 and cultured to 75% confluency. The extent of cell viability was measured by the MTT assay.

These results suggest that, differentiated rat neuroblastoma B103 cells may be useful as a neuronal cell line for *in vitro* studies to manipulate the expression of APP.

5.2 Expression of wild type but not mutant hAPP differentially maintained MEF2 in the phosphorylated state.

As all MEF2 family members are highly expressed in the CNS, we examined the expression levels of endogenous MEF2. Western analysis indicated that all four members of the MEF2 superfamily of transcription factors were present in differentiated B103 cells. However MEF2A and MEF2C were highly expressed, whereas only minimal levels of MEF2B and markedly reduced levels of MEF2D were observed. There were at least two major species of MEF2 proteins detectable in these cells, the faster and slower migrating bands at the expected molecular weight range for MEF2 proteins (56-60 kDa) (Figure 9a). To determine if hAPPwt or hAPPmut expression affects the expression level of MEF2 proteins, we examined the endogenous MEF2 expression levels by Western blot analysis of total cell lysates extracted from B103 cells transfected with mock, hAPPwt or hAPPmut probed with an anti-MEF2 antibody (C-21) that is reactive with

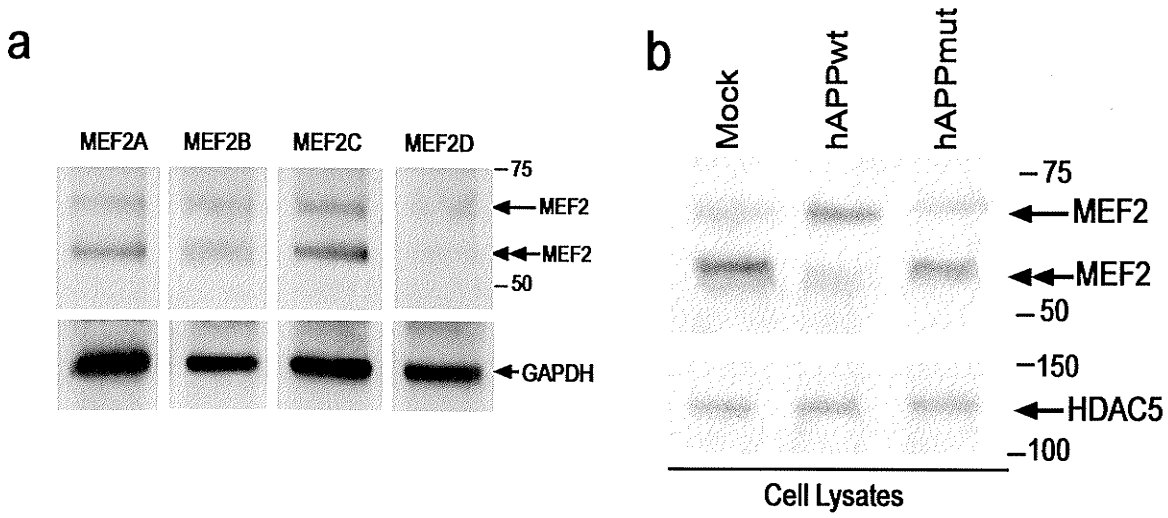

Figure 9. Characterization of MEF2 expression in B103 cells.

(a) Cellular protein extracts from differentiated B103 cells were separated by SDS-polyacrylamide gel electrophoresis (PAGE), and the immunoblots were probed with rabbit polyclonal anti-bodies against the MEF2 family of transcription factors. (b) Whole cell lysates were prepared from B103 cells stably transfected with hAPPwt, hAPPmut and mock plasmids. Protein extracts were separated by SDS-polyacrylamide gel electrophoresis and immunoblots were probed with rabbit polyclonal anti-MEF2 antibody.

MEF2A, -C, and -D. In these transfectants the two major migrating bands of MEF2 were observed. However, there was a significant increase ($P < 0.03$, $n = 5$) in the relative levels of the MEF2 slower migrating band of 9 ± 0.2 in hAPPwt compared with mock and hAPPmut expression with relative levels of the MEF2 slower migrating band of 3 ± 0.4 and 2.8 ± 0.3 respectively. In contrast, the relative levels of the MEF2 faster migrating species in hAPPwt was markedly lower (by 3 fold) compared with mock and hAPPmut (Figure 9b). MEF2 has been previously determined to be post-translationally modified by phosphorylation resulting in two major migrating species (76,78), therefore, we tested the possibility that the slower migrating band was the phosphorylated form of MEF2. To this end, cellular protein extracts from mock, hAPPwt, and hAPPmut cells were treated *in vitro* with calf intestinal alkaline phosphatase (AP), which dephosphorylates proteins. Treatment of cell lysates with AP reversed the mobility of MEF2 from slow to fast migration without change in the molecular weights of the MEF2 species. The slower migrating band of MEF2 in mock, hAPPwt and hAPPmut expressing cells disappeared after AP treatment, with a corresponding increase in the levels of the faster migrating bands (Figure 10a). These data demonstrate that the two major species of MEF2 that are visualized are largely, if not totally attributable to differential

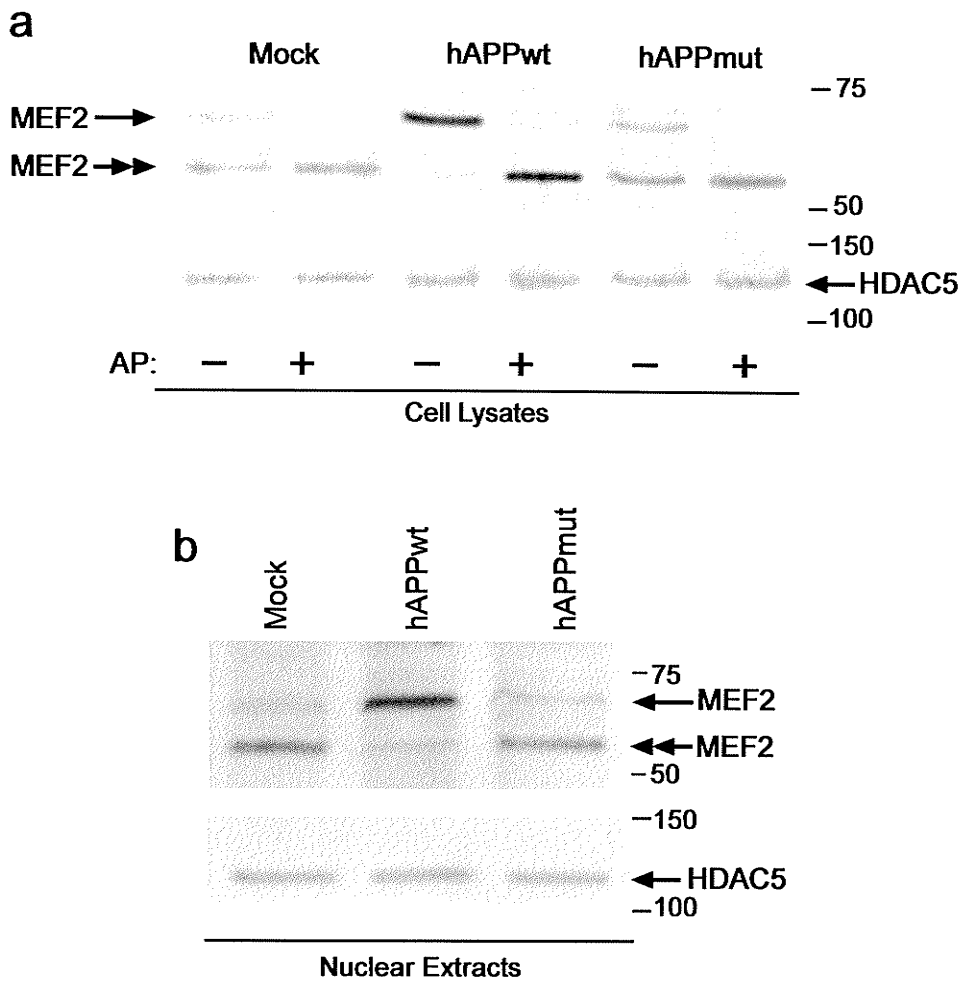

Figure 10. Phosphorylation state of total and nuclear MEF2 proteins in APPwt and APPmut cells. (a) Western blot analysis of MEF2 in cell lysates. Lanes labeled AP represents the treatment of protein extracts with calf intestinal alkaline phosphatase (AP). Double and single arrows indicate the position of MEF2 before (-) and after (+) AP treatment respectively. The identity of the slow migrating bands as the phoshorylated form of MEF2 was confirmed by incubation of protein extracts with AP. Similar results were obtained in 4 independent experiments for the Western blot analyses above. (b) Western blot analysis to illustrate MEF2 expression in nuclear extracts of transfected B103 cells. Total MEF2 nuclear proteins were analyzed by Western blotting with a rabbit polyclonal anti-MEF2 antibody. Arrows indicate the position of the two major migrating species of MEF2. The double arrow indicates the unphosphorylated form of MEF2.

phosphorylation, and that the slower migrating band corresponds to the phosphorylated species of MEF2. Because MEF2 is a transcription factor that affects gene expression (70,76,97), nuclear lysates were examined by Western analysis to determine the expression levels of MEF2. In the nuclear lysate of hAPPwt expressing cells, MEF2 expression was predominantly in the phosphorylated form compared with mock and hAPPmut (Figure 10b). The relative levels of the phosphorylated form of MEF2 in nuclear extracts of hAPPwt expressing cells was 6.9 ± 0.5, compared with 1.6 ± 0.4 in mock and 1.8 ± 0.2 in hAPPmut (Figure 11a). These results were consistent with the expression pattern of MEF2 in total cell lysates of mock, hAPPwt and hAPPmut (Figure 9b), suggesting that expression of hAPPwt mediated an increase in the differential phosphorylation of MEF2 in differentiated B103 cells. To provide further evidence that the slower band of MEF2 is the phosphorylated species, hAPPwt expressing cells were labeled *in vivo* with [γ^{32}P]orthophosphate and ^{35}S-methionine. Nuclear extracts from equal numbers of unlabeled and labeled hAPPwt cells were then immunoprecipitated with a monoclonal antibody against MEF2, and the radio-labeled, immunoprecipitated proteins were displayed by SDS-PAGE analysis. The antibody precipitated one band not present in control immunoprecipitations (Figure 11b, lanes 2 and 3). Most importantly, this

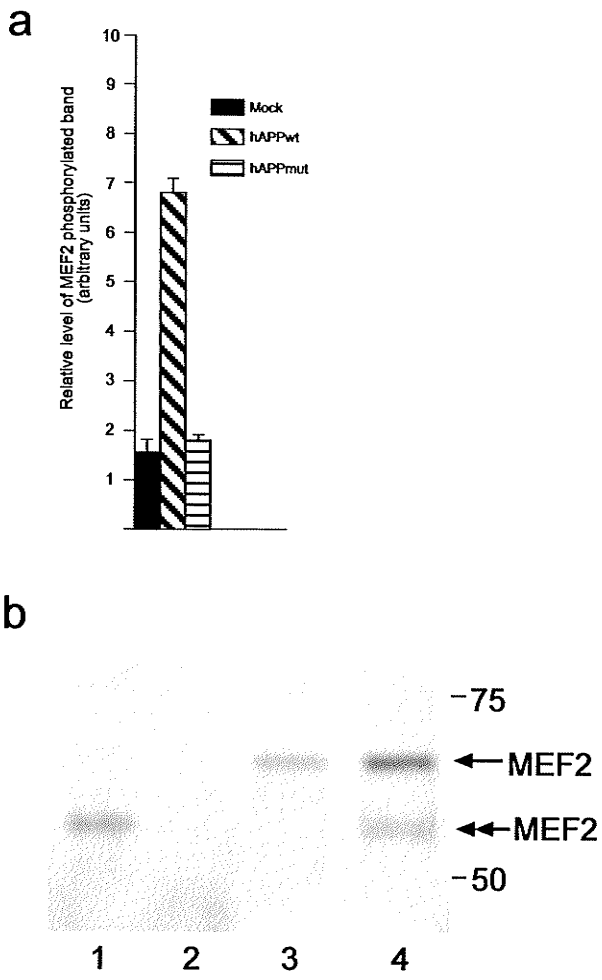

Figure 11. Relative levels of phosphorylated MEF2 immunoreactive bands. (a) This level was calculated by dividing the chemiluminescence signal (optical density x area of the phosphorylated MEF2 band) by the total chemiluminescence signal of MEF2 optical density peaks and normalized to the level of HDAC 5. The error bars are ± s.e.m, $n = 5$ (b) MEF2 is phosphorylated *in vivo*. *In vitro* translated ^{35}S methionine labeled MEF2A is a marker for unphosphorylated form of MEF2. Extracts from equivalent numbers of hAPPwt unlabeled cells (lane 2) and biosynthetically ^{32}P-labeled cells (lane 3) and ^{35}S methionine labeled cells (lane 4), were immunoprecipitated with anti-MEF2 antibody, and separated on 15% SDS-PAGE. The molecular weight markers in kDa are indicated on the right.

band corresponded to the slower but not the faster migrating band of MEF2 immunoprecipitated from [^{35}S] methionine labeled cells (Figure 11b, lane 4), and the faster migrating band of MEF2 corresponded to the molecular weight of an *in vitro* translated (unphosphorylated) MEF2 protein marker (Figure 11b, lane 1). This result confirms that the slower migrating band is the phosphorylated form of MEF2. To control for equal loading of protein in the Western blots, we examined the levels of histone deacetylase (HDAC 5), and there was no significant difference ($P > 0.05$, $n = 4$) in the expression levels of HDAC 5 in mock, hAPPwt and hAPPmut cells, suggesting that APP expression may not influence nuclear export of HDACs.

5.3 Wild type Alzheimer amyloid precursor protein induced phosphorylation of MEF2 is dependent on the p38 MAP kinase signaling pathway.

Previous studies indicated that MEF2 proteins are a known substrate of p38 MAPK (77,76). The similarities in the effects of APP and p38 MAPK on MEF2 phosphorylation, suggest that APP may activate p38 MAPK (phosphorylation of threonine (Thr) and tyrosine (Tyr) amino acid residues are required for the activation of p38 MAPK) to mediate MEF2

phosphorylation dependent transcriptional activity. To test this possibility, the phosphorylation state and activity of p38 MAPK was analyzed in mock, hAPPwt and hAPPmut transfected cells and these cells were also grown in the presence of p38 MAPK specific inhibitor, SB203580 (SB)(117) to determine the pattern of MEF2 expression. Western analysis showed that the relative expression levels of phospho-p38 MAPK (specific for phosphorylation at Thr 180 and Tyr 182) in hAPPwt cells was 390 ± 10 % significantly increased ($P < 0.03$, $n = 4$) compared with 190 ± 4% and 100% for mock and hAPPmut expression respectively (Fig. 12a,b). A significant difference ($P < 0.05$, $n = 4$) was observed in the relative phospho-p38 MAPK expression levels between hAPPmut and mock transfected cells. As phosphorylation of p38 MAPK parallels its activation, we measured the activity of p38 MAPKinase by a p38 MAPK assay using ATF-2 as a substrate for phosphorylation. These results are consistent with the phospho-p38 MAPK results. The hAPPwt expressing cells had a relative p38 MAPK activity of 285 ± 8% that was significantly increased ($P < 0.05$, $n = 5$) compared to mock and hAPPmut with values of 100% and 140 ± 9% respectively (Fig. 13a,b). If the APP induced phosphorylation of MEF2 is dependent on p38 MAPK pathway, then one would expect that the

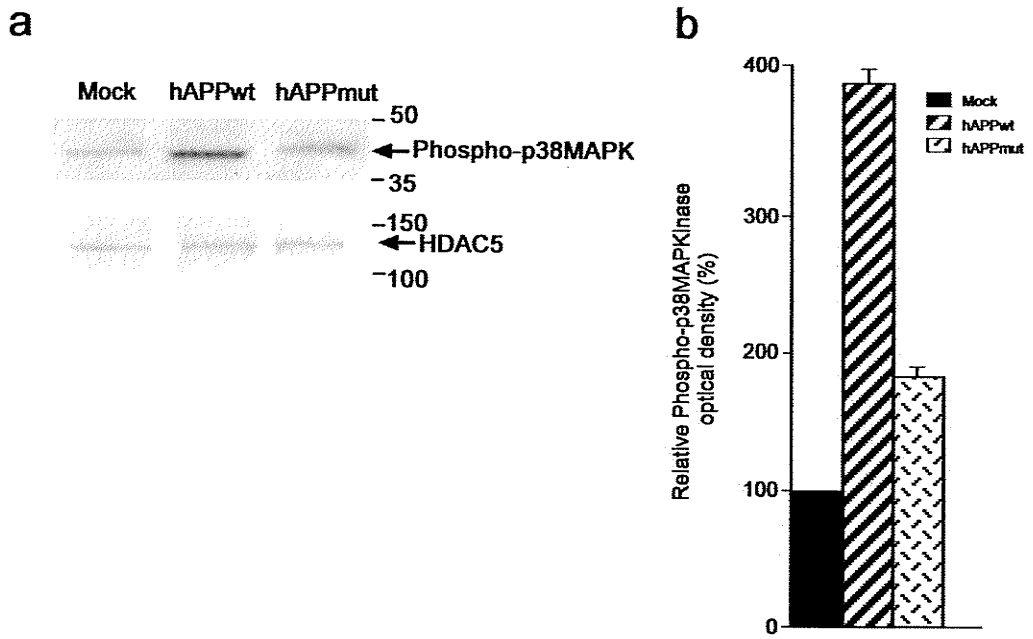

Figure 12. Effects of wild type and mutant APP on the phosphorylation p38 MAPK. (a) B103 cells stably transfected with hAPPwt, mut or mock expression vectors were grown in differentiation medium and harvested. A Western blot analysis of the active form of p38 MAPK (phospho-p38 MAPK) was performed by immunoblotting with an anti-phospho-specific (Thr180/Tyr182) p38 MAPK antibody. The p38 MAPK levels were determined for total protein loading control. (b) Relative phospho-p38 MAPK levels were calculated by dividing the chemiluminescence signal (optical density x area of the phosphorylated p38 MAPK band) by the total chemiluminescence signal of phosphorylated and unphosphorylated p38 MAPK optical density peak and the data graphed. The error bars are ± s.e.m, $n = 4$.

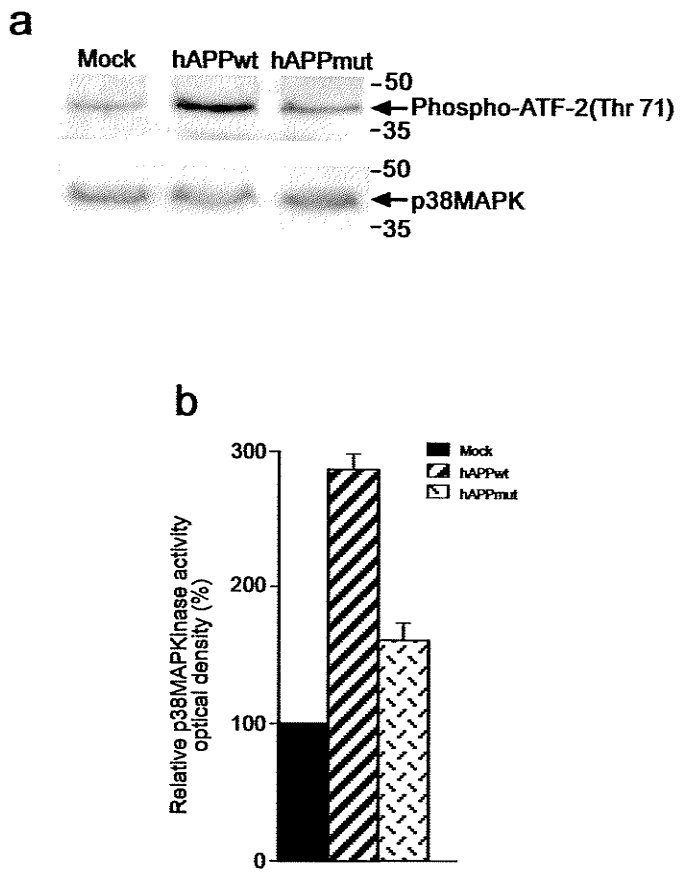

Figure 13. Effects of wild type and mutant APP on the activity of p38 MAPK. (a) Cell lysates were prepared from each of the above cell populations and cell extracts (200 μg) were incubated with p38 MAPK antibody. The kinase reaction was performed in the presence of 2 μg of GST-ATF-2 as substrate and 200 μM of cold ATP. Phosphorylation of ATF-2 at Thr71 was measured by Western blot using anti-specific phospho-ATF2 (Thr71) antibody as an extent of p38-MAPK activity.Total protein loading was controlled for by reprobing the immunoblot with anti-p38MAPK antibody. (b) Relative p38 MAPK activities were determined by dividing the chemiluminescence signal (optical density x area of the phosphorylated ATF2 band) by the total chemiluminescence signal of p38 MAPK optical density peak and the data graphed. The error bars are ± s.e.m, n = 5.

phosphorylation state of MEF2 would diminish in the presence of the specific inhibitor of p38 MAPK, SB. As expected, western blot analysis of nuclear extracts showed that in the presence of SB, the phosphorylated form of MEF2 (slower migrating band) was significantly decreased ($P < 0.05$, $n = 5$) in mock, hAPPwt and hAPPmut cells (Fig. 14a,b) and this corresponded to a parallel increase in the levels of the unphosphorylated (faster migrating band) of MEF2. The levels of p38 MAPK and HDAC5 in nuclear extracts from the transfected cells were not significantly different ($P > 0.05$, $n = 5$), suggesting that in B103 cells, nuclear localization of p38 MAPK is not affected by APP expression. These data demonstrate that hAPPwt signaling induces phosphorylation dependent activation of p38 MAPK that leads to phosphorylation of MEF2.

5.4 Wild type Alzheimer amyloid precursor protein induced CaMKII activity.

To further understand the mechanisms of how APP mediates phosphorylation of MEF2, we examined the possibility that multiple signaling pathways may be involved. In previous studies,

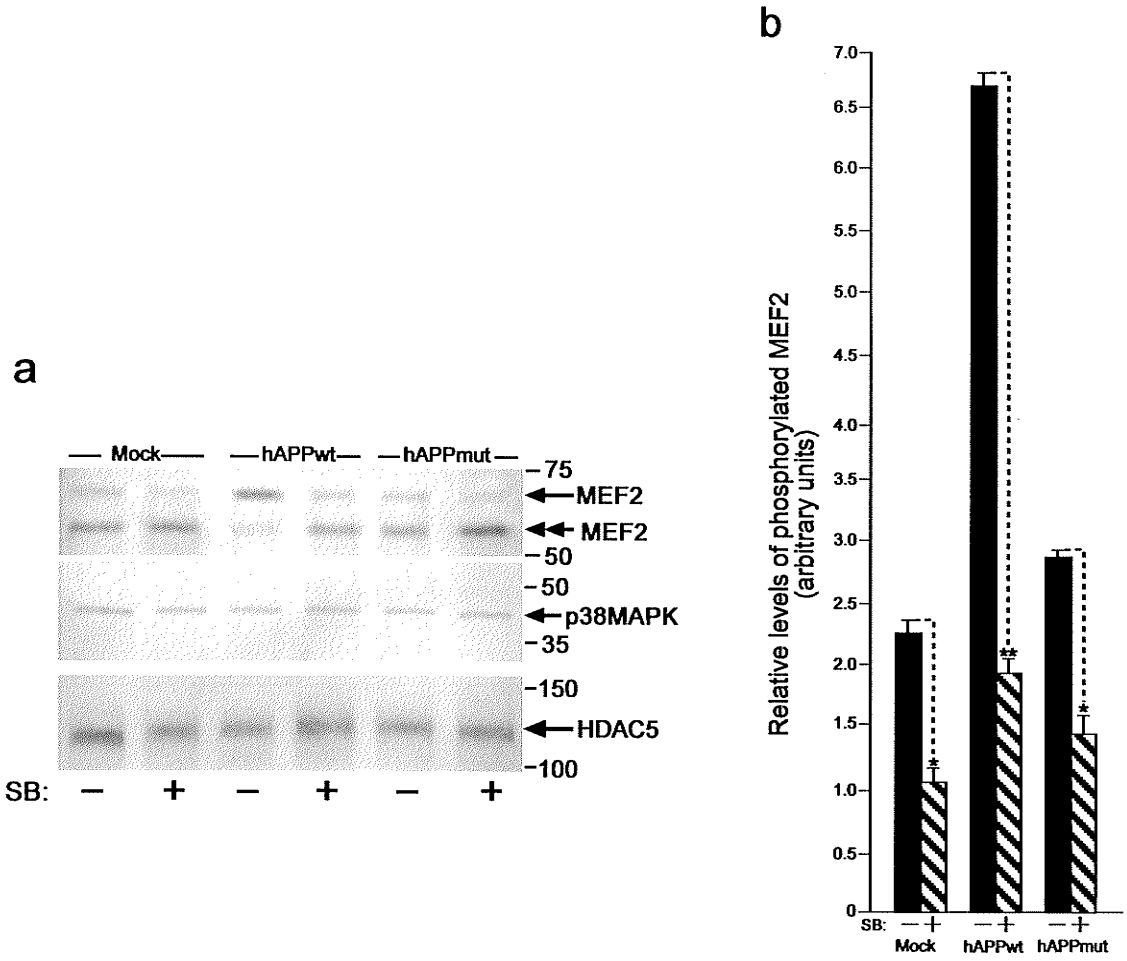

Figure 14. The effect of p38 inhibitors on the phosphorylation state of MEF2. (a) The levels of expression of the major migrating bands of MEF2 were determined in B103 transfectants in the presence and absence of the specific p38 MAPK inhibitor SB202190 hydrochloride (SB). B103 transfectants were grown in the undifferentiated state and transferred to serum free DMEM and cultured in Neurobasal A medium containing N-2 supplement for differentiation in the absence or presence of 2.5 μM SB for 72 hours. Total MEF2 nuclear proteins were analyzed by Western blotting with rabbit polyclonal anti-MEF2 antibody. Arrows indicate the position of the two major species of MEF2 before (-) and after (+) SB treatment. The slower migrating band (indicated by a single arrow) represents the phosphorylated form of MEF2. The immuno blots were reprobed for p38 MAPK and HDAC 5. (b) The relative level of phosphorylated MEF2 in the absence and presence of SB was calculated by dividing the chemiluminescence signal (optical density x area of of the phosphorylated MEF2 band) by the total chemiluminescence signal of MEF2 optical density and normalized to the level of p38 MAPK. The error bars are ± s.e.m, n = 5. The mol wt markers in kDa are indicated on the right.

calcium /calmodulin-dependent protein kinase II (CaMKII) activation has been found to increase the transcriptional activity of MEF2 (97,99), therefore we investigated the effect of APP expression on CaMKII expression and activity, and if CaMKII activity may contribute to the differential phosphorylation of MEF2. Western blot analysis showed that endogenous CaMKII and HDAC 5 expression levels in mock, hAPPwt and hAPPmut transfected cells were not significantly different ($P > 0.05$, $n = 5$), demonstrating that the expression of hAPPwt or hAPPmut had no effect on CaMKII expression levels (Figure 15a). To test whether APP expression affects CaMKII activity, a CaMKII assay that measured the phosphotransferase activity of CaMKII was performed. The CaMKII assay showed a significant increase ($P < 0.001$, $n = 5$) in CaMKII specific activity of 102 ± 3 in hAPPwt expressing cells compared with 10 ± 1 and 12 ± 2 CaMKII specific activity in mock and hAPPmut cells respectively. There was no significant difference ($P > 0.05$, $n = 5$) between CaMKII specific activity of mock and hAPPmut expressing cells (Figure 15b). The CaMKII activity in hAPPwt expressing cells was eliminated by treating hAPPwt cells with a CaMKII inhibitor, KN-93 (118), indicating that KN-93 is a specific inhibitor for CaMKII in B103 transfected cells. Western analysis of nuclear extracts of mock, hAPPwt and hAPPmut expressing cells that were cultured

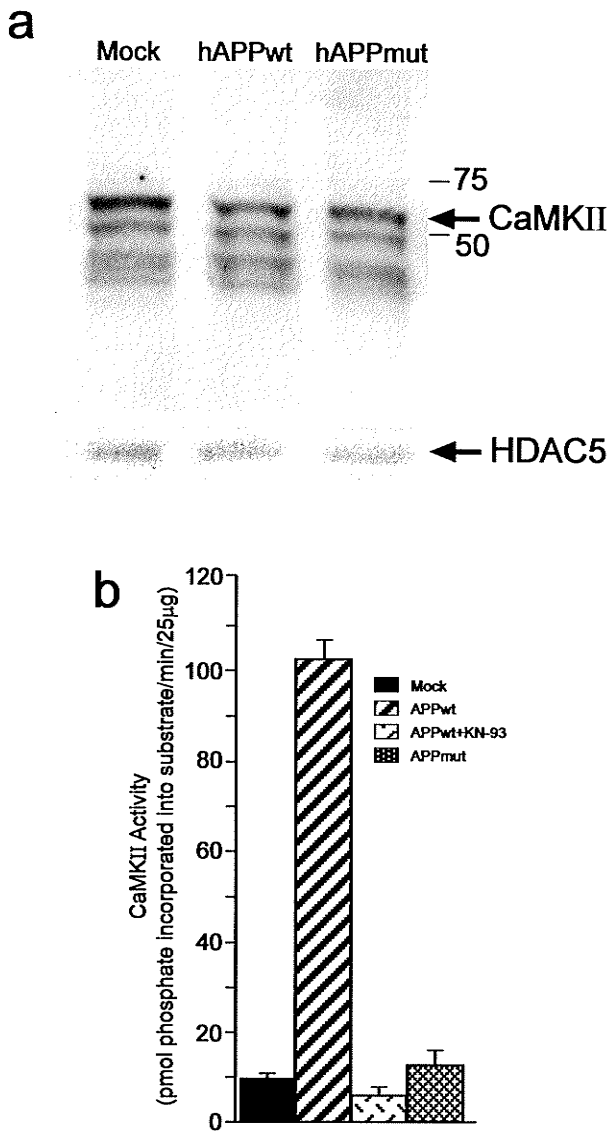

Figure 15. The effect of wild type and mutant hAPP on calcium/calmodulin kinase II (CaMKII) expression and activity. (a) Differentiated B103 transfectants were lysed and subjected to Western blot analysis. The protein-blotted membrane was first probed with monoclonal anti-CaMKII antibody and then reprobed by anti-rabbit polyclonal HDAC5 antibody after stripping for loading control. (b) Differentiating B103 transfectants were cultured in the absence or presence of 2.5 µM of the CaMKII specific inhibitor, KN-93 for 48 hours. Cells were lysed and the crude cell lysates were used for determining CaMKII activity. This activity was determined using the CaM kinase II assay kit (Upstate Biotech). The assay kit was designed to measure the phosphotransferase activity of CaMKII. The phosphorylated substrate is then separated from the residual [gamma^{32}P] ATP using phosphocellulose paper and quantitated by using a scintillation counter to determine the specific activity of CaMKII as phosphate incorporated into substrate peptide/min and graphed. The error bars are ± s.e.m, $n = 5$.

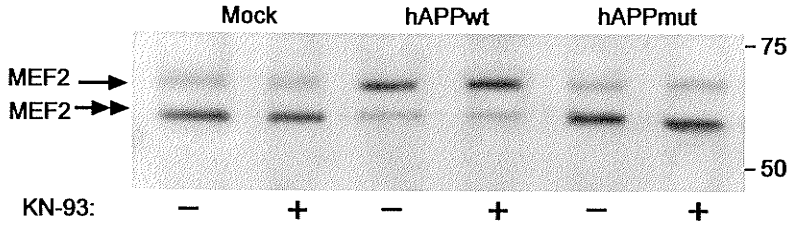

Figure 16. The effect of CaMKII inhibitors on the phosphorylation state of MEF2 proteins. The expression of MEF2 in nuclear extracts from B103 transfectants in the absence (-) or presence (+) of KN-93 was determined by Western blotting. Immunoblots were probed with rabbit polyclonal anti-MEF2 antibody, and loading of protein, was controlled for by reprobing with anti-HDAC5 antibody. Arrows indicate the position of the two major migration species of MEF2. The mol wt markers in kDa are indicated on the right.

in the presence of KN-93 showed no significant difference ($P > 0.05$, $n = 5$) in the relative levels of the slower and faster migrating forms of MEF2 compared with untreated cells (Figure 16). These results indicate that hAPPwt expression activates CaMKII activity without affecting the expression of CaMKII or nuclear export of HDACs. However, this increase in CaMKII activity may not be involved in the APP mediated phosphorylation of MEF2.

5.5 The DNA binding affinity of MEF2 is increased by expression of wild type but not mutant Alzheimer amyloid precursor protein.

Phosphorylation of MEF2 by the p38 MAPK pathway has been found to increase MEF2 transcription activity (76,99) by altering their ability to bind to DNA response elements (49) and to interact with co-activators and co-repressors of transcriptions (99,100,106,111). We tested whether the hAPPwt induced differential phosphorylation of MEF2 had any effect on the DNA binding activity of MEF2. To address this question, nuclear extracts from control and hAPP transfected cells were assayed by EMSA for their DNA binding activity to the MEF2 consensus binding site (CTAAAAATAA) (Figure 17). To test the relevance of over expressing

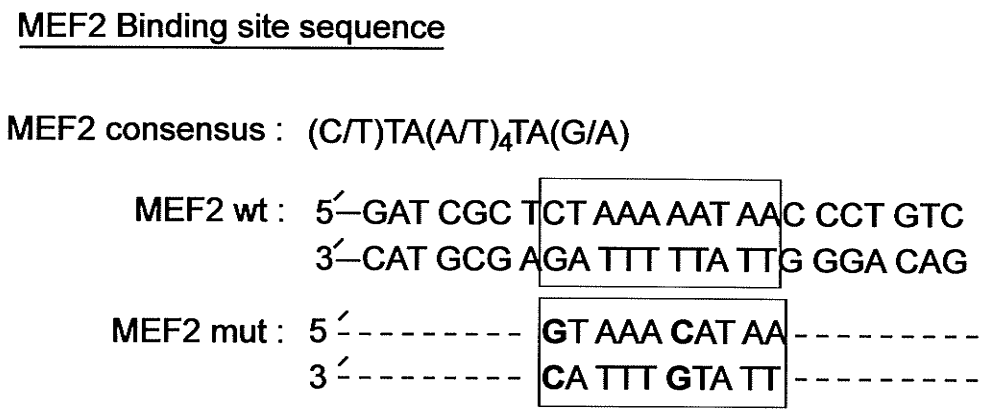

Figure 17. The MEF2 binding site consensus sequence for the wild type and mutant MEF2 *cis*-element probe used in electrophorectic mobility shift assay (EMSA). The base pair substitutions generated to mutate each site are indicated below the respective wild type sequence.

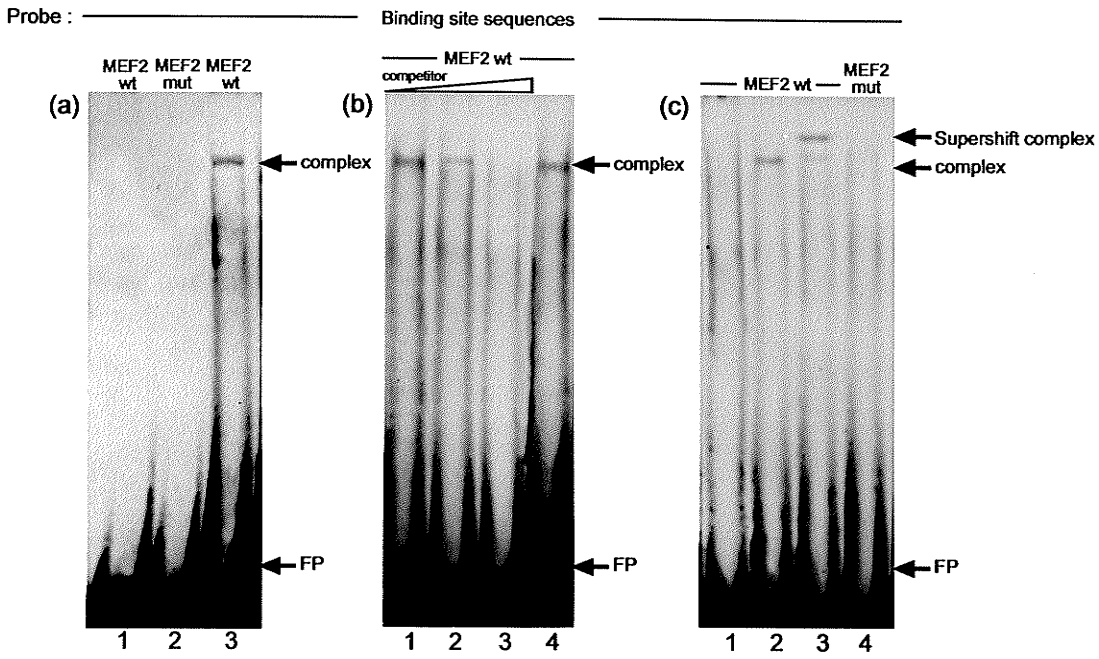

Figure 18. MEF2 is specific for binding to wild type but not the mutant MEF2 *cis*-element probe. (a) Electrophorectic mobility shift assay of 20 μg of B103 nuclear extract with MEF2wt/mut binding site sequence. Binding reactions contained no nuclear extract (lane1), nuclear extract (lanes 2 and 3). (b) Competition EMSA of 20 μg nuclear extracts from B103 cells with MEF2wt binding site DIG labeled probe. The probes were incubated in the binding reaction buffer with increasing concentration of molar excess cold (unlabeled) MEF2wt binding site oligomers. Control, no competitor (lane 1), 10 fold (lane 2), 30 fold (lane 3) molar excess of unlabeled probe and (lane 4), 10 fold of an unrelated competitor probe of NFkappaB *cis*-element. (c) EMSA of nuclear extracts with either wild type or mutant MEF2 binding site probes. The binding reactions contained no nuclear extracts (lane 1), nuclear extracts (lane 2), nuclear extracts and anti-MEF2 antibodies (lane 3) and nuclear extracts (lane 4). Positions of the MEF2-DNA and supershift complexes are indicated. Free DIG labeled probe is shown at the bottom of the gels.

MEF2 in the B103 cells, we first established by EMSA, that endogenous MEF2 bound the anticipated MEF2wt binding site, and as expected this binding activity was abolished when the MEF2mut binding site probe was used (Figure 18a). The MEF2 binding activity was gradually eliminated with increasing concentration of molar excess of cold (unlabeled) MEF2 DNA binding site oligomers in competition EMSA (Figure 18b, lanes 1 to 3). As a proof that MEF2 is contributing to the defined binding activity, excess molar of an unrelated competitor oligomer of NF kappaB binding site did not affect this binding activity (Figure 18b, lane 4). Furthermore, antibodies directed against MEF2 in EMSA showed the formation of a supershift complex that was abolished when MEF2 mutant binding site probes were used (Figure 18c). These results demonstrate that, the specificity of endogenous MEF2 binding activity in B103 cells is consistent with reports on other cell lines (49). Next, we next examined the effect of APP expression on MEF2 DNA binding activity. EMSA indicated that there was no significant difference ($P > 0.05$, $n = 5$) in the levels of MEF2–DNA complex from nuclear extracts of mock, hAPPwt and hAPPmut expressing cells (Figure 19a). However, this result does not mean that there is no change in MEF2 DNA binding activity, and to also eliminate bias due to unequal loading of MEF2-DNA complexes, we also determined the extent of

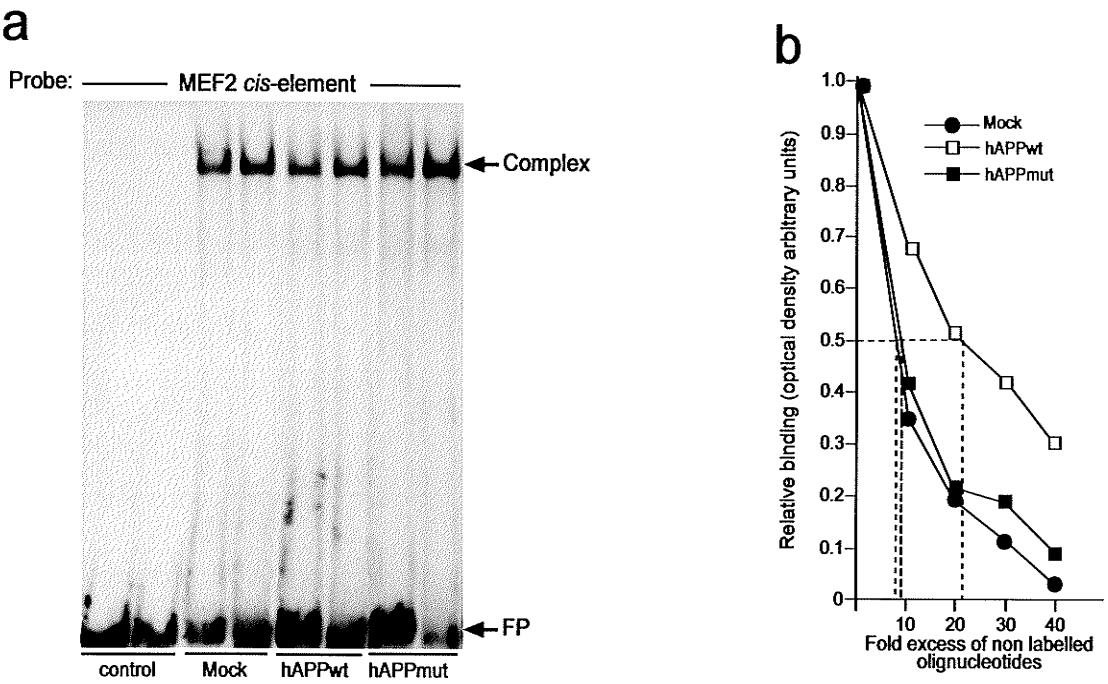

Figure 19. The effect of APPwt and APPmut expression on the DNA binding activity of MEF2 proteins. (a) Effects of mock, hAPPwt and hAPPmut expression on MEF2 DNA binding activity. Nuclear protein extracts from B103 transfected cells were used in EMSA with the MEF2wt binding site oligomer. The control lanes indicate that no nuclear extracts were used in the binding reactions. (b) The relative MEF2 DNA binding affinity was determined in an EMSA using excess molar concentration of cold MEF2wt binding site sequence to compete for the MEF2 nuclear binding. The relative binding was calculated by dividing the chemiluminescence signal (optical density of the MEF2-DNA complex x area of the band shift) by the amount of DIG labeled probe in the binding reaction buffer and normalized to arbitrary units.

MEF2 binding affinity in an EMSA with increasing concentration of molar excess unlabeled MEF2 *cis*-element oligomers as competitors. The data showed that, the relative binding affinity of MEF2 in hAPPwt nuclear extracts was reduced to 50% by 22 fold molar excess of cold competitor, compared with 8 and 9.5 fold of molar excess of cold competitor for mock and hAPPmut. (Figure 19b), suggesting that hAPPwt mediated an increase in the relative MEF2 DNA binding affinity, and could influence transcription of MEF2 dependent genes. To assess the factors that contributes to this increase in DNA binding activity, we examined whether APP expression may alter the intracellular distribution of MEF2. Indirect immunofluorescent analysis revealed that MEF2 is predominantly localized in the nuclei and there was no difference in the distribution pattern of MEF2 in mock, hAPPwt and hAPPmut transfected cells (Figure 20a). The percentage of MEF2 positive nuclei was 98 ± 2% in mock compared with 97 ± 5% and 97 ± 1% in hAPPwt and hAPPmut cells respectively. Thus, there was no significant difference ($\chi^2 = 35.1$; 1 degree of freedom; $P > 0.05$, $n = 5$) in the percentage of MEF2 positive nuclei of mock compared with hAPPwt and hAPPmut expression (Figure 20b), suggesting that subcellular localization of MEF2 does not play a role in the APP dependent increase in the MEF2-DNA binding activity.

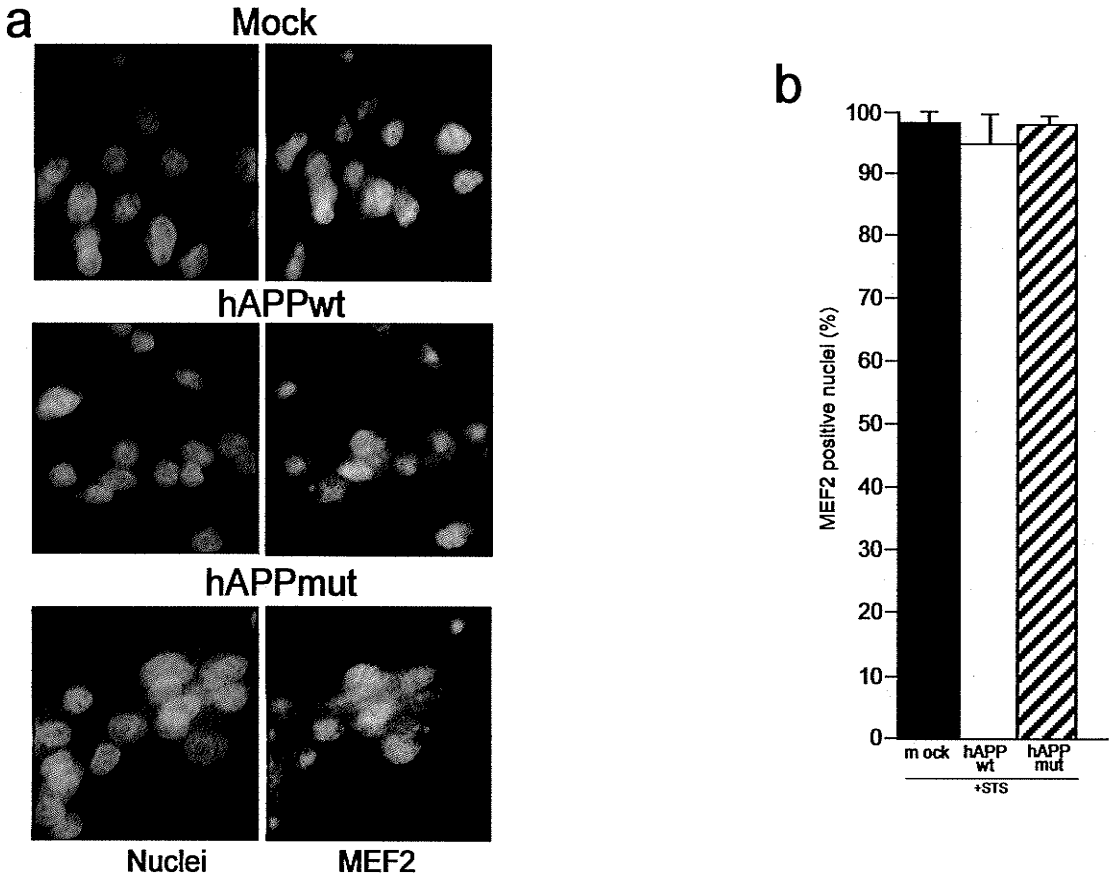

Figure 20. Intracellular distribution of MEF2 proteins. (a) There is similar intracellular distribution of MEF2 in differentiated B103 mock, hAPPwt and mut transfected cells. The MEF2 proteins were immunostained by using rabbit polyclonal anti-MEF2 antibody and images acquired with epiflourescent microscopy; x 40. Endogenous MEF2 in these cells shows a predominantly nuclear localization. Nuclei were counterstained with Hoechst 33258. (b) The frequency of MEF2 nuclear immunoreactivity was determined by assessing the number of positive nuclear MEF2 fluorescence divided by the total number of cells counted. Double blind analyses of cells were performed in numerous fields. The error bars are ± s.e.m, n = 5, and greater than 300 cells were scored per experiment.

5.6 Inhibition of p38 MAPK represses the wild type Alzheimer amyloid precursor protein mediated increase in MEF2 transcription activity.

To test the functional relevance of the hAPPwt induced MEF2 phosphorylation and increased DNA binding affinity, we examined the transcriptional activity of MEF2 proteins in cells expressing mock, hAPPwt and hAPPmut. To determine whether MEF2 could activate transcription from MEF2 dependent promoters, a CAT reporter gene driven by 2 copies of the MEF2 consensus binding sites (MEF2 x 2) upstream of the thymidine kinase (TK) minimal promoter (Figure 21a i) was transiently co-transfected with the pSVβ-galactosidase gene into mock, hAPPwt or hAPPmut expressing cells. The β-gal activity served as an internal control for transfection efficiency. Transfected cells were differentiated, and after 72 h, cell lysates were extracted and assayed for CAT activity. CAT activity assay was performed to determine the amount of CAT transcribed by measuring the optical density of radioactive ^{14}C chloramphenicol butyryl products relative to β-gal enzyme units for mock, hAPPwt, and hAPPmut cells (Figure 21a ii). Expression of hAPPwt significantly increased ($P < 0.01$, $n = 5$) the relative CAT activity by 495 ± 10% compared with the relative CAT activity of 100% in and 110 ± 7% for mock and hAPPmut

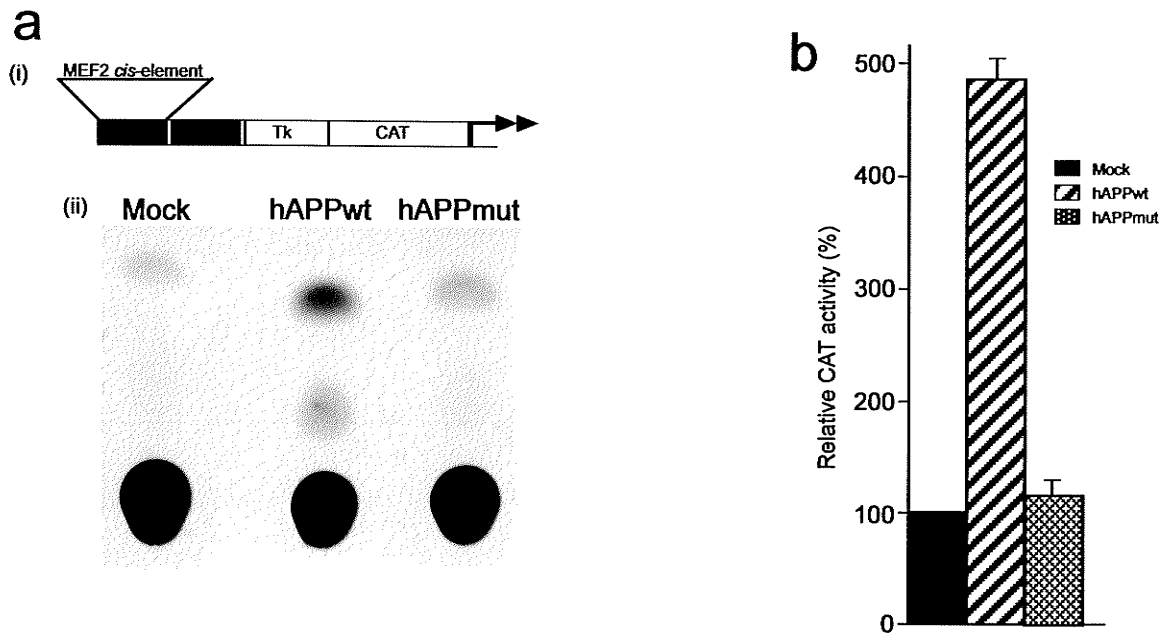

Figure 21. Wild type but not mutant APP expression activated a MEF2 responsive reporter gene. (a) i, Each plate of mock, hAPP6wt and hAPPmut stably transfected B103 cell cultures, was transiently transfected with 5 μg MEF2x2 CAT reporter gene and 3 μg of pSVβ-galactosidase construct (as an internal control for transfection efficiency). After transfection in the undifferentiated state, cells were cultured in differentiation medium. 72 h after transfection, cells extracts were prepared and CAT activity was determined. ii. A typical thin layer chromatography CAT assay autoradiogram is illustrated. Each transfection was repeated at least in three separate experiments with similar results. (b) The CAT activities were measured by both liquid scintillation counting and densitometry of radioactive ^{14}C chloramphenicol butyryl products and quantified relative to β-galactosidase enzyme activity. Fold stimulation of relative CAT activities were determined taking the CAT activity of the mock-stably transfected B103 cells as control (assigned the value of 100%) and graphed.

expressions respectively. There was no significant difference ($P > 0.05$, $n = 5$) in the relative CAT activity between hAPPmut and mock expressing cells (Figure 21b). Treatment of the transfected cells with the specific inhibitor of p38 MAPK, SB, significantly inhibited ($P < 0.03$, $n = 5$) the hAPPwt mediated increase in the transcriptional activity of MEF2 (Figure 22a). In contrast the specific inhibitor of CaMKII, KN-93 had no effect on the hAPPwt induced increase in MEF2 transcription activity (Figure 22b). These inhibitors had no effect on the viability of the transfected cells (figure 22c), suggesting that the inhibition of MEF2 activity is not a reflection of the cytotoxic effects of the p38 MAPK inhibitor, SB. These findings indicate that p38 MAPK but not CaMKII is involved in the activity of MEF2 transcription factor induced by APP.

5.7 The anti-apoptotic Alzheimer amyloid precursor protein signaling is dependent on MEF2 activation.

It has been previously shown that wild type but not mutant APP expression effectively protects against apoptosis in B103 cells under stressful conditions (40,41). To investigate the mechanisms involved in the

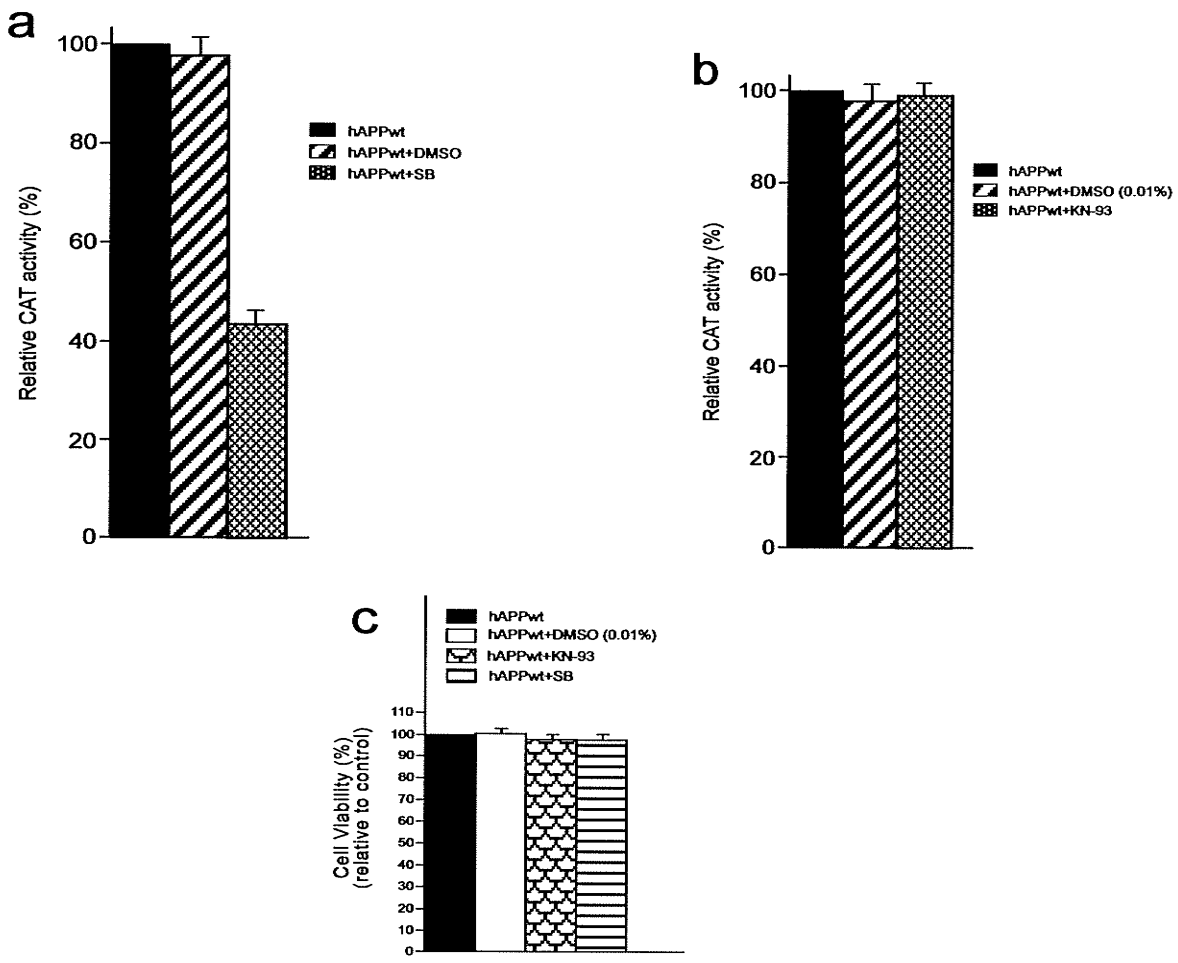

Figure 22. Activation of a MEF2-responsive reporter gene in the presence of p38 and CaMKII inhibitors. (a) Relative CAT activity of MEF2 reporter CAT gene transfectd into hAPPwt expressing cells, and cultured in the presence of p38 MAPK inhibitor, SB and absence (0.01%, DMSO) as vehicle for SB) (b) Relative CAT activity of the MEF2x2 reporter CAT gene transfectd into hAPPwt expressing cells, and cultured in the presence of CaMKII inhibitor, KN-93 and absence (0.01%, dimethyl sulfoxide (DMSO) as vehicle for KN-93. The error bars are ± s.e.m (which was not more than 2% of the mean value for any of the data points) $n = 5$. (c) Determination of the frequency of cell viability. Cells were cultured in the presence of specific inhibitors and the extent of cell viability measured by the MTT assay. The error bars are ± s.e.m, $n = 5$.

anti-apoptotic functions of APP, we focused on MEF2, a key transcription factor that regulates diverse cellular pathways. A TUNEL assay was performed to establish that DNA fragmentation is occurring concurrent with apoptosis when cells were treated with STS. The TUNEL assay was consistent with previous results, which showed that in the absence of an apoptotic inducing stimuli, hAPPmut transfected B103 cells showed no significant increase ($P > 0.05$, $n = 5$) in apoptosis compared with mock and hAPPwt tranfected cells (Figure 23). However, in the presence of STS treatment, hAPPwt expression significantly decreased ($P < 0.01$, $n = 5$) the level of apoptosis to 8.5 ± 2% compared with 23 ± 3% and 19 ± 3% for mock and hAPPmut expressing cells respectively. Because MEF2 has been observed to be essential for neurogenesis (65), and that expressing a dominant negative form of MEF2 in neuronal cells induced apoptosis during differentiation (67), we examined the possibility that MEF2 plays a role in mediating anti-apoptotic APP signaling. This assumption is further reinforced by the observation that MEF2 regulates neuronal activity dependent cell survival during development of neuronal cells (66). On the other hand, Ca^{+2} induced release of MEF2 increases apoptosis in T cells (101). We compared the effects of stably transfecting wild type or dominant negative MEF2 (MEF2Awt or MEF2A DN respectively) into hAPPwt or

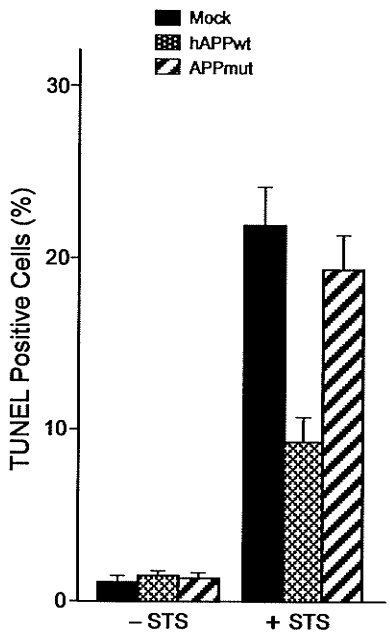

Figure 23. Wild-type, but not FAD-mutant hAPP695 protects APP-deficient B103 cells against apoptosis induced by 5 μM STS for 5h. The proportion of apoptotic cells (fragmented nuclei) were scored by TUNEL labeling. The error bars are ± s.e.m , $n = 4$.

hAPPmut expressing cells, to determine if APP exhibits its anti-apoptotic signaling in part by activating MEF2 transcriptional activity. To eliminate the bias due to dosage gene effects on apoptosis, western blot analysis of the transfected cells showed that expression levels of hAPPwt relative to GAPDH levels in hAPPwt, hAPPwt + MEF2Awt and hAPPwt + MEF2A DN were not significantly different ($P > 0.05$, $n = 5$) (Figure 21b). As expected the relative level of MEF2Awt in hAPPwt + MEF2Awt transfected cells was significantly greater (by 3 fold) compared with MEF2Awt levels in, mock, hAPPwt alone, and hAPPwt + MEF2A DN expressing cells. On the other hand, as expected the expression of MEF2A DN (detected by anti-GST antibodies to GST fusion protein tagged onto the MEF2A DN gene construct) (Figure 24a) was only detected in the hAPPwt + MEF2A DN transfected cells (Figure 24a). An interesting observation is that the MEF2A phosphorylation state is the same between the mock and APPwt expressing cells. In B103 cells MEF2C is the predominant isoform therefore we propose that the differential phosphorylation observed in the overall MEF2 levels are due to the phosphorylation of MEF2C not MEF2A. Using an EMSA, we established that transfection of MEF2Awt significantly enhanced ($P < 0.05$, $n = 5$) the amount of MEF2 DNA binding activity by 3-fold over endogenous MEF2 levels in hAPPwt expressing cells (Figure 24b, lanes 2

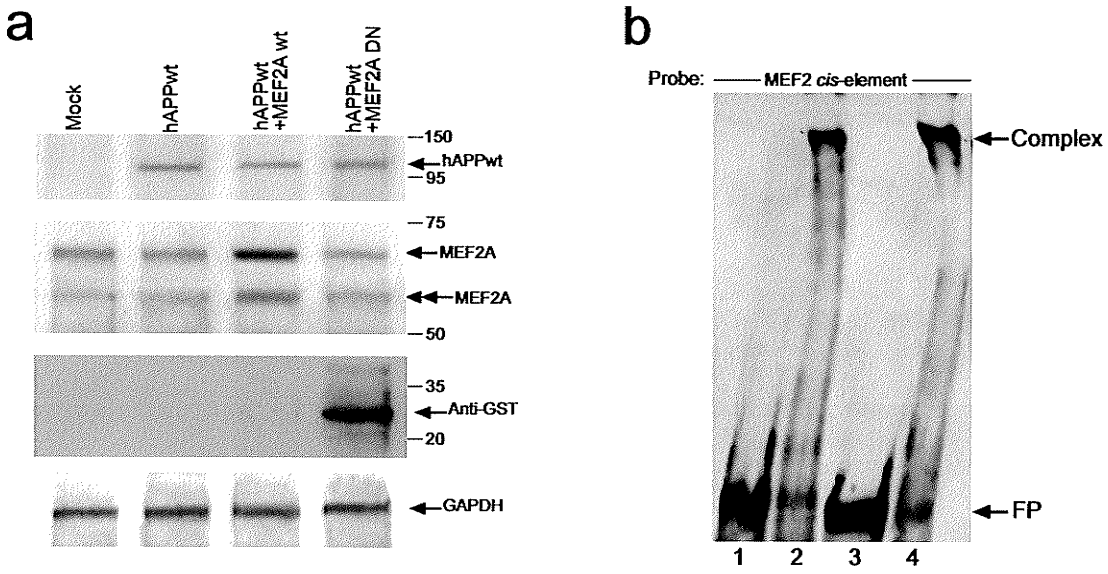

Figure 24. The expression of MEF2A DN in APP wt cells affects endogenous MEF2 DNA binding. (a) Westen blot analyses of total cell lysates to ascertain the expression of hAPPwt, MEF2Awt and MEF2A DN in B103 cells after stable transfections. It is noteworthy that the the relative levels of MEF2B, MEF2C and MEF2D were not significantly different in these cells.(b) Nuclear protein extracts from hAPP695wt B103 transfectants stably expressing MEF2Awt and DN plasmid constructs were used in EMSA with DIG labeled MEF2wt binding site probe. The arrows indicate the specific MEF2-DNA binding complex and unbound binding site probe (free probe). Lanes: (1) control, indicates no nuclear protein extracts were used in the binding reaction. (2) hAPPwt expression only. (3) hAPPwt + MEF2 DN. (4) hAPPwt + MEF2wt. Similar results were obtained in four separate experiments.

and 4). In contrast, transfection of MEF2A DN in hAPPwt expressing cells abrogated DNA binding activity of endogenous MEF2 (Figure 24b, lane 3) consistent with other reports [18,26]. Next, a TUNEL assay was then performed on hAPPwt cells transfected with MEF2Awt or MEF2A DN in the presence or absence of STS treatment as analyzed by flow cytometry (Figure 25a). In the absence of STS treatment, expression of MEF2A wt and MEF2A DN in hAPPwt expressing B103 cells showed no increase ($P > 0.05$) in apoptosis compared to hAPPwt expressing cells. Thus, the apoptosis (%) were: hAPPwt; 0.04%, hAPPwt + MEF2 DN; 0.02%, hAPPwt + MEF2A wt; 0.04%, demonstrating that expressing MEF2A DN does not induce apoptosis on its own in B103 cells in the absence of an apoptotic inducing agents. On the other hand, after STS treatment, hAPPwt + MEF2wt expressing cells had a significantly decreased ($P < 0.03$, $n = 4$) apoptosis level over hAPPwt expressing cells alone (8.42 ± 0.7% compared to 16.78 ± 0.8% respectively) (Figure 25b). However, cells expressing hAPPwt + MEF2A DN subjected to STS treatment had a significant increase ($P < 0.01$, $n = 4$) in apoptosis compared to hAPPwt and hAPPwt + MEF2Awt expressing cells (39.33 ± 3% compared with 16.78 ± 0.8% and 8.42 ± 0.7% respectively). It is noteworthy that, in the absence of STS treatment the extent of apoptosis for MEF2A and MEF2A DN expression in

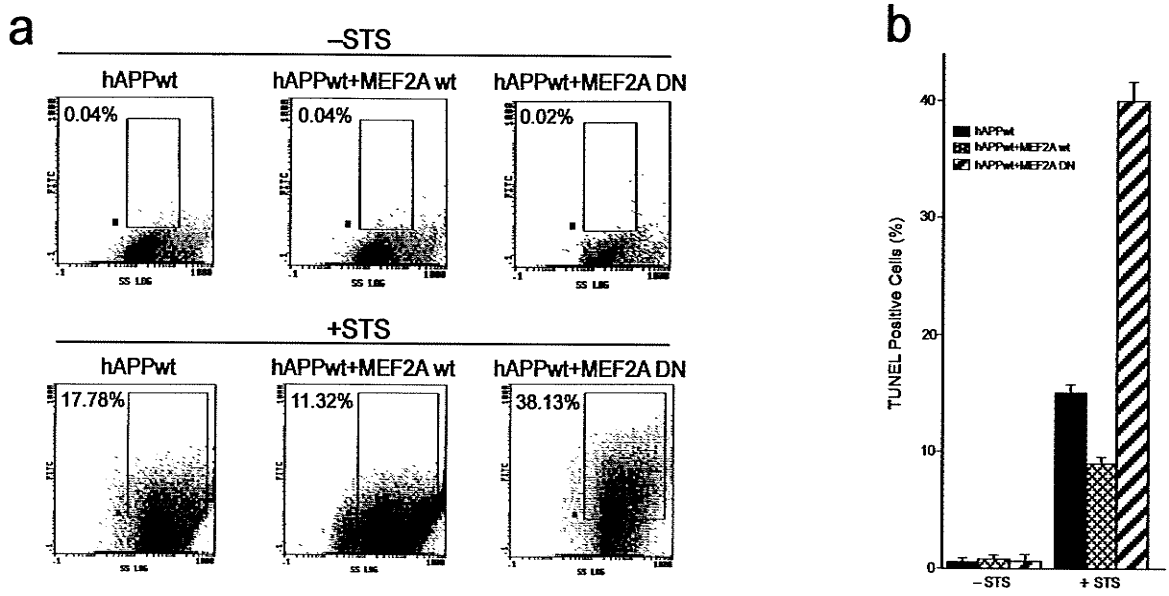

Figure 25. Inhibition of MEF2-DNA binding activity limited the anti-apoptotic capacity of Alzheimer amyloid precursor protein. (a) Effects of inhibition of MEF2 function in differentiated hAPPwt B103 transfected cells during staurosporine-induced apoptosis. A representative flow cytometric analysis of apoptotic cells in control (hAPPwt), hAPPwt + MEF2Awt and hAPPwt + MEF2A DN B103 cells before (- STS) and after treatment with 5 μM staurosporine for 5 h (+ STS). The numbers (inset) indicate the percentage of apoptotic cells (fragmented nuclei). (b) The percentage of apoptotic cells was scored by the TUNEL technique. The error bars are ± s.e.m, $n = 4$.

B103 cells (lacking endogenous APP) was not significantly different ($P > 0.05$, $n = 5$) with values of 0.03% and 0.05% respectively relative to 0.04% for hAPPwt expression However the expression of MEF2Awt or MEF2A DN alone in B103 cells, showed a significant increase ($P < 0.03$, $n = 5$) in STS induced apotosis compared with hAPPwt (33.54 ± 2% and 56.23 ± 21% respectively, compared with 16.78 ± 0.8%). These effects cannot be attributable to a difference in cytotoxicity due to the expression of wild type and dominant negative MEF2, because comparable levels of cell viability were observed between the transfected cells. The levels of cell viability (%) relative to control(assigned the value of 100%) as determined by the MTT assay were: MEF2Awt (95.7 ± 3%), MEF2A DN (97.2 ± 1%) hAPPwt (95.3 ± 2%), hAPPwt + MEF2Awt (95.8 ± 3%) and hAPPwt + MEF2A DN (96.7 ± 3%). These data demonstrate that MEF2 is plays a role in anti-apoptotic APP signaling. Once activated, MEF2 may regulate neuronal survival by stimulating MEF2 dependent gene transcription.

6.0 DISCUSSION

In the development of neuronal circuits, apoptosis is prevalent in neurons during the time they are forming synaptic contacts. Fifty percent of neurons die during this time in most regions of the developing nervous system. In the aging process and neurodegenerative disorders, induction of synapse loss and neuronal death have been proposed to utilize the same signaling mechanisms as in development (39). Evidence for this is shown in studies that have found that apoptosis contributes to neuronal loss seen in AD. Neuronal cells from tissue sections of brains from AD patients have been observed to exhibit apoptotic characteristics such as DNA fragmentation, and apoptotic like morphology. However, the morphological evidence might still be insufficient to formally indict apoptosis as the main cause of neurodegeneration associated with AD because there is also many cells that exhibit necrotic like death or maybe some alternative, non-classical form of apoptosis. The link between the apoptotic and necrotic death is not clear, but studies on APP, the precursor for the Aβ plaques may begin to explain this occurrence. Mutations in the APP gene that alter the processing of APP also alter its ability to carry out its normal anti-apoptotic role in neurons. Moreover, APP in normal function activates anti-apoptotic

pathways therefore, these mutations leave the cell more susceptible to undergoing apoptosis under stress as well as increasing the production of the Aβ plaque which has been shown to induce necrotic cell death by activating a local inflammatory response, affecting excitotoxicity, oxidative stress, the formation of free radicals and creating competition for low-affinity NGF receptors. To understand the mechanism behind the occurrence of cell death in AD a transgenic mouse model might be very useful to determine the time frame of induction of apoptotic and necrotic cell death and what role they play in overall degeneration.

Several studies have demonstrated the importance of APP in apoptosis and how FAD mutations impair or counteract specific APP functions (40, 41, 119, 120) However, largely unexplained is the molecular mechanisms involved in the regulation of apoptosis by APP and its mutant forms in contributing to neurodegeneration seen in AD. Therefore, studying APP pathways involved in inhibiting or promoting apoptosis is important in understanding the pathogenesis of AD, and in approaches to its treatment or prevention. What mechanisms are involved in anti-apoptotic APP signaling? To address this question, in this study we examined the role played by the transcription factor, MEF2 in anti-apoptotic APP pathways. MEF2 proteins have been extensively studied for their role in regulating

gene expression in myogenesis. However, MEF2 proteins are also present in the brain indicating that they may have important functions in the central nervous system, which is affirmed in studies that observe that MEF2 plays a role in neurogenesis and activity dependent neuronal survival (65).

One of the major mechanisms for stimulation of MEF2 transactivation is through the CaMKinase signaling pathway. This has led to extensive studies on the interactions of HDAC 4 and 5 (amongst the class II HDACs 4, 5, 6 and 7), with MEF2 resulting in repression of MEF2 dependent gene transcription (100,106). This repression can be overcome by CaMK dependent disruption of MEF2-HDAC complexes, leading to nuclear export of phosphorylated HDACs. We decided to examine the effect of APP expression on the nuclear levels of HDAC 5 but not HDAC 4, because HDAC 5, is shown to be affected by CaMK through the family of 14-3-3 proteins (chaperone proteins involved in mediation of localization of proteins) in stimulated cells (104). Interestingly, over expression of wild type or mutant APP had no effect on the level of HDAC 5 (Figure 9,10), indicating that APP may not directly influence nuclear export of the HDACs. Although, APP expression increased CaMKII activity, inhibition of this activity did not alter the phosphorylation state of MEF2, suggesting that APP induced phosphorylation of MEF2 may not be contributed to by

CaMKII (Figure 15). These results are in contrast to a recent study that has identified that CaMK may indirectly induce the phosphorylation of MEF2 in neurons by recruiting and activating ASK1 by phosphorylation evoked by calcium influx in membrane depolarization, which then activates MKK3/6 (upstream p38 activators). Therefore, this pathway may not be an important mechanism in CaMK signaling in B103 cells.

As CaMK primarily phosphorylates MEF2D (97), it may not be surprising that at least in these cells CaMKII may not play a role in directly phosphorylating MEF2 through APP signaling, because only MEF2A and MEF2C were highly expressed in these cells (Figure 9a). In addition, signaling pathways other than p38 MAPK and CaMK not investigated, such as PI3-kinase may mediate APP induced phosphorylation of MEF2 in a parallel but distinct route (75). This assumption is supported by the observations that APP activates PI3-kinase in insulin signaling (121).

We report that in differentiated neuroblastoma B103 cells, MEF2 is differentially maintained in the phosphorylated form when wild type but not mutant hAPP is expressed possibly implicating that APP signaling leads to phosphorylation of MEF2 (Figure 9). In previous studies p38 MAPK has been found to directly phosphorylate MEF2 induced by IGFR and G protein-linked receptor signaling. Concurrently, expression of wild type APP led to

phosphorylation dependent activation of p38 MAPK and inhibition of the p38 MAPK pathway with SB showed a decreased phosphorylation level of MEF2, also observed in previous studies, demonstrating that the observed APP induced phosphorylation of MEF2 involves the p38 MAPK pathway. This is likely to involve translocation of p38 MAPK to the nucleus, as western blots showed nuclear expression levels of p38 MAPK (Figure 5). However, the inhibitor of p38 MAPK used in these experiments may unknowingly affect other kinases, and there is also the possibility that multiple pathways could have an effect on the phosphorylation level of MEF2.

The roles of p38 MAPK cascades in neuronal death and survival are altered by the types of cells and the magnitude and timing of insults. Recent studies have shown that stimulation of the p38 pathway is anti-apoptotic during development but pro-apoptotic in mature neurons exposed to excitotoxic or other stress. Anti-apoptotic p38 signaling occurs in retinoic acid-induced neuronal differentiation of p19 embryonal carcinoma cells, in TNF-alpha signaling in PC12 cells (125), and in activity-dependant survival of primary cortical neurons (66). In contrast, the p38 signaling pathway has been found to be pro-apoptotic in PC12 cells, where nerve growth factor (NGF) withdrawl and $CoCl_2$ treatment lead to p38-induced apoptosis by

inducing gene expression that leads to activation of caspases and release of cytochrome c from the mitochondria (126,127). Also, p38 plays a pro-apoptotic role in glutamate and potassium deprivation in cerebellar granule neurons and ceramide-induced apoptosis of primary cortical neurons (128,129). The most accepted explanation for this discrepancy is that the physiological level of neuronal activity might control the p38 pathway as a mediator of cell survival. In contrast, once cells suffer strong stress beyond the physiological level, the p38 pathway might act as a stress-activated mediator of neuronal apoptosis (130). Recently, a mechanism has been reported that can account for a switch from the proneurogenic anti-apoptotic effects of the p38 MAPK-MEF2 transcription factor pathway into a pro-apoptotic cascade in mature neurons (113). It involves caspase activation by exposure of cerebrocortical neurons to an excitotoxic concentration of NMDA, which leads to the direct cleavage of MEF2 A, -C and –D in their transactivation domains by caspases. These cleaved products act as dominant negative transcription factors blocking the protective effect of MEF2 (113). These results suggest that activation of MEF2 is important in the survival pathways of neurons.

As p38 dependent phosphorylation of MEF2 has been shown to increase the transcriptional activity of MEF2 (76,77), we examined the

possible role of the anti-apoptotic p38/MEF2 pathway in APP signaling. Increased MEF2 DNA binding affinity (Figure 19b) and MEF2 dependent gene transcription of a reporter gene was observed in hAPPwt expressing cells (Figure 21a, b). This increase in MEF2 activity was not due to change in the MEF2 subcellular localization, as MEF2 was predominantly nuclear (Figure 21a, b). However, inhibition of p38 MAPK but not CaMKII led to a marked decrease in MEF2 dependent gene transcription (Figure 22 a, b) demonstrating that the APP induced phosphorylation of MEF2 mediated by p38 MAPK, could be required for the recruitment of an essential transcription co-factors (111) or release of co-repressors (99,100,106) resulting in increased MEF2 transactivation. This idea is consistent with recent reports that the transactivation activity of MEF2C is through p38 MAPK catalysed phosphorylation (79). Alternatively, APP expression may result in phosphorylation of MEF2 putative sites that are functionally distinct from those previously reported to result in a change in MEF2 DNA binding activity. However, our result is contrary to the observation that hypophosphorylation by calcineurin enhances MEF2 DNA binding activity and increased its transactivation in cerebellar granular neurons (68). This discrepancy may be due to the ability of the MEF2 proteins to activate

transcription dependent on the specific dimer composition of the DNA binding complex and the cellular context (122).

Next, we investigated the functional relevance of MEF2 transcriptional activity in anti-apoptotic APP signaling. Activation of MEF2 has been linked to the anti-apoptotic action of the p38 pathway, whereby p38-dependent phosphorylation of MEF2 activates anti-apoptotic genes in the differentiation of p19 cells (67), and in calcium-dependent survival of primary cortical neurons. Our results showed that inhibiting MEF2 DNA binding activity by expressing dominant negative MEF2A, limited the capacity of APP to effectively protect against STS-induced apoptosis, while expression of MEF2Awt enhanced anti-apoptotic APP effects (Figure 25). Taken together, these data indicate for the first time, that MEF2 activation may be required for the anti-apoptotic activity of wild type Alzheimer amyloid precursor protein. Thus, we propose a model where APP signaling affects activation of p38 MAPK pathways that leads to increased MEF2 transcription activity by post-translational modification due to phosphorylation. Once activated, MEF2 regulates neuronal survival by stimulating MEF2 dependent gene transcription (Fig. 7). This model illustrates the relationship between APP and p38 MAPK that converge on MEF2. It is noteworthy that APP can activate MEF2 independent of p38

MAPK. Such pathways may involve Akt, and PI3-kinase. How does this model apply to the pathogenesis of AD? Disruption of this function by mutations in APP, aberrations in the p38 MAPK/MEF2 pathways may enhance neuronal apoptosis due to secondary insults, and could contribute to neuronal degeneration seen in AD.

Some future directions that could be taken to clarify and enhance these results would be to co-transfect B103 cells with DN p38 and DN CaMK. This would strengthen the result that APPwt induces phosphorylation through activation of p38. Using a Gal4 reporter assay with the transactivation domain of all MEF2 isoforms would identify if the increase in transactivation of MEF2 is due to the increase in DNA binding affinity observed and what isoforms are involved. In addition, mutagenesis of specific residues in MEF2 known to be phosphorylated by p38 in muscle would identify if these sites are the same in neuronal B103 cells. Also, to complete the experiments in this study on other neuronal cell lines to identify if there is heterogeneity in MEF2 action among different neuronal cells.

A novel study has recently identified that APP signaling leads to activation of PI3-K (121) and APP has also been found to activate Ras (unpublished results). Both of these pathways lead to activation of MEF2 in

p38-dependent and p38-independent pathways, therefore they are implicated in activating the anti-apoptotic APP signaling pathway but this remains to be clarified.

MEF2 has been shown to display complex regulation by the formation of different dimer partners with MEF2. Dimer composition varies between cell types and in response to different signals in the same cell type. Identification of these dimers has been studied in muscle but is relatively unknown in neuronal cells. Activation of MEF2 increases transcription of gene important in the survival of neuronal cells, but specific anti-apoptotic genes activated by APP stimulation in neuronal cells are not known. This is an important observation that could have therapeutic implications in patients that have the familial Alzheimer's disease mutation in APP that does not exhibit a protective effect in neuronal cells. Using MatInspector V2.2 (131) we searched for potential MEF2 binding sites in apoptosis-regulating factors that may play a role in the pathology of AD. Bcl-2 and Bcl-x_L act as anti-apoptotic regulators that can prevent neuronal cells death induced by various stimuli, and have been found to have higher expression levels in brain cells from patients with AD (132). Inspecting the promoter region of mouse Bcl-2 and Bcl-x, we found two potential MEF2 binding sites in Bcl-x (AF133277 PubMed) at positions 1303 and 1311. Investigation into the

function of these potential MEF2 sites in Bcl-x and searching for other proteins with potential sites could lead to the identification of anti-apoptotic targets of MEF2. Finally, identification of the expression and activation levels of the key players in the p38/MEF2 pathway in human AD brain tissues compared to normal or transgenic mice models that carry a mutation in the APP gene may help to implicate the physiological importance of this pathway in the neurodegeneration seen in AD.

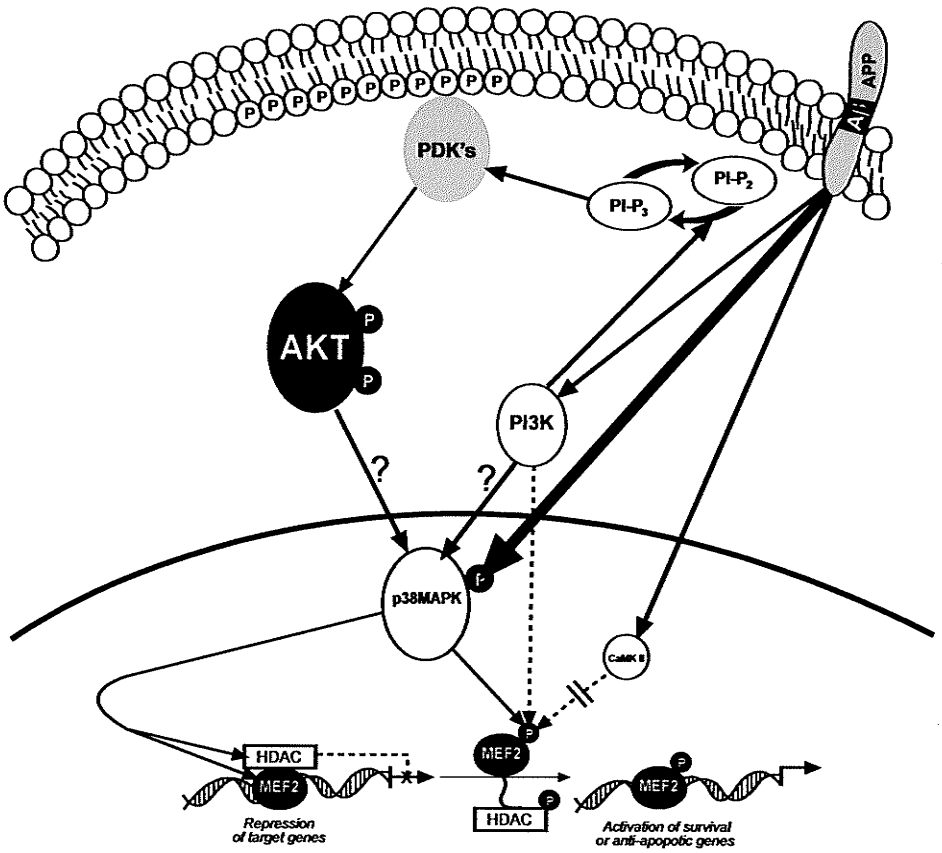

Figure 26. The p38 MAPK pathway links APP with MEF2 in anti-apoptotic signaling. The Alzheimer amyloid precursor protein induces phosphorylation dependent activation of p38 MAPK. Activated p38 MAPK may phosphorylate MEF2, and consequently an increase in MEF2 dependent gene transcriptions. Alternatively, APP may also activate MEF2 through the PI3-kinase/Akt pathways

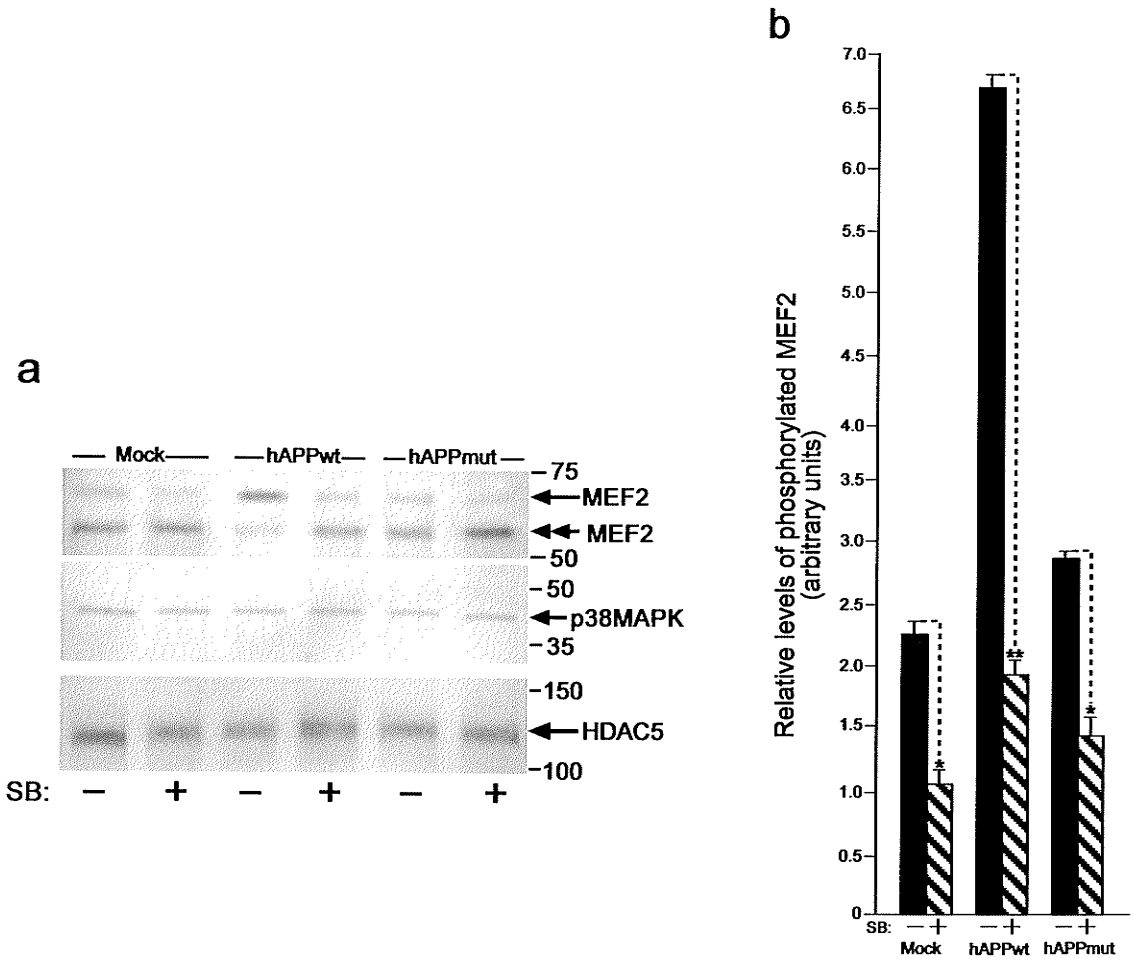

Figure 14. The effect of p38 inhibitors on the phosphorylation state of MEF2. (a) The levels of expression of the major migrating bands of MEF2 were determined in B103 transfectants in the presence and absence of the specific p38 MAPK inhibitor SB202190 hydrochloride (SB). B103 transfectants were grown in the undifferentiated state and transferred to serum free DMEM and cultured in Neurobasal A medium containing N-2 supplement for differentiation in the absence or presence of 2.5 μM SB for 72 hours. Total MEF2 nuclear proteins were analyzed by Western blotting with rabbit polyclonal anti-MEF2 antibody. Arrows indicate the position of the two major species of MEF2 before (-) and after (+) SB treatment. The slower migrating band (indicated by a single arrow) represents the phosphorylated form of MEF2. The immuno blots were reprobed for p38 MAPK and HDAC 5. (b) The relative level of phosphorylated MEF2 in the absence and presence of SB was calculated by dividing the chemiluminescence signal (optical density x area of of the phosphorylated MEF2 band) by the total chemiluminescence signal of MEF2 optical density and normalized to the level of p38 MAPK. The error bars are ± s.e.m, n = 5. The mol wt markers in kDa are indicated on the right.

7.0 REFERENCES

1 T. Yamazaki, D.J. Selkoe, and E.H. Koo (1995) Trafficking of cell surface beta-amyloid precursor protein: retrograde and transcytotic transport in cultured neurons. J. Cell Biol. 129, 431-42.

2 N. Kitaguchi, Y. Takahashi, Y. Tokushima, S. Shiojiri, and H. Ito (1988) Novel precursor of Alzheimer's disease amyloid protein shows protease inhibitory activity. Nature. 331, 530-32.

3 Ponte, P., Gonzalex-DeWhitt, P., Schilling, J., Miller, J., Hsu, D., Greenberg, B., Davis, K., Wallace, W., Lieberburg, I., and Fuller, F. (1988) A new A4 amyloid mRNA contains a domain homologous to serine protease inhibitors. Nature 331 525-27.

4 D.J. Selkoe (1994) Cell biology of the amyloid beta-protein precursor and the mechanism of Alzheimer's disease. Annu Rev Cell Biol. 10, 373-403.

5 S. Gauthier (2002) Advances in the pharmacotherapy of Alzheimer's disease. J.A.M.C. 166, 616-23.

6 P.E. Fraser, L. Levesque, and D.R. McLachlan (1993) Biochemistry of Alzheimer's disease amyloid plaques. Clinical Biochemistry. 26, 339-49.

7 C. Haass, and D.J. Selkoe (1993) Cellular processing of beta-amyloid precursor protein and the genesis of amyloid beta-peptide. Cell. 75, 1039-42.

8 D.J. Selkoe (1999) Translating cell biology into therapeutic advances in Alzheimer's disease. Nature. 399, Suppl: A23-31.

9 J. Kang, H.G. Lemaire, A. Unterbeck, J.M. Salbaum, C.L. Masters, K.H. Grzeschik, G. Multhaup, K. Beyreuther, B. Muller-Hill (1987) The precursor of Alzheimer's disease amyloid A4 protein resembles a cell-surface receptor. Nature. 325, 733-736.

10 J.W. Tamkun, D.W. DeSimone, D. Fonda, R.S. Patel, C. Buck, A.F. Horwitz, R.O. Hynes (1986) Structure of integrin, a glycoprotein involved in the transmembrane linkage between fibronectin and actin, Cell. 46, 271-82.

11 I. Nishimoto, T. Okamoto, Y. Matsura, S. Takahashi, T. Okamoto, Y. Murayama, E. Ogata (1993) Alzheimer amyloid precursor protein complexes with brain GTP-binding protein Go. Nature. 362, 75-79.

12 F. Fiore, N. Zambrano, G. Minopoli, V. Donini, A. Duilio, T. Russo (1995) The regions of Fe65 protein homologous to the phosphotyrosine interaction/phosphotyrosine binding domain of Shc bind the intracellular domain of the Alzheimer's amyloid precursor protein, J. Biol. Chem. 270, 1-5.

13 N. Chow, J.R. Korenberg, X. Chen, R.I. Neve (1996) APP-BP1, a novel protein that binds to the carboxyl-terminal region of the amyloid precursor protein. J. Biol. Chem. 271, 11339-11346.

14 D.M. McLoughlin, C.C. Miller (1996) The intracellular cytoplasmic domain of the Alzheimer's disease amyloid precursor protein interacts with phosphotyrosine-binding domain proteins in the yeast two-hybrid system. FEBS Letts. 397, 197-200.

15 U. Schuch, M.J. Lohse, and M. Schachner (1989) Neural cell adhesion molecules influence second messenger systems. Neuron. 3, 13-20.

16 S.M. Strittmatter, M.C. Fishman, and X.P. Zhu (1994) Activated mutants of the α subunit of G_0 promote an increased number of neurites per cell. J. Neurosci. 14, 2327-38.

17 K. Sebok, D. Woodside, A. Al-Aoukaty, A.D. Ho, S. Gluck, and A.Z. Maghazachi (1993) IL-8 induces the locomotion of human IL-2-activted natural killer cells. Involvement of a guanine nucleotide binding (G0) protein. J. Immunol. 150, 1524-34.

18 T. Okamoto, S. Takeda, Y. Murayama, E. Ogata, I. Nishimoto (1995) Ligand-dependant G protein coupling function of amyloid transmembrane precursor. J. Biol. Chem. 270, 4205-4208.

19 T. Ikezu, T. Okamoto, K. Komatsuzaki, T. Matsui, J.A.J. Martyn, and I. Nishimoto (1996) Negative transactivation of cAMP response element by familial Alzheimer's mutants of APP. EMBO J. 15, 2468-75.

20 U. Giambarella, T. Yamatsuji, T. Okamoto, T. Matsui, T. Ikezu, Y. Murayama, M.A. Levine, A. Katz, N. Gautan, I. Nishimoto (1997) G-protein beta gamma complex-mediated apoptosis by familial Alzheimer's disease mutant of APP. EMBO J. 16, 4897-4907.

21 N. Zambrano, J.D. Buxbaum, G. Minopoli, F. Fiore, P. De Candia, S. De Renzis, R. Faraonio, S. Sabo, J. Cheetham, M. Sudol, and T. Russo (1997) Interaction of the phosphotyrosine interaction/phosphotyrosine binding-related domains of Fe65 with wild-type and mutant Alzheimer's beta-amyloid precursor proteins. J. Biol. Chem. 272, 6399-405.

22 N. Zambrano, G. Minopoli, P. de Candia, T. Russo (1998) The Fe65 adaptor protein interacts through its PID1 domain with the transcription factor CP2/LSF/LBP1. J. Biol. Chem. 273, 20128-20133.

23 M.K. Shirra, Q. Zhu, H. Huang, D. Pallas, andU. Hansen (1994) One exon of the human LSF gene includes conserved regions involved in novel DNA-binding and dimerization motifs. Mol. Cell Biol. 14, 5076-87.

24 J.L. Volker, L.E. Rameh, Q. Zhu, J. DeCaprio, and U. Hansen (1997) Mitogenic stimulation of resting T cells causes rapid phosphorylation of the transcription factor LSF and increased DNA-binding activity. Genes Dev. 11, 1435-46.

25 J.B. Yoon, G. Li, and R.G. Roeder (1994) Characterization of a family of related cellular transcription factors which can modulate human immunodeficiency virus type 1 transcription *in vitro*. Mol. Cell Biol. 14, 1776-85.

26 Z. Bing, S.A. Reddy, Y. Ren, J. Qin, and W.S. Liao (1999) Purification and characterization of the serum amyloid A3 enhancer factor. J. Biol. Chem. 274, 24649-656.

27 K.F. Lau, C.C. Miller, B.H. Anderton, and P.C. Shaw (1999) Molecular cloning and characterization of the human glycogen synthase kinase-3beta promoter. Genomics. 60, 121-128.

28 F.B. Gertler, K. Niebuhr, M. Reinhard, J. Wehland, and P. Soriano (1996) Mena, a relative of VASP and Drosophila Enabled, is implicated in the control of microfilament dynamics. Cell 87, 227-39.

29 T. Russo, R. Faraonio, G. Minopoli, P. De Candia, S. De Renzis, and N. Zambrano (1998) Fe65 and the protein network centered around the cytosolic domain of the Alzheimer's β-amyloid precursor protein. FEBS. 434, 1-7.

30 C.S. Ho, V. Marinescu, M.L. Steinbilb, J.R. Gaut, R.S. Turner, and E.L. Stuenkel. (2002) Synergistic effects of Munc18a and X11 proteins on amyloid precursor protein metabolism. J. Biol. Chem. 277, 27021-28.

31 H. Taru, Y Kirino, T. Suzuki (2002) JIP scaffold proteins in the modulation of amyloid precursor protein metabolism. J. Biol. Chem. 277, 27567-574.

32 H. Taru, K. Iijima, M. Hase, Y. Kirino, Y. Yagi, and T. Suzuki (2002) Interaction of Alzheimer's beta-amyloid precursor family proteins with scaffold proteins of the JNK signaling cascade. J. Biol. Chem. 277, 20070-78.

33 M.H. Scheinfeld, R. Roncarati, P. Vito, P.A. Lopez, M. Abdallah, and L. D'Adamio (2002) Jun NH2-terminal kinase (JNK) interacting protein 1 (JIP1) binds the cytoplasmic domain of the Alzheimer's beta-amyloid precursor protein (APP). J. Biol. Chem. 277, 3767-75.

34 N. Chow, J.R. Korenberg, X.N. Chen, and R.L. Neve (1996) APP-BP1, a novel protein that binds to the carboxyl-terminal region of the amyloid precursor protein. J. Biol. Chem. 271, 11339-346.

35 Y. Chen, D.L. McPhie, J. Hirschberg, and R.L. Neve (2000) The amyloid precursor protein-binding APP-BP1 drives the cell cycle through the S-M checkpoint and causes apoptosis in neurons. J. Biol. Chem. 275, 8929-8935.

36 P.E. Tarr, R. Roncarati, G. Pelicci, P.G. Pelicci and L. D'Adamino (2002) Tyrosine phosphorylation of the beta-amyloid precursor protein cytoplasmic tail promotes interaction with Shc. J. Bio. Chem. 277, 16798-804.

37 C.B. Thompson, (1995) Apoptosis in the pathogenesis and treatment of disease. Science. 267, 1456-1462.

38 C.W. Cotman, and J.H. Su (1996) Mechanism of neuronal death in Alzheimer's disease. Brain Pathol. 6, 493-506.

39 M.P. Mattson, W. Duan (1999) "Apoptotic" biochemical cascades in synaptic compartments: roles in adaptive plasticity and neurodegenerative disorders, J. Neurosci. Res. 58, 152-166.

40 X. Xu, D. Yang, T. Wyss-Coray, J. Yan, L. Gan, Y. Sun L. Mucke (1999) Wild-Type but not Alzheimer-mutant amyloid precursor protein confers resistance against p53-mediated apoptosis. Proc. Natl. Acad. Sci. 96, 7547-7552.

41 I. Nishimura, T. Uetsuki, S.U. Dani, Y Onsawa, I. Saito, H. Okamura, Y Uchiyama, K, Yoshikawa (1998) Degeneration *in vivo* of rat hippocampal neurons by wild-type Alzheimer amyloid precursor protein overexpressed by adenovirus-mediated gene transfer. J. Neruosci. 18, 2387-2398.

42 A. Eckert, B. Steiner, C. Marques, S. Leutz, H. Romig, C. Haass, and W.E. Muller (2002) Elevated vulnerability to oxidative stress-induced cell death and activation of caspase-3 by the Swedish amyloid precursor protein mutation. J. Neurosci. Res. 64, 183-192.

43 W. Araki, and R.J. Wurtman (1998) Increased expression of amyloid precursor protein and amyloid precursor-like protein 2 during trophic factor withdrawl-induced death of neuronal PC12 cells. Brain Res. Mol. Brain Res. 56, 169-77.

44 Q. Guo, N. Robinson, and M.P. Mattson (1998) Secreted beta-amyloid precursor protein counteracts the proapoptotic action of mutant presenilin-1 by activation of NF-kappaB and stabilization of calcium homeostasis. J. Biol. Chem. 273, 12341-12351.

45 E. Masliah, C.E. Westland, E.M. Rockenstein, C.R. Abraham. M. Mallory, I. Veinberg, E. Sheldon, and L. Mucke (1997) Amyloid precursor proteins protect neurons of transgenic mice against acute and chronic excitotoxic injuries *in vivo*. Neurosci. 78, 135-146.

46 D.L. McPhie, T. Golde, C.B. Eckman, D. Yager, J.B. Brant, and R.L. Neve (2001) Beta-secretase cleavage of the amyloid precursor protein mediates neuronal apoptosis caused by familial Alzheimer's disease mutations. Brain Res. Mol. Brain Res. 98, 103-113.

47 P. Kienlen-Campard, S. Miolet, B. Tasiaux, J.N. Octave (2002) Intracellular amyloid-beta 1-42, but not extracellular soluble amyloid-beta peptides, induces neuronal apoptosis. J. Biol. Chem. 277, 15666-670.

48 D. Leifer, D. Krainc, Yu, Y-T., McDermott, J., Breitbart, R.E., Heng, J., Neve, R.L., Kosofsky, B., Nadal-Ginard, B., Lipton, S.A (1993) MEF2C, a MADS/MEF2-family transcription factor expressed in a laminar distribution in cerebral cortex. Proc. Natl. Acad. Sci. USA. 90, 1546-1550.

49 J.D. Molkentin, L. Li, E.N. Olson (1996) Phosphorylation of the MADS-box transcription factor MEF2C enhances its DNA binding activity. J. Biol. Chem. 271, 17199-17204.

50 Q. Lin, J. Schwarz, C. Bucana, E.N. Olson (1997) Control of mouse cardiac morphogenesis and myogenesis by transcription factor MEF2C. Science 276, 1404-1407.

51 A. Zetser, E. Gredinger, and E. Bengal (1999) p38 mitogen-activated protein kinase pathway promotes skeletal muscle differentiation. J. Biol. Chem. 274, 5193-5200.

52 Q. Lin, J. Lu, H. Yanagisawa, R. Webb, G.E. Lyons, J.A. Richardson, and E.N. Olson (1998) Requirement of the MADS-box transcription factor MEF2C for vascular development. Development 125, 4565-74.

53 X. Lin, S. Shah, and R.F. Bullet (1996) The expression of MEF2 genes is implicated in CNS neuronal differentiation. Brain Res. Mol. Brain Res. 42, 307-316.

54 J.D. Molkentin, B.L. Black, J.F. Martin, E.N. Olson (1995) Cooperative activation of muscle gene expression by MEF2 and myogenic bHLH proteins. Cell.83, 1125-1136.

55 S.V. Subramanian, and B. Nadal-Ginard (1996) Early expression of the different isoforms of the myocyte enhancer factor-2 (MEF2) protein in myogenic as well as non-myogenic cell lineages during mouse embryogenesis. Mech. Dev. 57, 103-112.

56 O.I. Ornatsky, J.J. Andreucci, J.C. McDermott, A dominant-negative form of transcription factor MEF2 inhibits myogenesis J. Biol. Chem. 272 (1997) 33271-33278.

57 Y. Katoh, J.D. Molkentin, V. Dave, E.N. Olson, and M. Periasamy (1998) MEF2B is a component of a smooth muscle-specific complex that binds an A/T-rich element important for smooth muscle myosin heavy chain gene expression. J. Biol. Chem. 273, 1511-18.

58 A. Taylor, K.A. Webster, T.A. Gustafson, and L. Kedes (1997) The anti-cancer agent distamycin A displaces essential transcription factors and selectively inhibits myogenic differentiation. Mol. Cell Biochem. 169, 61-72.

59 R. Di Lisi, C. Millino, E. Calabria, F. Alturda, S. Schiaffino, and S. Ausoni (1998) Combinatorial *cis*-acting elements control tissue-specific activation of the cardiac troponin I gene *in vitro* and *in vivo*. J. Biol. Chem. 273, 25371-380.

60 Q. Wang, C.D. Sigmund, and J.J. Lin (2000) Identification of cis elements in the cardiac troponin T gene conferring specific expression in cardiac muscle of transgenic mice. Circ. Res. 86, 478-484.

61 S. Ferrari, S. Molinari, R. Melchionna, M.G. Cusella-De Angelis, R. Battini, L. De Angelis, R. Kelly, and G. Cossu (1997) Absence of MEF2 binding to the A/T-rich element in the muscle creatine kinase

(MCK) enhancer correlates with lack of early expression of the MCK gene in embryonic mammalian muscle. Cell Growth Differ. 8, 23-24.

62 K. Esser, T. Nelson, V. Lupa-Kimball, and E. Blough (1999) The CACC box and myocyte enhancer factor-2 sites within the myosin light chain 2 slow promoter cooperate in regulating nerve-specific transcription in skeletal muscle. J. Biol. Chem. 274, 12095-102.

63 A.G. Ridgeway, S. Wilton, and I.S. Skerjanc (2000) Myocyte enhancer factor 2C and myogenin up-regulate each other's expression and induce the development of skeletal muscle in P19 cells. J. Biol. Chem. 275, 41-46.

64 T. Maeda, M.P. Gupta, and A.F.R. Stewart (2002) TEF-1 and MEF2 transcription factors interact to regulate muscle-specific promoters. Biochem. Biophys. Res. Comm. 294, 791-797.

65 G.E. Lyons, B.K. Micales, Schwartz, J., Martins, J.F. and Olson, E.N. Expression of MEF2 genes in the central nervous system suggests a role in neuronal maturation, J. Neurosci.15 (1995) 5727-5738.

66 Z. Mao, A. Bonni, F. Xia, M. Nadal-Vicens, M.E. Greenberg, Neuronal activity-dependent cell survival mediated by transcription factor MEF2, Science. 286 (1999) 785-790.

67 S. Okamoto, D. Krainc, K. Sherman, S.A. Lipton, Anti-apoptotic role of the p38 mitogen activated protein kinase-myocyte enhancer factor-2 pathway during neuronal differentiation, Proc. Natl. Acad. Sci. 97 (2000) 7561-7566.

68 Z. Mao, M. Wiedmann, Calcineurin enhances MEF2 DNA binding activity in calcium-dependent survival of cerebellar granule neurons, J. Biol. Chem. 274 (1999) 31102-31107.

69 I.S. Skerjanc, and S. Wilton (2000) Myocyte enhancer factor 2C upregulates MASH-1 expression and induces neurogenesis in P19 cells. FEBS Lett. 472, 53-56.

70 O.I. Ornatsky, J.C. McDermott, MEF2 protein expression, DNA binding specificity and complex composition, and transcriptional

activity in muscle and non-muscle cells, J. Biol. Chem. 271, (1996) 24927-24933.

71 O.A. Coso, S. Montaner, C. Fromm, J.C. Lacal, R. Prywes, H. Teramoto, and J.S. Gutkind (1997) Signaling from G protein-coupled receptors to the c-jun promoter involves the MEF2 transcription factor. J. Biol. Chem. 272, 20691-697.

72 M.J. Marinissen, M. Chiariello, M. Pallante, and J.S Gutkind (1999) A network of mitogen-activated protein kinases links G protein-coupled receptors to the c-*jun* promoter: a role for c-Jun NH_2-terminal kinase, p38s, and extracellular signal-regulated kinase 5. Mol. Cell Biol. 19, 4289-4301.

73 D. Krainc, G. Bai, S. Okamoto, M. Carles, J.W. Kusiak, R.N. Brent, and S.A. Lipton (1998) Synergistic activation of the N-methyl-D-aspartate receptor subunit 1 promoter by myocyte enhancer factor 2C and Sp1. J. Biol. Chem. 273, 26218-224.

74 D. Kranic, G. Bai, S. Okamoto, M. Carles, J.W. Kusiak, R.N. Brent, and S.A. Lipton (1998) Synergistic activation of the N-methyl-D-aspartate receptor subunit1 promoter by myocyte enhancer factor 2C and Sp1. J. Biol. Chem. 273, 26218-224.

75 Y. Tamir, E. Bengal, Phosphoinositide 3-kinase induces the transcriptional activity of MEF2 proteins during muscle differentiation, J. Biol. Chem. 275 (2000) 34424-34432.

76 M. Zhao, L. New, V.V. Kravchenko, Y. Kato, H. Gram, F. Padova, E.N. Olson, R.J. Ulevitch, J. Han, Regulation of the MEF2 family of transcription factors by p38, Mol. Cell. Biol. 19 (1999) 21-30.

77 S. Yang, A. Galanis, A. Sharrocks, Targeting of p38 mitogen-activated protein kinases to MEF2 transcription factors, Mol. Cell biol. 19 (1999) 4028-4038.

78 O.I. Ornatsky, D.M. Cox, P. Tangirala, J.J. Andreucci, Z.A. Quinn, J.L. Wrana, R. Prywes, Y. Yu, J.C. McDermott, Post-translational control of the MEF2A transcriptional regulatory protein, Nuc. Acids Res. 27 (1999) 2646-2654.

79 J. Han, Y. Jiang, Z. Li, V.V. Kravchenko, and R.J. Ulevitch (1997) Activation of the transcription factor MEF2C by the MAP kinase p38 in inflammation. Nature 386, 296-299.

80 Y. Kato, M. Zhao, A. Morikawa, T. Sugiyama, D. Chakravortty, N. Koide, T. Yoshida, R.I. Tapping, Y. Yang, T. Yokochi, and J-D. Lee (2000) Big mitogen-activated kinase regulates multiple members of the MEF2 protein family. J. Biol. Chem. 275, 18534-540.

81 C-C. Yang, O.I. Ornatsky, J.C. McDermott, T.F. Cruz, and C.A. Prody (1998) Interaction of myocyte enhancer factor 2 (MEF2) with a mitogen-activated protein kinase, ERK5/BMK1. Nucleic Acids Res. 26, 4771-777.

82 Q. Xu, and Z. Wu (2000) The insulin-like growth factor-phosphatidylinositol 3-kinase-Akt signaling pathway regulates myogenin expression in normal myogenic cells but not in rhabdomyosarcoma-derived RD cells. J. Biol. Chem. 275, 36750-757.

83 S.M. Rosenthal, and Z.Q. Cheng (1995) Opposing early and late effects of insulin-like growth factor I on differentiation and the cell cycle regulatory retinoblastoma protein in skeletal myoblasts. Proc Natl Acad Sci U S A. 92, 10307-11.

84 J.C. Engert, E.B. Berglund, and N. Rosenthal (1996) Proliferation precedes differentiation in IGF-I-stimulated myogenesis. J Cell Biol. 135, 431-40.

85 B.H. Jiang, J.Z. Zheng, and P.K. Vogt (1998) An essential role of phosphatidylinositol 3-kinase in myogenic differentiation. Proc Natl Acad Sci U S A. 95, 14179-83.

86 S. Kaneko, R.I. Feldman, L. Yu, Z. Wu, T. Gritsko, S.A. Shelley, S.V. Nicosia, T. Nobori, and J.Q. Cheng (2002) Positive feedback regulation between Akt2 and MyoD during muscle differentiation. Cloning of Akt2 promoter. J. Biol. Chem. 277, 23230-235.

87 B. Pasche (2001) Role of transforming growth factor beta in cancer. J. Cellular Physiol. 186, 153-168.

88 Z.A. Quinn, C-C. Yang, J.L. Wrana, and J.C. McDermott (2001) Smad proteins function as co-modulators for MEF2 transcriptional regulatory proteins. Nucleic Acids Res. 29, 732-42.

89 L.A. Pinna (2002) Protein kinase CK2: a challenge to canons. J. Cell Science 115, 3873-3878.

90 S. Halpain, J.A. Girault, and P. Greengard (1990) Activation of NMDA receptors induces dephosphorylation of DARPP-32 in rat striatal slices. Nature. 343, 369-72.

91 J. Liu, J.D. Farmer, W.S. Lane, J. Friedman, I. Weissman, and S.L. Schreiber (1991) Calcineurin is a common target of cyclophilin-cyclosporin A and FKBP-FK506 complexes. Cell 66, 807-15.

92 J. Jain, P.G. McCaffrey, T.K. Kerppola, J.N. Lambert, G.L. Verdine, T. Curran, and A. Rao (1993) The T-cell transcription factor NFATp is a substrate for calcineurin and interacts with Fos and Jun. Nature. 365, 352-5.

93 T.A. McKinsey, C.L. Zhang, and E.N. Olson (2002) MEF2: a calcium-dependent regulator of cell division, differentiation and death. T.I.B.S. 27, 40-47.

94 Q. Xu, L. Yu, L. Liu, C.F. Cheung, X. Li, S-P. Yee, X-J. Yang, and Z. Wu (2002) Calcium-calmodulin-dependent protein kinase-, and calcineurin-mediated signaling pathways transcriptionally regulate myogenin expression. Mol. Biol. Cell 13, 1940-52.

95 H. Wu, F.J. Naya, T.A. McKinsey, B. Mercer, J.M. Shelton E.R. Chin A.R. Simard, R.N. Michel, R. Bassel-Duby, E.N. Olson, and R.S. Williams. MEF2 responds to multiple calcium-regulated signals in the control of skeletal muscle fiber type. EMBO J. 19, 1963-73.

96 H. Youn, L. Sun, R. Prywes, J.O. Liu, Apoptosis of T cells mediated by Ca^{2+}-induced release of the transcription factor MEF2, Science. 286 (1999) 790-793.

97 F. Blaser, N. Ho, R. Prywes, T.A. Chatila, Ca(2+)-dependent gene expression mediated by MEF2 transcription factors, J. Biol. Chem. 275 (2000) 197-209.

98 E.A. Miska, C. Karlsson, E. Langley, S.J. Nielsen, J. Pines and T. Kouzarides (1999) HDAC4 deacetylase associates with and represses the MEF2 transcription factor. EMBO J. 18, 5099-5107.

99 J. Lu, T.A. McKinsey, R.L. Nicol, E.N. Olson, Signal-dependent activation of the MEF2 transcription factor by dissociation from histone deacetylases, Proc. Natl. Acad. Sci.97 (2000) 4070-4075.

100 H-D. Youn, C.M. Grozinger, and J.O. Liu (2000) Calcium regulates transcriptional repression of myocyte enhancer factor 2 by histone deacetylase 4. J. Biol. Chem. 275, 22563-567.

101 C. Lemercier, A. Verdel, B. Galloo, S. Curtet, M.P. Brocard, and S. Khochbin (2000) mHDA1/HDAC5 histone deacetylase interacts with and represses MEF2A transcriptional activity. J. Biol. Chem. 275, 15594-599.

102 C.M. Grozinger, C.A. Hassig, and S.L. Schreiber (1999) Three proteins define a class of human histone deacetylases related to yeast Hda1p. Proc Natl Acad Sci U S A. 96, 4868-73.

103 3S. Borghi, S. Molinari, G. Razzini, F. Parise, R. Battini, and S. Ferrari (2001) The nuclear localization domain of the MEF2 family of transcription factors shows member-specific features and mediates the nuclear import of histone deacetylase 4. J. Cell Sci. 114, 4477-4483.

104 T.A. McKinsey, C.L. Zhang, and E.N. Olson (2000) Activation of the myocyte enhancer factor-2 transcription factor by calcium/calmodulin-dependent protein kinase-stimulated binding of 14-3-3 to histone deacetylases 5. P.N.A.S. 97, 14400-14405.

105 T.A. McKinsey, C.L. Zhang, J. Lu, and E.N. Olson (2000) Signal-dependent nuclear export of a histone deacetylases regulates muscle differentiation. Nature 408, 106-111.

106 J. Lu, T.A. McKinsey, C, Zhang, E.N. Olson, Regulation of skeletal myogenesis by association of the MEF2 transcription factor with class II histone deacetylases, Mol. Cell. 6 (2000) 233-244.

107 S.J. Choi, S.Y. Park, and T.H. Han (2001) 14-3-3tau associates with and activates the MEF2D transcription factor during muscle cell differentiation. Nucleic Acids Res. 29, 2836-42.

108 X.Q. Gong, and L. Li (2002) Dermo-1, a multifunctional basic helix-loop-helix protein, represses MyoD transactivation via the HLH domain, MEF2 interaction, and chromatin deacetylation. J. Biol. Chem. 277, 12310-317.

109 C.L. Zhang, T.A. M,Kinsey, J.R. Lu, and E.N. Olson (2001) Association of COOH-terminal-binding protein (CtBP) and MEF2-interacting transcription repressor (MITR) contributes to transcriptional repression of the MEF2 transcription factor. J. Biol. Chem. 276, 35-39.

110 H.D. Youn, and J.O. Liu (2000) Cabin1 represses MEF2-dependent Nur77 expression and T cell apoptosis by controlling association of histone deacetylases and acetylases with MEF2. Immunity 13, 85-94.

111 V. Sartorelli, J. Huang, Y. Hamamori, and L. Kedes (1997) Molecular mechanisms of myogenic coactivation by p300: direct interaction with the activation domain of MyoD and with the MADS box of MEF2C. Mol. Cell Biol. 17, 1010-1026.

112 M. Li, D.A. Linseman, M.P. Allen, M.K. Meintzer, X. Wang, T. Laessig, M.E. Wierman, and K.A. Heidenreich (2001) Myocyte enhancer factor 2A and 2D undergo phosphorylation and caspase-mediated degradation during apoptosis of rat cerebellar granule neurons. J. Neurosci. 21, 6544-552.

113 S. Okamoto, Z. Li, C. Ju, M.N. Scholzke, E. Mathews, J. Cui, G.S. Salvesen, E. Bossy-Wetzel, and S.A. Lipton (2002) Dominant-interfering forms of MEF2 generated by caspase cleavage contribute to NMDA-induced neuronal apoptosis. P.N.A.S. 99, 3974-79.

114 R.B. Dyer, N.K. Herzog, Isolation of intact nuclei for nuclear extract preparation from a fragile B-lymphocyte cell line, Biotechniques. 19 (1995) 192-195.

115 C. Gorman, in: DNA Cloning (IRL Press). 2 (1985) 143-149.

116 D. Schubert, C. Behl, The expression of amyloid beta protein precursor protects nerve cells from beta-amyloid and glutamate toxicity and alters their interaction with the extracellular matrix, Brain Res. 629 (1993) 275-282.

117 C.L. Manthey, S.W. Wang, S.D. Kinney, Z. Yao, SB202190, a selective inhibitor of p38 mitogen-activated protein kinase, is a powerful regulator of LPS-induced mRNAs in monocytes, J Leukoc Biol. 64 (1998) 407-417.

118 P.D. Marley, K.A. Thomson, The Calcium-calmodulin dependent protein kinase II inhibitors KN-62 and KN-93, and their inactive analogues KN-64 and KN-92, inhibit nicotinic activation of tyrosine hydroxylase in nicotinic activation in bovine chromaffin cells, Biochem. Biophys. Res. Commun. 221 (1996) 15-18.

119 M. Masumura, R. Hata, I. Nishimura, T.U. Etsuki, T. Sawada, K. Yoshikawa, Caspase-3 activation and inflammatory responses in rat hippocampus inoculated with a recombinant adenovirus expressing the Alzheimer's amyloid precursor protein, Mol. Brain Res. 80 (2000) 219-227.

120 A. Ecket, B. Steiner, C. Marques, S. Leutz, H. Ronig, C. Haass, W. Muller, Elevated vulnerability to oxidative stress-induced cell death and activation of caspase-3 by the Swedish amyloid precursor protein mutation, J. Neurosci Res. 64 (2001) 183-192.

121 C.W. Wallace, C.A. Akar, B. Wolozin, Amyloid precursor protein requires the insulin signaling pathway for neurotrophic activity, Mol. Brain. Res. 52 (1997) 213-227.

122 J.F. Martin, J.J. Schwarz, E.N. Olson, Myocyte enhancer factor (MEF) 2C: a tissue restricted member of the MEF-2 family of transcription factors, Proc. Natl. Acad. Sci. 90 (1993) 5282-5286.

123 J. Tan, T. Town, F. Crawford, T. Mori, A. DelleDonne, R. Crescentini, D. Obregon, R.A. Flavell and M.J. Mullan, Role of CD40 ligand in amyloidosis in transgenic Alzheimer's mice, Nature 1038 (2002) 968-972.

124 J. Hu, K.T. Akama, G.A. Krafft, B.A. Chromy, and L.J. Van Eldik, Amyloid-beta peptide activtes cultured astrocytes: morphological alterations, cytokine induction and nitric oxide release, 785 (1998) 195-206.

125 Y. Yuk, H. Rhim, S.Y. Yi, and Y.S. Yoo, Role of p38 in the regulation of apoptosis signaling induced by TNF-alpha in differentiated PC12 cells. J. Biochem. Mol. Biol. 35 (2002) 267-72.

126 G.S. De Zutter, and R.J. Davis, Pro-apoptotic gene expression mediated by the p38 mitogen-activated protein kinase signal transduction pathway, PNAS. 98, (2001) 6168-73.

127 W. Zou, J. Zeng, M. Zhuo, W. Xu, L. Sun, J. Wang, and X. Liu, Involvement of caspase-3 and p38 mitogen-activated protein kinase in cobalt chloride-induced apoptosis in PC12 cells, J. Neurosci, Res. 67 (2002) 837-43.

128 R. Nath, K. McGinnis, S. Dutta, B. Shivers, and K.K. Wang, Inhibition of p38 kinase mimics survival signal-linked protection against apoptosis in rat cerebellar granule neurons, Cell Mol. Biol. Lett. 6 (2001) 173-84.

129 S. Willaime, P. Vanhoutte, J. Caboche, Y. Lemaigre-Dubreuil, J. Mariani, and B. Brugg (2001) Ceramide-induced apoptosis in cortical neurons is mediated by an increase in p38 phosphorylation and not by the decrease in ERK phosphorylation. Eur. J. of Neuroscience 13, 2037-2046.

130 K. Takeda, and H. Ichijo (2002) Neuronal p38 MAPK signaling: an emerging regulator of cell fate and function in the nervous system. Genes to Cells 7, 1099-1111.

131 E. Wingender, X. Chen, R. Hehl, H. Karas, I. Liebich, V. Matys, T. Meinhardt, M. Prub, I. Reuter, and F. Schacherer (2000) Transfac: an integral system for gene expression regulation. N. A. Res. 28, 316-319.

132 S. Shimohama (2000) Apoptosis in Alzheimer's disease-an update. Apoptosis 5, 9-16.